博士論文

Physical training regulates the serotonin 2A receptor sensitivity of neuronal cells in the central nervous system and contributes to alleviation of spasticity after spinal cord injury

（運動は中枢神経系における
神経細胞のセロトニン 2A 受容体感受性を調節し、
脊髄損傷後痙縮の改善に寄与する）

リュウ　ヨンジェ
(Ryu Youngjae)

Table of contents

List of Abbreviations

5-HT	5-Hydroxytryptophan
5-HTP	5-Hydroxytryptophan
BBB locomotor score	the Basso Beattie and Bresnahan locomotor score
BWST	Body weight supported treadmill
ChAT	Choline acetyltransferase
CNS	Central nervous system
DAPI	4’,6-diaminido-2-phenylindole
EMG	Electromyography
FSS	Fluid shear stress
GFAP	Glial fibrillary acidic protein
IR	Immunoreactivity
MG	Medial gastrocnemius muscle
PFC	Prefrontal cortex
PHM	Passive head motion
PKC	Protein kinase C
SCI	Spinal cord injury
SERT	Serotonin transporter
TA	Tibialis anterior muscle
TMT	Treadmill training
TUJ-1	Class III β-tubulin
WT	Water temperature

General introduction

Section 1. The effect of physical training on mental and neurological disorders and its underlying mechanism

Physical training (exercise) has been widely recognized to be the most effective and safest practice to maintain our health for a long time and have been clinically adapted as a therapeutic approach for human and veterinary medicine. 'Physical training' or 'Exercise' can be defined as "structured and repetitive physical activity designed to maintain or improve physical fitness"[1]. World health organization defines 'physical activity' as "any bodily movement produced by skeletal muscles that requires energy expenditure" from the resting condition[2]. It is generally known that physical training has numerous beneficial effects on body system mainly via increasing blood flow, oxygen consumption and metabolic cascades[1,3]. It is also accepted that, as the aspect of nervous system, exercise leads psychological benefits (*e.g.*, releasing stress or anxiety, alleviating depression) as well as even neuro-regeneration[4-6]. Moreover, physical training is recognized as a therapeutic approach to treat a variety of health problems, including cardiovascular disorders, metabolic diseases and mental illnesses. Thus, to understand the underlying mechanism by which exercise exerts its effects is meaningful not only to maintain good health for a long time, but to provide novel strategies toward more effective and safer treatments for various diseases. Numerous scientific reports elicited therapeutic effects of physical training, and most of those evidences are converging into cardiovascular or metabolic mechanisms: improve glucose metabolism, enhance endothelial remodeling, increase insulin sensitivity, reduce systemic inflammation, reduce low density lipoprotein etc[1,7-10].

Although the molecular mechanisms behind the beneficial effects of physical training on psycho-neurologic disease are still poorly understood, it is reported that exercise induces synaptic remodeling, neuronal plasticity and hippocampal neurogenesis via releasing various

nervous growth factors such as brain derived neurologic factor (BDNF) and insulin growth factor -1 (IGF-1)[11-13]. There is accumulating evidence that physical training shows clinical effects on mental disorders including schizophrenia, anxiety and depression[14,15] which are particularly relating to disorder of serotonergic functions[16-18]. For example, many studies described physical activities such as running or walking increase stress resistance, resolve anxiety and exert beneficial effects on depression[6,14,19,20]. In regard to serotonin (5-hydroxytryptamine; 5-HT) system, it is known that exercise induces elevation of 5-HT levels and regulates the expression of 5-HT receptors such as 5-HT_{1A} receptor in the brain[21-23]. These reports indicate that physical activities by exercise could modulate 5-HT system in the central nervous system (CNS). On the other hand, related to serotonergic system, not only confined to mental disorder, physical training also shows beneficial effects on spinal disorders including spasticity and improves patient's locomotive functions after spinal cord injury as in the sense of rehabilitation[24-27]. Taken together, it is assumed that regulation of 5-HT system plays an important role in therapeutic mechanisms of exercise after the CNS disorders.

Section 2. Regulation of serotonin in the central nervous system

Serotonin (5-HT) is a core monoamine neurotransmitter in the CNS. 5-HT and its receptors, consistent of at least 15 serotonin receptors which are members of G protein-coupled receptor (GPCR) family[28], are essential to regulate brain functions and maintenances such as sleep, emotion, sensory-motor functions and cognition[16,29]. Dysregulation of 5-HT system cause many mental disorders including depression, anxiety, insomnia and other behavioral abnormalities. For example, low level of 5-HT in the CSN is deeply related to the depressive patient[30,31]. The collapse of 5-HT regulation is also known as an upregulation of 5-HT_{2A} receptor in the frontal cortex in depressive and bipolar disorder patients[32]. Excessive 5-HT and desensitized 5-HT_{1A} receptor in the medulla and connected cortex regions are correlated with anxiety[30]. In dogs, increased or decreased 5-HT_{2A} receptor is related to aggressive behaviors or anxious behaviors[33]. Therefore, biological functions and activation mechanisms of 5-HT signaling have been focused to treat these mental disorders.

Cellular responses mediated by 5-HT receptors are regulated by desensitization of the receptors, which is generally occurred after an agonist administration[28,34,35]. It is generally recognized that ligand dependent regulation of 5-HT receptors accompanies the internalization and desensitization of receptors via endocytosis[36]. 5-HT receptors under desensitization show short- or long-term reactive changes which eventually modulate biological responses[35,36]. Although it is reasonable to assume that beneficial effects of physical training on the CNS are produced via the regulation of both ligand and/or receptor sensitivity, numerous reports have been focused on the facts that physical trainings increase the level of 5-HT in the brain as well as spinal cord, while the effects of exercise on the ligand-independent 5-HT receptor sensitivity have not been paid much attention and still remained unclear. To elucidate whether and how physical activity regulates 5-HT receptor sensitivity will be helpful for better understanding

about mechanisms of the effect of exercise and be useful for developing novel therapeutic strategies or rehabilitative program for serotonin-related CNS disorders.

Section 3. Spasticity and hypersensitivity of serotonin receptor

To examine the effect of physical training on 5-HT receptor with a clinical implication, spasticity after spinal cord injury (SCI) have been investigated. Spasticity is one of the common and chronic complications after traumatic SCI. Traditionally, spasticity is often defined as a velocity dependent increase in the stretch reflex caused by hyperexcitability of spinal circuits[37]. More widely, in clinical, spasticity is referred as sustaining involuntary muscular activations resulting from a lesion of upper motor neurons (UMN)[38]. In the sense of biological phenomenon, spasticity could be characterized in spontaneous activations of motor neuron pools without conscious control[39]. Traumatic disconnection between UMN and lower motor neurons (LMN) following SCI is known to result in hyperexcitability of spinal reflexes and subsequent spastic symptoms including muscle spasms, muscular hypertonia, and clonus[25,38-40].

While it is not clearly studied when the symptoms of spasticity occur after the injury, it is generally considered that spastic symptoms gradually emerge in the sub-acute phase after injury and interfere with voluntary physical performance throughout the chronic phase[41]. In spinalized rodent models, spastic signs are also observed, with progressive muscular stiffness and tail spasm starting 3–4 weeks after SCI[42,43]. Spasticity frequently impairs voluntary motor control, and its severity varies among individuals with SCI. It is reported that approximately 65–80% of patients with SCI present with muscle spasticity, whereas others have reported that 50–60% of patients complain of spastic symptoms that interfere with voluntary motion[40,44,45]. Basically, medications are often prescribed to treat spastic symptoms[25,41,46]. Although systemic administration of oral drugs such as GABAnergic (gamma-aminobutyric acid) drugs are frequently used to correct the hyperactive state of spinal motor neurons, they have a limitation

in their side effects and controlling severe symptoms[47-49]. Therefore, the underlying mechanisms of spasticity and voluntary motor control is needed to establish further improvement of symptoms and development new therapeutic interventions for spasticity. Although several studies on spasticity using the contusive injury animal models have shown an increased muscle resistance and spinal hyperreflexia after SCI[50-52], individual variation in spastic symptoms, even if the animals were received same types or degree of injury, remains an obstacle for the detailed analysis of molecular mechanisms underlying spasticity. Therefore, novel objective method is required to quantitatively evaluate spasticity in an appropriate SCI model for accurate analysis.

Exaggeration of spinal reflexes resulted in muscular hypertonia is the key feature of spasticity. Mechanisms underlying hyperexcitability of spinal circuit are variously suggested: decreased inhibitory inputs, increased excitatory synaptic inputs and upregulated motor neuron excitability[42,53-58]. Traditionally, loss of balances between excitatory and inhibitory descending spinal tracts such as reticulospinal tract has been regarded as a crucial reason of the onset of spasticity[59].

Recently, hypersensitivity of 5-HT and up-regulation of its receptors below the injury site after SCI have been reported to be related to the hyperexcitability of spinal motor neurons and consequent spasticity[55,56,58,60,61]. The depletion of 5-HT from the descending tract following SCI is accompanied by the upregulation of its receptor on motor neurons, leading to both ligand-dependent and ligand-independent activation of the receptor which induces a persistent depolarization[58,62,63]. Among the 5-HT receptors, it is reported that 5-HT_{2A}, 5-HT_{2B}, and 5-HT_{2C} receptors are closely related to the hyperexcitability of motor neurons after SCI[56]. After SCI, gradual and robust up-regulation of the expression of 5-HT_2 receptors on the spinal motor neurons below to the lesion site was observed[58,62-64]. Thus, 5-HT receptor antagonists,

including cyproheptadine, have been studied to alleviate spastic symptoms[65,66]. Although it is assumed that 5-HT signaling is important to develop spasticity after SCI, there have been no basic research about quantitative assessment of spastic behaviors focused on 5-HT receptor in the spinal cord with or without interventions, so far.

Section 4. Potential of regulation of serotonergic system for developing novel therapeutic strategy and rehabilitative therapy

It is generally recognized that physical training (e.g. treadmill training or cycling) is efficient to manage spasticity[24,25]. Recent studies on animal models and human subjects have shown that physical training after SCI restores the balance between excitatory and inhibitory functions of propriospinal neurons, which modulate spinal motor neurons, thereby alleviating spastic symptoms[67-69]. Clinically, treadmill training in human patients with SCI is reported to reduce the spasticity in their lower limbs[24,70]. However, it is not enough studied using proper spasticity models for evaluating the effect of physical training on the spastic behaviors *in vivo* in related to examining 5-HT receptors. Moreover, it would be expected to apply a combination therapy including physical therapy and medications which modulate 5-HT receptor sensitivity, aiming for an additive or synergistic therapeutic effect on spasticity. Since rehabilitation programs with medication targeting spasticity have not been extensively examined in human and animal studies, there is a need to research the effect of combination therapies including physical training with using a proper animal model of spasticity.

Section 5. Mechanical factor generated from physical training and a behavior assessment related to serotonin receptor

Physical training (exercise) shows beneficial effects on various neurological or mental disorders including depression, schizophrenia and the other cognitive or behavioral diseases. Moreover, physical training helps to alleviate spinal diseases such as spasticity, as described above. However, the direct mechanism how exercise modulates 5-HT system, especially about the sensitivity of 5-HT receptors, is largely unknown. Thus, to elucidate the underlying mechanism is expected to give new insights of developing novel therapeutic strategies for treating various 5-HT related CNS diseases. To find out how physical training exerts its effects on the CNS related to 5-HT receptor regulation, I focused on mechanical components which induced by physical activity itself, such as generated forces, rather than a ligand stimulation or secreted biological factors. It is known that interstitial fluid, the fluid between cells, is consisted of up to 15-20% of volume of the brain, could be changed its velocity or direction by physical activity[71,72]. It is reported that cerebral interstitial fluid diffuses naturally in different direction and at various velocities at the different parts of the brain[73,74]. When the fluid flows, fluid shear stress is occurred on the surface of objects and offer a mechanical stress to the cells. In biological fields, fluid shear stress is widely researched for blood vessel and blood flow studies[75-77]. From those researches, it is proved that fluid shear stress can induce biological modulations on the cells and promote endocytosis of receptors, especially G protein-coupled receptors (GPCRs)[78] Physical training could generate mechanical forces on the CNS including brain and spinal cord. Because of generated forces during the movement of part of the body such as the head, tissues and cells will be also affected by that forces. In that context, it is hypothesized that the fluid sheer stress caused by diffusion of cerebral intestinal fluid during physical training may directly influence on the regulation of 5-HT receptor in the CNS.

Section 6. Objective of the study

Above all, the main aims of my studies, in this thesis, were to evaluate the effect of physical training and to explore its mechanism on the 5-HT receptor regulation in the CNS.

At ***Chapter 1***, a novel method to assess spasticity using the swimming test was developed and examined for quantitative evaluation of the effect of physical training for further clinical implications.

At ***Chapter 2***, spastic animals were received treadmill training with or without serotonergic interventions which were a 5-HT_2 receptor antagonist and selective serotonin re-uptake inhibitor (SSRI) to evaluate the effect of combination therapy with physical training and medications on spasticity. After the interventions, spasticity was evaluated and the expression of 5-HT_{2A} receptor was analyzed.

Finally, at ***Chapter 3***, to explain whether and how the physical training affects 5-HT receptor sensitivity, I demonstrated that mechanical perturbation applied to nervous cells is an important factor that regulates the sensitivity of 5-HT receptor. I utilized the property of brain and 5-HT_{2A} receptor-related brain functions which are used as a reminiscent model to understand how the mechanical stress regulates the sensitivity of 5-HT receptor on the spinal neurons and to investigate the related mechanism more properly.

Chapter 1.

The swimming test for evaluating spasticity

after contusive spinal cord injury

Introduction

Impairments in locomotive and neurological functions, as the consequences of upper motor neurons (UMN) lesions, are frequently followed by traumatic spinal cord injury (SCI). Spasticity is a frequent chronic complication in individuals with SCI. It presents as various symptoms such as spasm, clonus, and hyperreflexia, and decrease the quality of life of the patients.

The pathophysiology of spasticity has been well studied in rodent models mainly using complete spinal cord transection models, wherein supraspinal input is completely disconnected beyond the lesion[79,80]. These studies have provided insights into spasticity mechanisms, including exaggerated spinal reflexes, alternations in synapses, and changes in the expression of motor neuron receptors after SCI[42,53-58]. However, inflammatory tissue reactions and the spared neural network, which exerts a critical influence on the spinal circuitry after injury, differ greatly between the complete spinalized model and the contusive model with incomplete paralysis[81-83]. Considering that most patients with spasticity have a traumatic contusive spinal cord injury, using an incomplete contusive rodent model is more appropriate for clinical translation than the use of a complete transection model.

To examine the exaggerated spinal reflex after SCI, Hoffman reflex test (the H-reflex) is commonly used to assess the spinal circuit excitability and synaptic transmission from Ia afferents to spinal motor neurons with spasticity. This electrophysiological method directly presents the excitability of spinal monosynaptic reflex and, thus, used as a diagnostic method. However, the H-reflex can only attribute to interpret the monosynaptic connection between the sensory fibers to spinal motor neurons, it is hard to represent overall features of the spastic symptoms or behavioral phenotypes derived by UMN or other circumstances. Although several

studies on spasticity using contusive injury animal models have shown increased muscle resistance and spinal hyperreflexia after SCI[50-52], individual variation in spastic symptoms remains an obstacle for the detailed analysis of molecular mechanisms underlying spasticity. Therefore, methods need to be developed to evaluate spasticity in a contusive SCI model to enable further objective quantification and analysis of spasticity. In this point of view, I focused to the swimming test which is a well-established approach for evaluating behavior after SCI[84,85]. Gonzenbach et al. reported muscle spasms in an incomplete transection SCI rat model during swimming [86]. However, to my knowledge, there are no criteria for evaluating spastic behaviors in a contusive SCI model.

As described in the ***Section 3*** of ***General introduction***, hypersensitivity of serotonin (5-HT) receptor is considered as one of the crucial reasons for development of spasticity. However, it has not been investigated whether the severity of spasticity is associated with the changes in 5-HT receptors.

Therefore, in this chapter, I attempted to use a swimming test for the screening and quantification of spasticity, as well as to determining its validity in a contusive SCI rat model. In particular, I sought to determine whether a swimming test can be effectively used to quantify spastic behaviors and to determine the severity of spasticity connected with the spinal motor-neuronal reflex test as well as the expression of 5-HT_{2A} receptor on the spinal motor neurons using a contusive SCI rat model. These findings are expected to help in the design of future experiments and representative models used to improve our understanding of the mechanisms underlying the development of spasticity following SCI.

Materials and methods

Experimental animals, surgery, and post-operative care

Ten-week-old female Sprague-Dawley rats (n = 60, 200–300 g, Charles River Japan) were used in this experiment. Fifty rats received the contusive injury, and 10 were used as uninjured controls. The rats were anesthetized with a mixture of 2 mg/kg of midazolam (Sandoz), 2.5 mg/kg of butorphanol (Meiji Seika, Japan) and 0.15 mg/kg of medetomidine (Kyoritsu Seiyaku, Japan) via intraperitoneal injection (i.p.). After shaving, povidone-iodine (Meiji Seika, Japan) was used for preoperative skin preparation and the body temperature of animals was kept warm using heat pad. Dorsal laminectomy was used to expose thoracic spinal cord. Then, rats were received a 250-kilodyne (kd) contusive injury from an Infinite Horizon impactor device (Precision Systems and Instrumentation, VA, USA) at the 8th thoracic level. After surgery, the injured rats were treated with a single shot of antibiotic (Baytril, 5 mg/kg, SC, Bayer). Manual bladder expression was conducted twice per day until the injured rats spontaneously urinated. The housing room was under a 12-hour/12-hour light/dark cycle and the temperature was maintained at 23°C. Food and water were supplied *ad libitum*. Uninjured rats were used as controls. All animal experiments were approved by the ethical committee of the National Rehabilitation Center for Persons with Disabilities.

Swimming tests

Swimming tests were performed in a rectangular Plexiglas chamber (150 × 14.5 × 40 cm) filled with tap water to a depth of approximately 20–23 cm. The water temperature was maintained at 23°C, which is considered to be an optimal temperature for the rat swimming test [86]. The swimming direction of the rats was controlled from the right to the left side of the

chamber using a ramp. To allow animals to escape easily, an island was attached to the left side of the chamber. Assessment of swimming was conducted within a point of 100 cm distance before the ending point (**Fig. 1-1A**). Swimming from the start point to the end point was regarded as a single run of the swimming test. I performed the swimming test over 5 runs 3 weeks after SCI and over 10 runs each 4, 5, and 6 weeks after SCI. If the SCI rats had at least one clonus phase or a spastic phase in a single run during the test, they were classified as a "spasticity-positive" rat (for criteria for clonus and spastic phases, see the *Results* section). Even if the animals had multiple or mixed phases during a run, the run was considered to be a "spasticity-positive" run because it was difficult to independently determine the clonus and spastic episodes. If both spastic and clonus phases were observed during a run, the run was classified as a clonus phase run. Importantly, behaviors related to defecating or urinating during swimming were excluded. All swimming tests were videotaped using a Sony Handycam HDR-CX700 camera at 60 frames per second. Video analyses and motion capturing were performed using Vegas Pro software (Sony, Japan)

EMG telemetry implantation and recording

I implanted an EMG telemetry device (model: F40-EET, DSI/Receiver model: RPC-1, DSI, MN, USA) to obtain EMG data while the rats moved freely. The EMG telemetry device was inserted between 3 and 4 weeks after the SCI. The device was implanted at the same age in the uninjured animals. The rats (n = 15) were anesthetized using pentobarbital sodium (50 mg/kg, i.p.). After anesthesia, the body of the EMG telemetry device was inserted subcutaneously into the neck region and fixed using sutures. The EMG wires were led via subcutaneous injection and implanted intramuscularly into the left tibial anterialis (TA) muscle, which acts as an ankle flexor, and the left medial gastrocnemius (MG) muscle, which has the opposite action as an ankle extensor. The wires were tightly fixed using 6-0 nylon sutures.

EMG recording was performed at least 3 days after surgery. After EMG implantation, the rats were treated with a single shot of antibiotic (Baytril, 5 mg/kg, SC, Bayer). The EMG signal (sampled at 1,000 Hz) was digitized and filtered using a high-pass filter (30 Hz). EMG recordings were synchronized with a video recording using a light cue trigger. Spike2 software (CED, Cambridge, England) was used for the EMG recording and analysis. All EMG recordings were obtained in an electromagnetic-shielded room. EMGs obtained over 1 second during spastic behaviors were used to determine the mean amplitude of muscle activity using MATLAB software (Mathworks). Video analyses and motion capturing were performed using Vegas Pro software (Sony, Japan)

Twenty-hour cage observation

Cage observations were conducted 4 weeks after SCI from 16:00 on the first day to 12:00 on the following day. Each rat (n = 10) with an implanted EMG telemetry device was individually housed in a large plastic cage (40 × 25 × 18 cm) under dim light. Video was captured using a web camera during simultaneous EMG recording. EMG recording was synchronized to the video recording using a light-cue trigger. For quantitative evaluation, I counted the numbers of clonus and spasm episodes during the 20-hour cage observations, which were confirmed with using EMG recordings (see the *Results* section). Behaviors during defecation or urination were excluded. The same rats that were used for the cage observations were used for the EMG recordings on a treadmill (Robomedica, Inc., CA, USA) with body weight support 4 weeks after SCI to examine muscle activity during voluntary motion. EMG recordings during 10 cycles of walking gaits on a treadmill were obtained at a rate of 7.5 m/minute.

Hoffmann reflex (H-reflex) recording

To test H-reflex, we chose the plantar muscle for its ease of separation and robustness of H-reflex when stimulates the tibial nerve in rodent SCI models[87-89]. Moreover, the changes of plantar reflex is analogous to the other hind limb muscles, such as gastrocnemius and anterior tibialis muscle, in a rat SCI model was reported[89].

Animals were anesthetized using chloral hydrate anesthesia (2.5 g/kg, i.p., Sigma). After anesthesia, limbs and body of animals were fixed with tape. The distal tibial nerve was exposed by small incision and a bipolar cuff was hooked on to the nerve at ankle level. Next, a pair of recording electrodes was subcutaneously inserted into the plantar muscle of the hind limb on the same side[87]. In order to determine the rate-dependent depression (RDD) of the H-reflex, we stimulated the nerve with a stimulator (1-2 V of stimulation intensity, Nihon Kohden, Japan) at 0.2, 0.5, 1, 2, and 5 Hz respectively. The electromyography (EMG) signal was transferred to an amplifier (NEC Biotop 6R12, Nihon Kohden, Japan) and band-pass filtered (5-3000 Hz; sampling rate, 5,000 Hz). The amplitudes of the M and H waves were calculated as an average peak-to-peak value of 15 waves of each waveform. The rate-dependent changes at each stimulation frequency were calculated as a percentage of the response at 0.2 Hz.

Tissue processing and immunohistochemistry

Six weeks after SCI, the rats were deeply anesthetized using sodium pentobarbital, perfused with PBS, and fixed using a 4% PFA solution delivered transcardially. The cervical region and the lumbar region (C1–C3 of the cervical enlargement and L4–L6 of the lumbar enlargement, respectively), and the epicenter of the SCI were removed and post-fixed in a 4% PFA solution for an additional 24 hours at 4°C. The tissues were cut transversely into 20 μm-thick sections on a cryostat (Leica CM3050S, Leica Microsystems). The tissue sections were

incubated with diluted primary antibodies (goat-anti choline acetyltransferase, 1:100, EMD Millipore, #AB144P; rabbit-anti serotonin 2A receptor, 1:200, EMD Millipore, #PC176; rabbit-anti NeuN, 1:500, #MAB377, Millipore; goat-anti serotonin, 1:500, Abcam, #ab66047; mouse-anti glial fibrillary acidic protein (GFAP), 1:500, EMD Millipore, #MAB360) overnight. The next day, the sections were incubated with fluorescent secondary antibodies (Alexa Fluor 488 and 568 for each species-of primary antibody, 1:200, Life Technologies) and DAPI (1:1,000, Sigma) for 2 hours. All images were acquired using a BZ-9000 HS All-in-one Fluorescence Microscope (Keyence BZ-9000).

The area of immunoreactivity (IR) was measured using Image J software (National Institutes of Health, USA). Serotonin 2A receptor (5-HT_{2A}) levels were measured according to the methods described by Kong et al.[63]. In brief, I set thresholds for each images using auto-thresholding methods (Image J software) and binarized. Next, I calculated the 5-HT_{2A} receptor-labeled area corresponding to the ChAT (choline acetyltransferase)-labeled areas of the soma and proximal dendrites of the spinal motor neurons located in the ventral horn. Quantification of the area of serotonin (5-HT) staining was limited to the ventral horn of the spinal cord. Images of the ventral horn obtained at 20× magnification were analyzed for 5-HT immunoreactivity. Five sections (each section was separated by over 300 μm) were used for image analyses of the 5-HT_{2A} receptor and 5-HT fibers. The spared area of the epicenter of the injury was calculated by measuring the GFAP(+) area in each spinal section outline area.

Statistical analyses

All the quantitative data are presented as means ± the standard error of the mean (SEM). Statistical analyses were conducted by using SPSS software (Version 18, IBM SPSS, Inc.). Differences were considered as significant at *P* values below 0.05.

Results

Spastic behaviors during swimming: clonus phase and spastic phase

Uninjured rats showed rapid and clear reciprocal activity of TA and MG muscle during swimming runs (**Fig. 1-1B**). After the mid-thoracic SCI, the injured rats were almost entirely dependent on their forelimbs during swimming. However, they occasionally used their hindlimbs in normal reciprocal strokes but with a slower cycle (< 2 Hz) compared to uninjured rats (4–5 Hz). During the normal strokes, the injured rats had clear reciprocal muscular activations in their hindlimbs, although some portions of the EMG pattern were overlapping (**Fig. 1-1C**). I defined normal and reciprocal activation of the hindlimbs as the "normal stroke phase" for EMG comparisons. After at least 3 weeks of SCI, the injured rats had typical symptoms of spasticity during swimming. These symptoms were referred to as the "clonus phase" or the "spastic phase". The clonus phase presented as rapid (5–8 Hz) jerking movements of either one or both legs during swimming. During this phase, simultaneously recorded EMGs showed reciprocal, high intensity bursts of TA and MG muscle activity (**Fig 1-1C and 1-2A**). It is notable that the clonus phase was often observed immediately after the rats stretched or contracted their hindlimbs. The spastic phase typically presented as a ventro-flexed trunk posture with stretched hind limbs during swimming (**Fig. 1-1C**). A common feature of the spastic phase was the extended hindlimb posture, which was represented by co-contraction patterns and high bursts of the TA and MG muscle activity. The spastic behaviors, which were divided into the clonus phase and the spastic phase, were observed either simultaneously or independently within a single swimming run and were easily verified during the swimming test. Given that some of the common spastic symptoms observed after SCI include hyperreflexia, clonus, hypertonus of the muscles, and muscular spasm in both human patients and animal

models [39,90], I postulated that the clonus phase and the spastic phase observed during swimming represent the spastic symptoms of contusive SCI rats. The mean amplitude of muscle activity during the spastic phase in SCI rats was significantly higher than that during the normal stroke phase of both SCI and uninjured rats (n = 4 for uninjured rats, n = 5 for SCI rats, one-way ANOVA with Tukey's post-hoc test; **Fig. 1-2A**). In summary, the symptoms of spasticity in the contusive SCI rat model were observed during the swimming test.

The swimming test can be used to classify SCI rats according to frequency of spastic behaviors

In the swimming experiment, I calculated the frequency of spastic behavior. The histogram of the occurrence frequency indicates the existence of two groups based on spastic behavior (n = 50 SCI rats; **Fig. 1-2B**). Because the groups were apparently divided based on 40% frequency, I used a cut-off of 40% (i.e., 4 or more "spasticity-positive" runs among the 10 swimming runs) as the criterion for grouping SCI rats into the "spasticity-strong group." The other SCI rats were grouped into the "spasticity-weak group".

Three weeks after SCI, over 50% of the SCI rats were placed in the spasticity-strong group. However, some of the SCI rats in the spasticity-weak group were subsequently classified in the spasticity-strong group 4 weeks after SCI. The percentage of rats in the spasticity-strong group reached a plateau 4 to 5 weeks after SCI (n = 36 tested SCI rats, **Fig. 1-2C**). The spared tissue area of the epicenter of the injured site, which was measured by staining for GFAP at 6 weeks after SCI, was not significantly different between the two groups (n = 5 per group, P = 0.787, Student's two-tailed *t*-test; **Fig. 1-2D**). These results indicate that the SCI rats can be grouped according to severity based on the occurrence frequency of spastic behaviors, including the clonus phase and the spastic phase, during the swimming test.

Spasticity during the swimming test was consistent and reproducible

To determine whether the occurrence of spastic behaviors and the amplitude of muscle activity of each rat change over time, I performed the swimming tests weekly from 4 to 6 weeks after SCI. In the spasticity-strong group, the occurrence frequency of clonus and spastic phases during the 10 swimming runs was not significantly different from 3 weeks to 6 weeks after SCI (n = 10, $P = 0.499$, one-way ANOVA with Tukey's post-hoc test; **Fig. 1-3A**). Furthermore, the mean amplitude of muscle activity during spasticity did not differ significantly between test periods in the spasticity-strong group (n = 6, $P = 0.119$ for TA, $P = 0.846$ for MG, Kruskal-Wallis H-test; **Fig. 1-3B**). These results suggest that the occurrence frequency of spastic behaviors and the amplitude of muscle activity tend to be consistent during the time course, at least over the observation period.

The spasticity-strong group had more hyperexcitability of the spinal reflex circuit

To examine differences in the hyperexcitability of the monosynaptic lumbar spinal circuit between the spasticity-strong and spasticity-weak groups, the rate-dependent depression (RDD) of the Hoffman reflex, was obtained 6 weeks after SCI (**Fig. 1-4A** and **1-4B**). The Hoffman reflex (H-reflex) test is a standard tool for evaluating spasticity based on the activities of alpha motor neurons in animal models and human patients[87,91,92]. The M-wave is not changed upon a RDD of the H-reflex test because it is the output of direct stimulation of motor neuronal axon. On the other hand, in the normal condition, the H-wave is altered by different stimulation rates since it is the monosynaptic reflex wave via afferent Ia sensory fibers and spinal motor neurons.

As shown in **Fig. 1-4B** and **Fig. 1-5A**, the M-wave remained unchanged after the stimulation frequency was applied (n = 7–8 per group, two-way ANOVA with Bonferroni's post-hoc correction). The RDD of the H-wave for all SCI rats, including both spasticity-strong and spasticity-weak groups, was significantly less depressed than that of uninjured rats at stimulation frequencies of 2 Hz and 5 Hz, respectively (n = 7 for uninjured rats, n = 15 for SCI rats, two-way ANOVA with Bonferroni's post-hoc correction; **Fig. 1-4B** and **1-5B**). The RDD of the spasticity-strong group was significantly more decreased than that of the spasticity-weak group at the stimulation frequency of 5 Hz. Furthermore, only the spasticity-strong group had statistically significant differences at stimulation frequencies of 1 Hz, 2 Hz, and 5 Hz compared to the uninjured group (n = 7–8 per group, two-way ANOVA with Bonferroni's post-hoc correction; **Fig. 1-5C**). These results suggest that the spasticity-strong group of SCI rats had more hyperexcitability of the lumbar circuit than the spasticity-weak group, which is consistent with the results of the behavioral screening performed during the swimming test.

The spasticity-strong group has more up-regulated serotonin receptor expression in spinal motor neurons

To determine whether 5-HT and its receptor influence the variation between the spasticity groups, I examined serotonin (5-HT) fibers and 5-HT_{2A} receptors in both upper (cervical) and lower (lumbar) spinal regions based on a report by Kong et al. [63], who showed that expression of the serotonin 2A receptor was robustly increased after spinal cord transection in a rat model. Consistent with previous reports, the IR of the 5-HT_{2A} receptor was greatly upregulated in the region below the epicenter of the spinal cord after SCI (**Fig. 1-6A**). Furthermore, expression of the 5-HT_{2A} receptor in the lumbar motor neurons of the spasticity-strong group was significantly more upregulated compared to that of the spasticity-weak group (n = 5–6 per

group, $P < 0.001$, one-way ANOVA with Bonferroni's post-hoc correction; **Fig. 1-6B**). Conversely, the positive area of the 5-HT fibers in the ventral horn of the lumbar spinal cord was significantly reduced after SCI when compared to that of the uninjured rats. The 5-HT-positive area in the spasticity-strong group was also decreased when compared to that of the spasticity-weak group. However, this difference was not statistically significant (n = 5–6 per group, $P > 0.05$, one-way ANOVA with Bonferroni's post-hoc correction; **Fig. 1-6C** and **1-6D**). The IR areas of 5-HT_{2A} receptors and 5-HT fibers in the ventral horn of the cervical spinal cord did not show any significant differences between groups (n = 5–6 per group, $P = 0.141$ for 5-HT_{2A} receptor and $P = 0.264$ for 5-HT fibers, one-way ANOVA; **Fig. 1-6C** and **1-6D**). Plots of reserved 5-HT fibers and expression patterns of the 5-HT_{2A} receptor in each animal suggest the presence of a strong relationship between the reserved 5-HT fiber area and 5-HT_{2A} receptor density in the lumbar spinal cord ($r^2 = 0.602$, $p = 0.001$, logarithmic regression analysis; **Fig. 1-6E**). The plot in **Fig. 1-6E** also shows that uninjured rats have high 5-HT/5-HT_{2A} receptor ratios, while spasticity-strong rats have low 5-HT/5-HT_{2A} receptor ratios and spasticity-weak rats have intermediate ratios. These results indicate that the altered 5-HT/5-HT_{2A} receptor ratio in the lumbar spinal cord may correlate with the frequency of spastic behaviors observed in the swimming test.

Types and occurrence of spastic behaviors during the 20-hour observation period confirm the results of the swimming test

To examine the correlation between spastic symptoms observed in the swimming test (**Fig. 1-1A**) and spastic behaviors under free-moving conditions on the ground, I conducted EMG recordings of the same SCI rats, which were tested and grouped using the swimming test, over 20 hours. The recordings were synchronized with video capture during normal behavior in a housing cage. Four weeks after SCI, the SCI rats had an episodic EMG pattern corresponding to a clonus or spasm episode in a cage situation (**Fig. 1-7A**). Clonus during cage observations occurred episodically and was spontaneously accompanied by long-term (over 3 seconds based on the EMG recordings) reciprocal bursts of TA and MG muscle activity and abnormal motions, such as whirling of the tail. Spasms during the cage observations also occurred spontaneously with hyper-stretched limbs or hyper-contracted limbs, even when the rats were apparently sleeping or resting. The EMG patterns of the spasms during cage observations were represented by simultaneous and extensive bursts of TA and MG muscle activities. Since the muscle activities obtained during continuous gaits in the injured rats could not be assessed under normal cage conditions, I obtained a baseline amplitude for the gait on the treadmill. The mean amplitude of spastic muscle activity during the cage observations was significantly higher than that observed over 10 gait cycles on a body weight-supported treadmill in the same rats (n = 5, $P = 0.023$ for TA and $P = 0.002$ for MG, Student's two-tailed *t*-test; **Fig. 1-7B**). The spasticity-strong group, which was assigned based on the results of the swimming test, had significantly more spasm and clonus episodes than the spasticity-weak group during the 20-hour observation period (n = 5 per group, $P = 0.021$ for spasm, $P = 0.037$ for clonus and $P = 0.022$ for total, Student's two-tailed *t*-test; **Fig. 1-7C**). Uninjured rats did not have any spasm or clonus episodes during the 20-hour observation period (n = 3). The average counted number of spasm and clonus episodes peaked in the early morning (08:00–09:00) and early evening (17:00–19:00) (n = 5 per group; **Fig. 1-7D**), which is consistent with other reports regarding the spastic symptoms of rats and humans [86,93]. These results indicate

that the spasticity-strong group of SCI rats had more severe spasticity symptom than the spasticity-weak group during cage observation as well as during the swimming test.

Discussion

I observed spastic behaviors during a swimming test in contusive SCI rats. The spastic behavior consisted of clonus and spastic phases. These behaviors were easily reproducible and detectable, and could be readily quantified based on occurrence frequency. In addition, the swimming test could discriminate SCI rats with different severities of spasticity. I used this test to classify the rats into the spasticity-strong group and the spasticity-weak group based on the occurrence frequency of the spastic behaviors. Moreover, I confirmed the feasibility of this grouping using the H-reflex test, immunohistochemistry for the 5-HT receptor, and the 20-hour cage observations. All measures consistently showed that the spasticity-strong group, which was assigned based on the swimming test, had more severe changes related to upper motor neuron syndrome compared to the spasticity-weak group. Furthermore, the percentage of SCI rats that were placed in the spasticity-strong group and the time course of spasticity after SCI are largely consistent with the results of a previous study using an incomplete transection rat model[86]. Therefore, the swimming test results reflect the severity of upper motor neuron syndrome, at least to some extent.

While I observed variations in severity among the spasticity-strong and spasticity-weak groups in the swimming test, I assume that the division into the two groups is reliable based on the results of multiple other modalities. Considering that incomplete SCI results in various degrees of spasticity[40,44,45], it is important to obtain homogenous experimental groups for SCI research. I thus suggest that the swimming test is a useful screening tool for incomplete SCI models.

I tested the hyperexcitability of the lumbar spinal circuit using the H-reflex test, which is a standard method of measuring hyperreflexia in both humans and animal models[57,69,81,94]. I

found that the spasticity-strong group had lower RDDs in the H-reflex, as well as increased expression of the 5-HT_{2A} receptor in the lumbar spinal motor neurons compared with the spasticity-weak group. Overexpression of the 5-HT receptor causes hypersensitivity to 5-HT, which is related to spasticity[62]. Therefore, I expected that such hypersensitivity to 5-HT, caused by the overexpression of 5-HT receptors, may be the primary reason for the reduced RDD in the spasticity-strong group.

Hypersensitivity of 5-HT and up-regulation of 5-HT receptors below the injury site after SCI have previously been reported to be related to the hyperexcitability of spinal motor neurons and consequent spasticity[55,56,58,60,61,95]. It is known that several types of 5-HT2 receptors, such as 5-HT_{2A}, 5-HT_{2B}, and 5-HT_{2C}, are closely related to the hyperexcitability of motor neurons after SCI[58]. However, immunohistochemical studies have clearly shown robust elevation of the 5-HT_{2A} receptor after SCI and reported the upregulation of mRNA for this receptor[63,96]. Therefore, I selected the 5-HT_{2A} receptor as a representative serotonin receptor that is mainly expressed in spinal motor neurons for the present immunohistochemistry analysis[63,97]. My results indicate a correlation between the degree of 5-HT hypersensitivity and the severity of spasticity given the same severity of SCI.

During the 20-hour cage observations, I noted some spasticity-related behaviors in the "spasticity-weak" rats. Nevertheless, the total occurrence of spasm and clonus episodes was significantly lower in this group than in the spasticity-strong group. Therefore, my results suggest that the severity of spasticity in a contusive SCI rat model may be reflected by the occurrence frequency of spastic behaviors.

My assessment using behavioral features may not directly reflect velocity-dependent muscle rigidity, which is the classical criterion for spasticity[37]. It should be noted that there are other established assays that use ankle-rotation evoked EMG responses[51,52]. Nevertheless, according to my EMG and H-reflex results, the behavioral patterns of the SCI rats during the

swimming test correspond well to patterns of spastic symptoms observed in human patients with respect to 1) muscle spasms, 2) clonus, 3) co-contraction of the muscles, and 4) hypertonia and hyperreflexia. Therefore, the swimming test is able to show direct manifestations of clinically relevant symptoms of spasticity and may be useful for subsequent behavioral assessments. This test provides an advantage in prospective design by defining homogenous samples.

In this chapter, my study has several limitations. First, the correlation of spastic behavior frequency during the swimming test and the H reflex test was not perfectly matched as a linear correlation. Despite this limitation, I believe that the swimming test is useful for screening incomplete SCI rats to obtain more homogenous experimental groups. Second, spastic behaviors during the swimming test may not be able to be used to discriminate between voluntary attempts and involuntary movements. However, I found that those behaviors were unique, which allowed us to distinguish between the spasticity-strong and spasticity-weak groups. Furthermore, the behavioral assessment has the advantages of ease and repeatability for longitudinal experiments.

In summary, my results suggest that quantification and screening of spasticity in contusive SCI rats is possible by measuring the occurrence frequency of spastic behaviors during a swimming test. These results present that swimming test may help to discriminate spasticity-weak rats from spasticity-strong rats after SCI. Also, the expression of 5-HT_{2A} receptor is connected to the severity of spasticity during a swimming test. Taken together, my findings suggest that the swimming test is an effective method for evaluating symptoms of spasticity and developing treatments targeting spasticity after SCI.

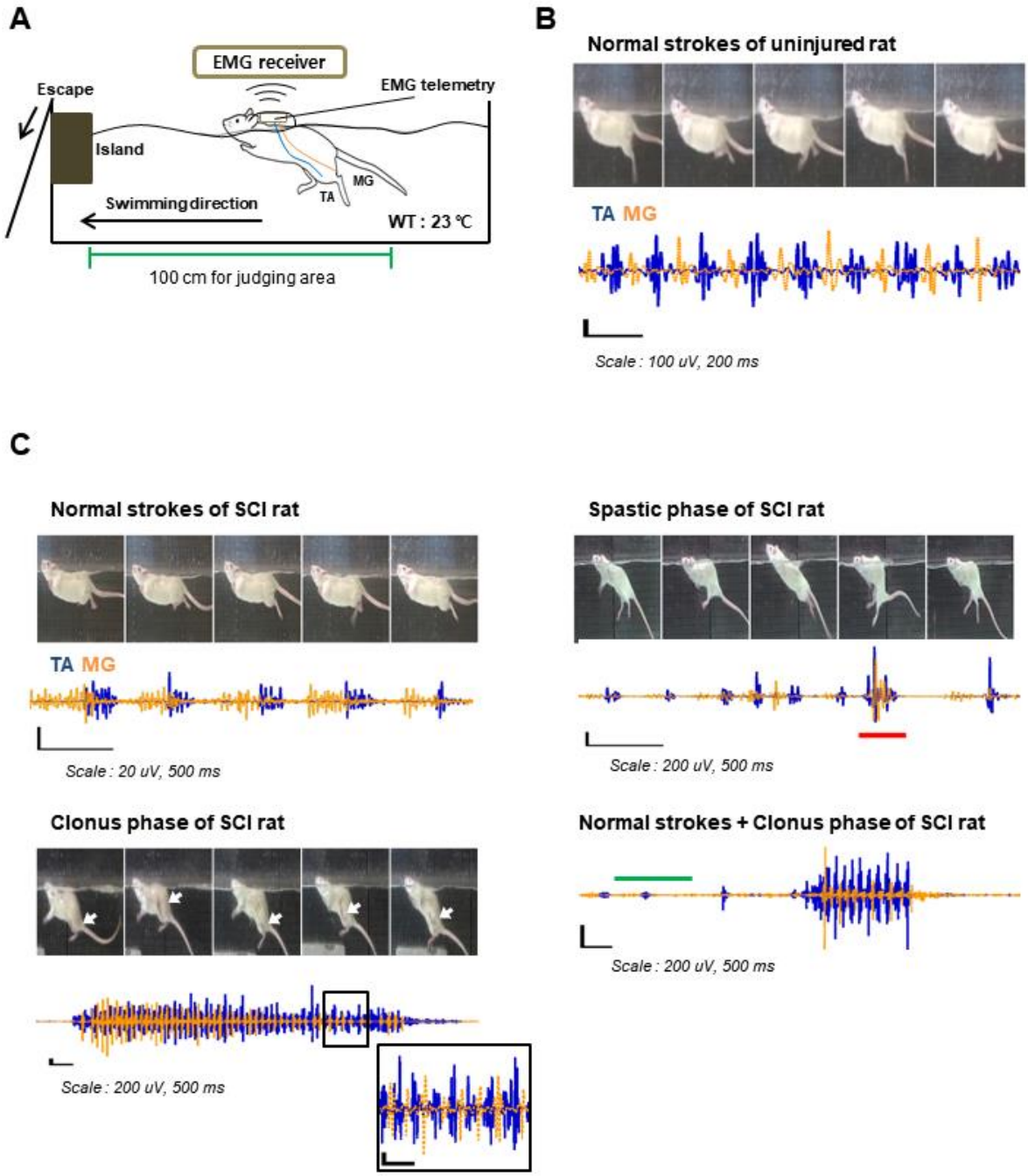
A
EMG receiver
Escape
EMG telemetry
Island
MG
TA
Swimming direction
WT : 23 ℃
100 cm for judging area
B
Normal strokes of uninjured rat
TA MG
Scale : 100 uV, 200 ms
C
Normal strokes of SCI rat
TA MG
Scale : 20 uV, 500 ms
Spastic phase of SCI rat
Scale : 200 uV, 500 ms
Clonus phase of SCI rat
Scale : 200 uV, 500 ms
Normal strokes + Clonus phase of SCI rat
Scale : 200 uV, 500 ms

Figure 1-1. Experimental circumstance and types of spastic behaviors during the swimming test

(**A**) Configuration of the EMG recording device during the swimming test. (**B**) Representative sequential captured images and corresponding recorded muscle activity of the left TA (blue) and the left MG (orange) muscle of an uninjured rat during a swimming run. (**C**) Representative sequential captured images and corresponding recorded muscle activity of the left TA (blue) and the left MG (orange) muscle of SCI rats during the swimming tests showing each type of spasticity (the clonus phase and spastic phase). The black box represents a magnified image of the recorded EMG. The red bar on the recorded EMG of the spastic phase indicates co-contraction of the TA and MG muscles. The green bar on the bottom image corresponds to the normal reciprocal stroke phase. White arrows indicate the location of the hind paw of the rat during the clonus phase. Note that all EMG figures were normalized to the peak amplitudes of TA muscle activity.

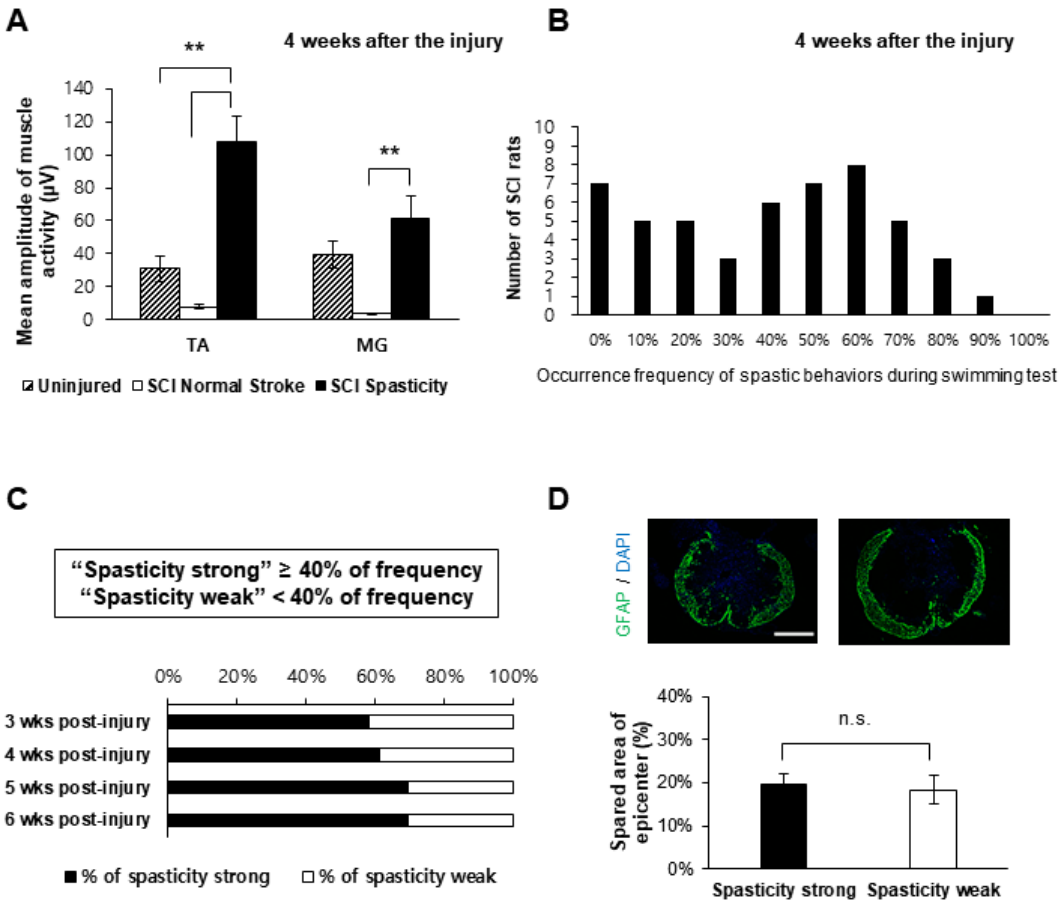

Figure 1-2. Occurrence frequency of spastic behaviors during the swimming test varies among the SCI rats

(**A**) Mean amplitude of recorded muscle activity during spastic behaviors (SCI spasticity; black bar) compared with the mean amplitude of muscle activity during normal reciprocal strokes (SCI normal stroke; white bar) of SCI rats and uninjured rats (Uninjured; dashed bar) at 4 weeks after SCI. (**B**) The number of the SCI rats with each occurrence frequency of spastic behaviors during swimming test at 4weeks after the injury. (**C**) Percentage of the spasticity-strong rats from 3 to 6 weeks after SCI. Injured rats were classified as "spasticity-strong" if they showed the occurrence frequency over 40% during the swimming test. (**D**) Average percentage of the spared area of the epicenter of the injury measured by the GFAP (+) area after SCI in the spasticity-strong group and -weak group. **, $P < 0.01$, n.s., not significant.

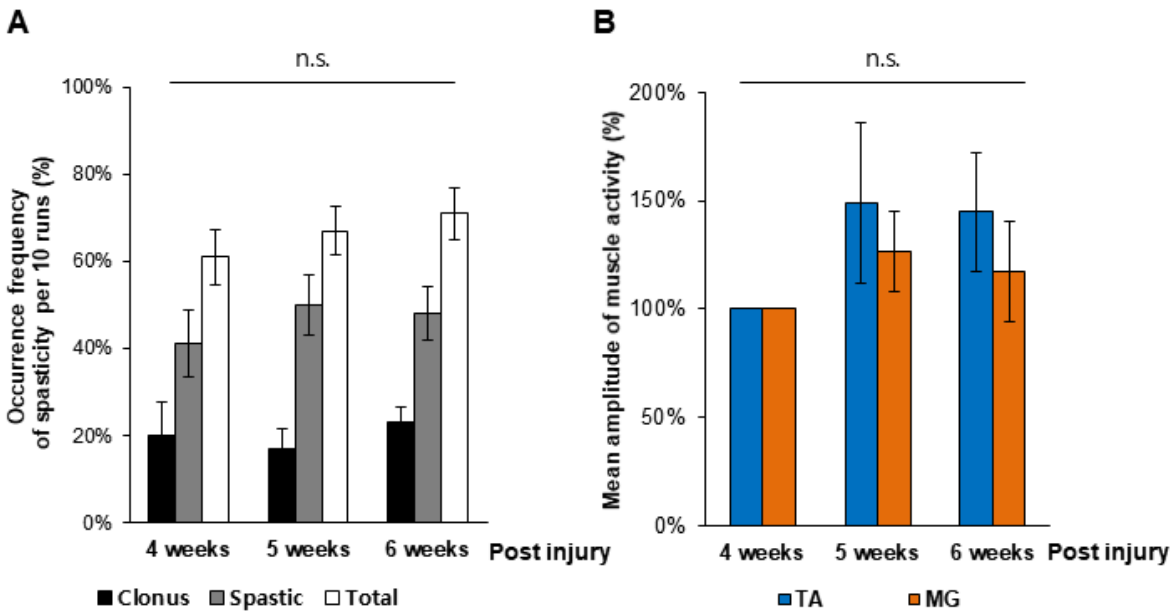

Figure 1-3. The occurrence frequencies of spastic behaviors and corresponding amplitudes of muscle activity during the test period

(**A**) The occurrence frequency and percentage of each type of spasticity observed in the spasticity-strong group during the swimming tests from 4 to 6 weeks after SCI (clonus, black bars; spastic, grey bars; total, white bars). (**B**) The mean amplitude of muscle activity of spastic behaviors in the spasticity-strong group during the swimming test from 4 to 6 weeks after SCI recorded from the left TA muscle (blue) and the left MG muscle (orange). Mean amplitudes of muscle activity at 4 weeks were considered to be 100%. n.s., not significant.

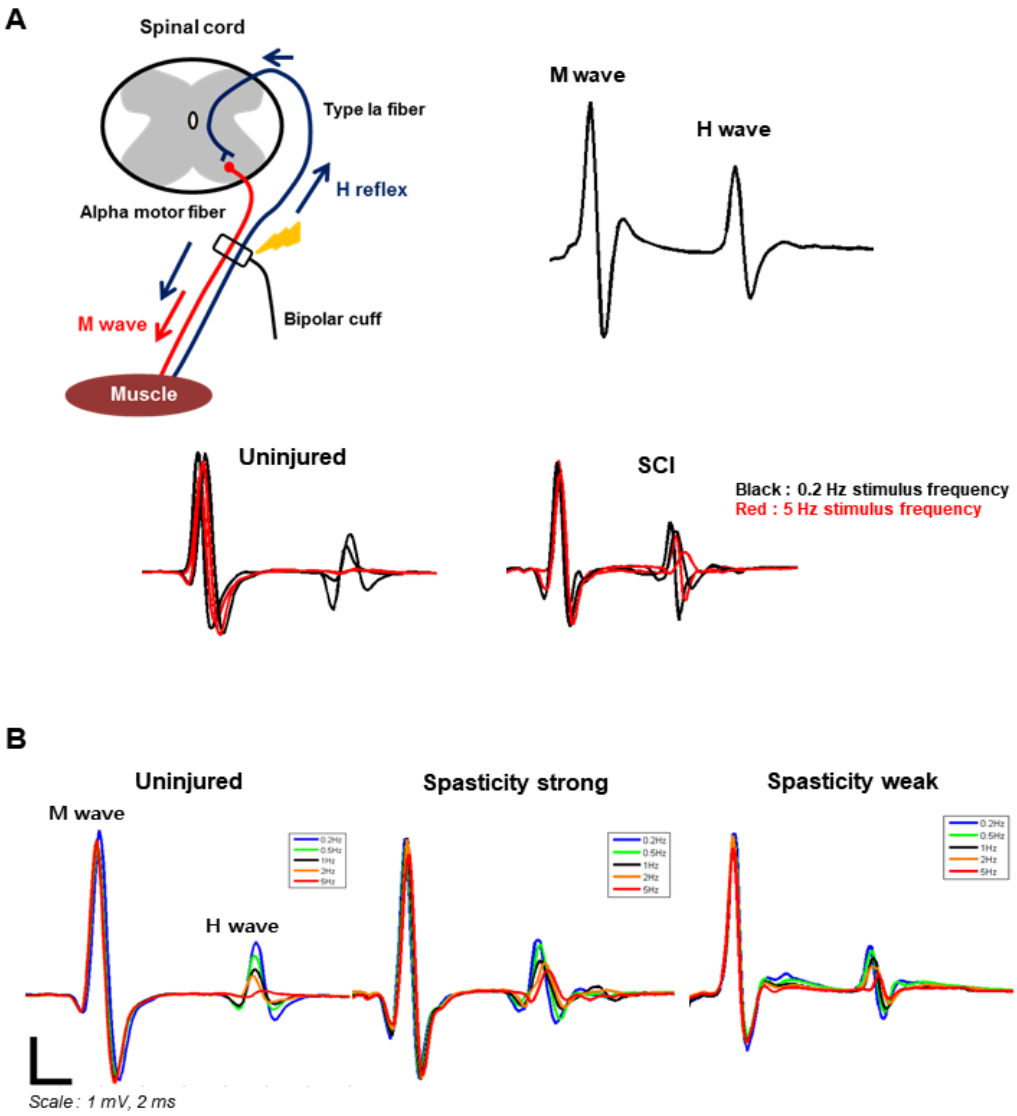

Figure 1-4. Rate-dependent depression (RDD) of the H-wave reflects the excitability of spinal reflex

(**A**) Schematic illustration of the Hoffmann reflex (H-reflex) test and representative M and H waveforms are presented (right). The H wave in SCI rats was depressed when stimulated with a high frequency (5 Hz, red line; right, bottom), compared to the uninjured rats (left, bottom). (**B**) Representative H-reflex waveforms of uninjured, spasticity-strong, and -weak groups were shown. Different colors indicate different stimulation frequency: 0.2 Hz (blue), 0.5 Hz (Green), 1 Hz (Black), 2 Hz (orange), and 5 Hz (red).

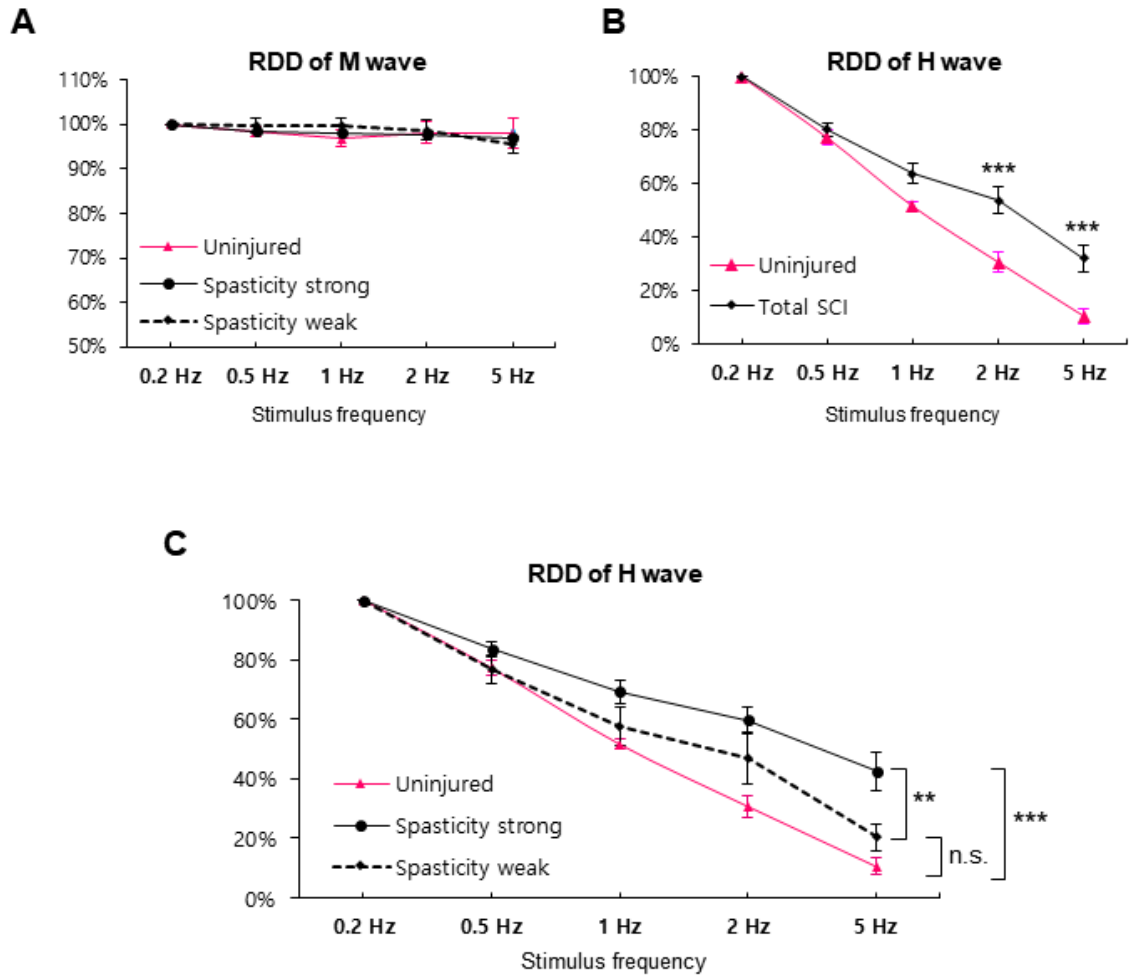

Figure 1-5. SCI rats show spinal hyperreflexia, in which the spasticity strong group present more decreased RDD

(**A**) Rate-dependent depression (RDD) of the M-wave is shown. The mean amplitude at 0.2-Hz stimulation was set to the baseline amplitude as 100%. Uninjured (magenta line), spasticity-strong group (solid black line), -weak group (black-dashed line). (**B**) RDD of H-wave in the uninjured (magenta line) and total SCI group (black; includes spasticity-strong and -weak rats). (**C**) Comparison of the RDD values of the H-wave between groups. The RDD of the spasticity-strong group (solid black line), -weak group (black-dashed line), and uninjured rats (magenta line). **, $P < 0.01$, ***, $P \leq 0.001$.

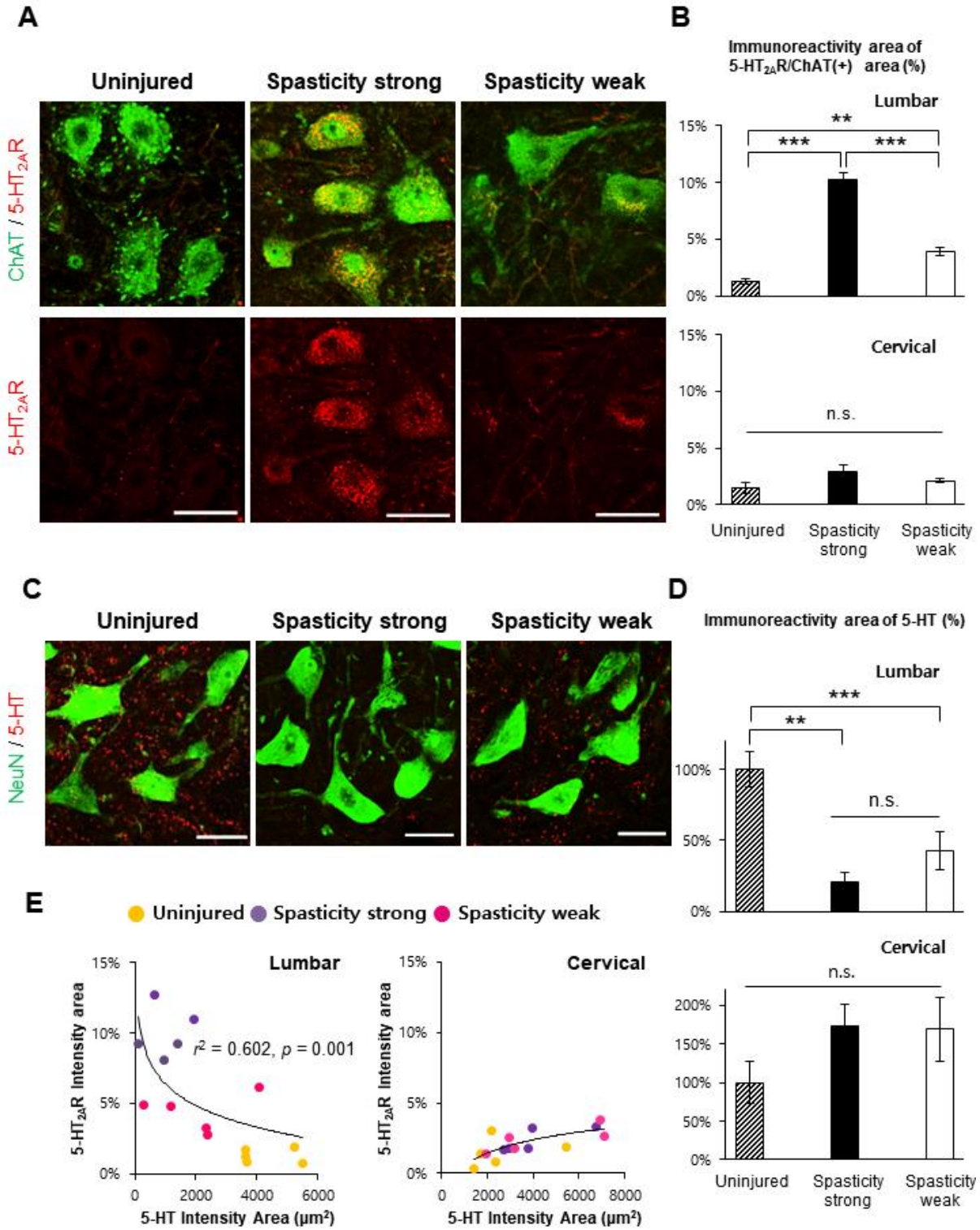
A
Uninjured
Spasticity strong
Spasticity weak
ChAT / 5-HT2AR
5-HT2AR
B
Immunoreactivity area of 5-HT2AR/ChAT(+) area (%)
Lumbar
**
***
***
15%
10%
5%
0%
Cervical
n.s.
Uninjured
Spasticity strong
Spasticity weak
C
Uninjured
Spasticity strong
Spasticity weak
NeuN / 5-HT
D
Immunoreactivity area of 5-HT (%)
Lumbar
***
**
n.s.
100%
50%
0%
Cervical
n.s.
200%
150%
100%
50%
0%
Uninjured
Spasticity strong
Spasticity weak
E
Uninjured
Spasticity strong
Spasticity weak
Lumbar
Cervical
5-HT2AR Intensity area
15%
10%
5%
0%
r2 = 0.602, p = 0.001
0
2000
4000
6000
8000
5-HT Intensity Area (μm2)

Figure 1-6. Immunohistochemistry and quantification of 5-HT$_{2A}$ receptor and 5-HT in SCI groups and uninjured rats indicate the imbalance of 5-HT system after SCI

(**A**) Robust up-regulation of the 5-HT$_{2A}$ receptor (5-HT$_{2A}$R) at the lumbar motor neurons of the spasticity-strong group compared with the -weak group and uninjured group (scale bars: 50 μm). (**B**) Quantification of the 5-HT$_{2A}$ receptor-positive (+) area within spinal motor neurons labeled as ChAT positive (+) at both the cervical region and the lumbar region (uninjured group, dashed bars; spasticity-strong group, black bars; spasticity-weak group, white bars). (**C**) The 5-HT fibers were almost completely lost after 250-kd contusive SCI, but were more reduced at the spasticity-strong group (scale bars: 50 μm). (**D**) Quantification of the area of 5-HT fibers at both the cervical and the lumbar ventral horn region (uninjured group, dashed bars; spasticity-strong group, black bars; spasticity-weak group, white bars). Values were normalized considering the value for uninjured rats as 100%. (**E**) Plots of the quantification of 5-HT$_{2A}$ receptor expression and 5-HT fibers at the cervical and lumbar region, respectively in uninjured (yellow), spasticity-strong group (purple), and -weak group (magenta). **, $P < 0.01$, ***, $P < 0.001$, n.s., not significant.

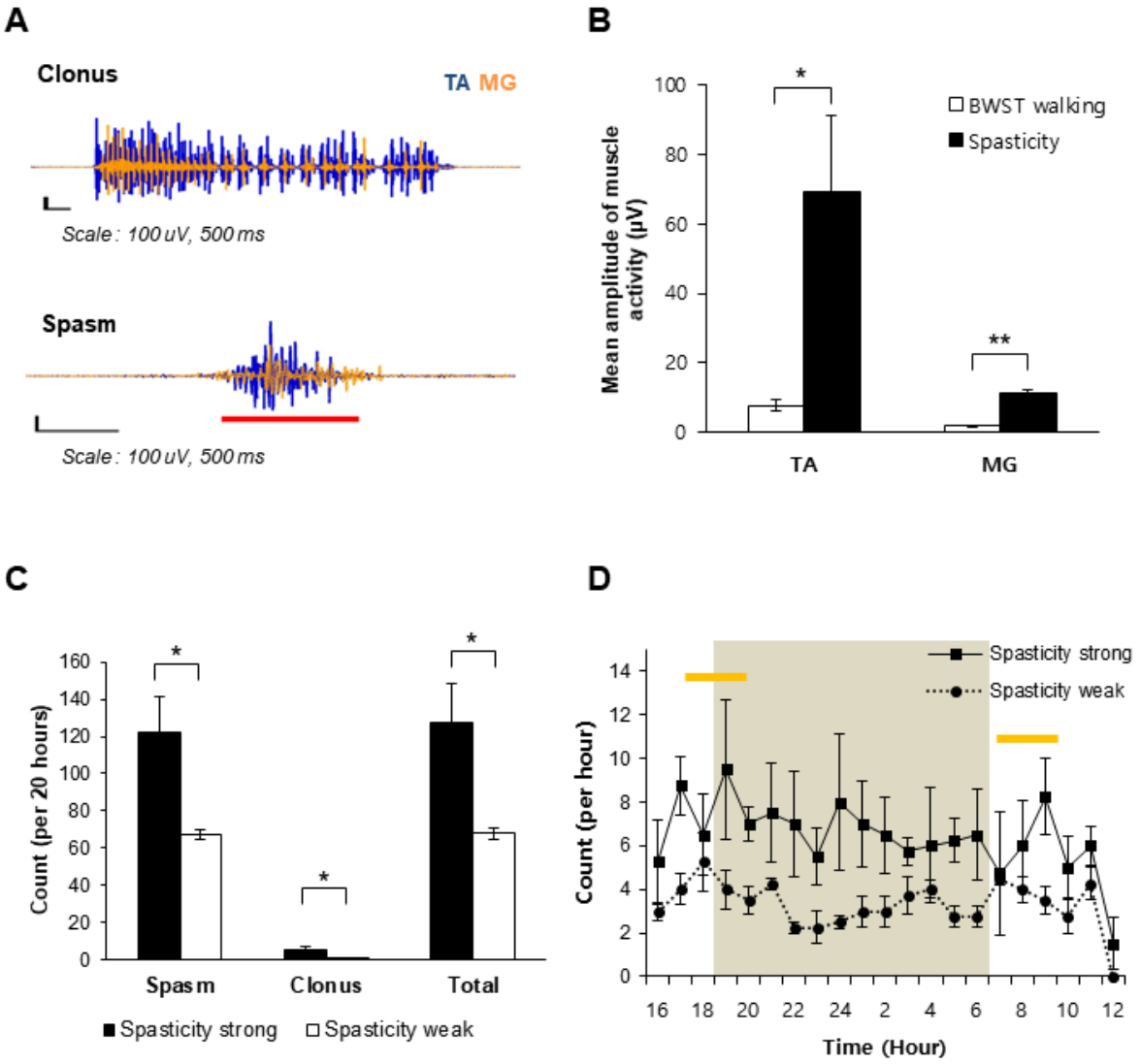
A
Clonus
TA MG
Scale : 100 uV, 500 ms
Spasm
Scale : 100 uV, 500 ms
B
Mean amplitude of muscle activity (μV)
BWST walking
Spasticity
TA
MG
C
Count (per 20 hours)
Spasm
Clonus
Total
Spasticity strong
Spasticity weak
D
Count (per hour)
Spasticity strong
Spasticity weak
Time (Hour)

Figure 1-7. EMG results and occurrence frequency of spastic behaviors during the 20-hour cage observation is consistent with the results of swimming test

(**A**) Recorded EMG results for the clonus and spasm in SCI rat during 20-hour cage observations obtained from the left TA muscle (blue) and the left MG muscle (orange). The red bar indicates co-contraction of the TA and MG muscle activities. Note that all EMG figures were normalized to the peak amplitudes of TA muscle activity. (**B**) Mean amplitude of muscle activity during spastic behaviors compared with the mean amplitude of muscle activity during 10 gait cycles on BWST 4 weeks after SCI. (**C**) The occurrence of each type of spastic behaviors during 20-hour cage observations in the spasticity-strong group (black bars) and -weak group (white bars) at 4 weeks after SCI. (**D**) The occurrence of spastic behaviors in the spasticity-strong group (solid black line) and -weak group (black-dashed line) shown by each recorded hour. The shaded area shows the default dark time (18:00 to 6:00) of the housing room. The yellow bars indicate the peak time points for the counted spastic behaviors. *, $P < 0.05$, **, $P < 0.01$.

Chapter 2.

Effects of physical training combined with serotonergic interventions on spasticity after contusive spinal cord injury

Introduction

Spasticity usually emerges during the course of recovery from spinal cord injury (SCI). Hyperactivity of spinal motor neurons due to the disconnection between the upper motor neuron and spinal motor neuron is crucial to the manifestation of spasticity[39,44]. Medication and physical therapy are often prescribed to treat spastic symptoms[25,41,46]. While oral drugs such as GABAnergic drugs are frequently used to correct the hyperactive state of spinal motor neurons, they have a limitation in controlling severe symptoms[47,49].

Hypersensitivity of the serotonin (5-hydroxytryptamine; 5-HT) receptor is considered to be crucial to the hyperactivity of spinal motor neurons[56,58,60]. The depletion of 5-HT from the descending tract is accompanied by the upregulation of the expression of its receptor on motor neurons, leading to both ligand-dependent and ligand-independent activation of the receptor[58,62,63]. Thus, 5-HT receptor antagonists, including cyproheptadine, have been studied for their ability to alleviate spastic symptoms[65,66]. The 5-HT functions can be also modified by selective serotonin re-uptake inhibitors (SSRIs), such as fluoxetine, which are well known for their role as antidepressants[98]. They achieve such effects by not only increasing the 5-HT concentration by blocking the 5-HT transporter, but also by decreasing the sensitivity of 5-HT_{1A} receptor[99]. Moreover, SSRIs desensitize other 5-HT receptors, including the 5-HT_{2A} receptor[100,101].

Recent studies on animal models and human subjects have also shown that physical training (*e.g.* treadmill training or cycling) after SCI restores the balance between excitatory and inhibitory functions of propriospinal neurons, which modulate spinal motor neurons, thereby alleviating spastic symptoms[67-69]. Clinically, treadmill training in patients with SCI is reported to reduce the spasticity in their lower limbs[24,70]. In order to potentiate the therapeutic

effects on spasticity, it would be desirable to administer combination therapy including medication and physical therapy, aiming for an additive or synergistic effect. However, rehabilitation programs with medication targeting spasticity have not been extensively examined in human or animal studies.

In the ***Chapter 1***, I determined that the severity of spastic symptoms in a rat model of SCI was correlated with the increase in the expression of 5-HT_{2A} receptor. Therefore, I assumed that drugs modulating the 5-HT system are promising candidates and combination therapy with physical training additively or synergistically suppress the spastic symptoms after SCI.

In this chapter, I examined the effects of combinatorial interventions that included the administration of a 5-HT receptor antagonist and a SSRI with or without treadmill training for targeting spasticity, using a rat model of contusive SCI with severe spasticity. My results will help in understanding the underlying mechanisms in the alleviation of spasticity following SCI and in the design of effective rehabilitation strategies.

Materials and methods

Animals

All the experiments were performed according to the guidelines of the ethics committee of the National Rehabilitation Center for Persons with Disabilities. A total of 64 adult female Sprague-Dawley rats (200 to 300 g, Charles river Japan, Yokohama) were used for the experiments. The animals were housed under a 12 h/12 h light cycle with controlled temperature (23-25°C). Food and water were supplied *ad libitum.*

Spinal cord injury

The animals were anesthetized with a combination of 2 mg/kg of midazolam (Sandoz), 2.5 mg/kg of butorphanol (Meiji Seika, Japan), and 0.15 mg/kg of medetomidine (Kyoritsu Seiyaku, Japan) via intraperitoneal injection (i.p.). After anesthesia, rats were received a thoracic laminectomy, and then, a 250-kilodyne (kd) contusive injury at the 8th thoracic vertebral level with an Infinite Horizon impactor device (Precision Systems and Instrumentation, VA, USA). After the surgery, the injured rats were administered a single shot of antibiotic (Baytril, 5 mg/kg, SC, Bayer). Manual bladder expression was performed twice a day until the injured rats were able to urinate themselves.

Swimming test and behavior scoring

Swimming tests were performed at 4 weeks, and the rats were divided into two groups, namely spasticity-strong and spasticity-weak groups, based on their score of the swimming test as shown in the ***Chapter 1*** (‘Pre-test’ shown in **Fig. 2-1A**). To examine clearly the effects of the interventions on spasticity, only spasticity-strong rats were used in this chapter. The

spasticity-strong rats were randomly divided into six groups, and conducted interventions including treadmill training (hereafter referred to as TMT in this chapter), TMT with fluoxetine (a SSRI), TMT with cyproheptadine (a 5-HT_2 receptor antagonist), only fluoxetine, and only cyproheptadine (n = 5 to 6 per group) for 2 weeks as shown in **Fig. 2-1A**. The non-intervention group was used as a control (n = 10). While the rats were given the therapeutic intervention, the percentage of spasticity-positive runs in the 10 runs of swimming was calculated at 5 and 6 weeks after SCI ('1st test' and '2nd test' shown in **Fig. 2-1A**).

According to the Basso, Beattie, and Bresnahan (BBB) locomotor score[102], I scored the hind limb function of injured rats in each group at weekly intervals after a SCI. The rats were scored while moving freely on a table within 4-min assessment periods.

Treadmill training and serotonergic interventions

The rats were trained on the treadmill (7 m/min, 30 min/d; Robomedica, Inc., CA, USA) with a body weight support starting 4 weeks after the SCI (the end of the pre-swimming test) for 2 weeks. The animals were given a harness that was connected to a part of the treadmill apparatus for supporting their body weight. The level of counterweight for body weight support was adjusted to 50 to 70% of the body weight of the animals so that rats could perform a plantar placement of their hindlimbs. Next, the injured rats were trained in a quadrupedal position. Usually, the injured rats can continue planter stepping without any assistance. When the rats exhibited dorsal stepping or dragging of their hindlimbs, the researchers manually re-positioned the animals, temporarily supported their belly, or adjusted their hindlimb (**Fig. 2-1B**).

Fluoxetine hydrochloride and cyproheptadine hydrochloride sesquihydrate were purchased from Sigma. Systemic administrations of fluoxetine (5 mg/kg, i.p.) or cyproheptadine (5 mg/kg, i.p.) were given daily for 14 days from the 4 weeks after the injury

(**Fig. 2-1A**). Drugs were administrated once a day after the treadmill training or swimming test. Drugs were not administered in a blinded manner.

Hoffmann reflex (H-reflex) recording

The Hoffmann reflex (H-reflex) was measured and the rate dependent depression (RDD) of H-reflex was determined as described in the ***Chapter 1*** at 6 weeks after SCI, while the animals were under chloral hydrate anesthesia (2.5 g/kg, i.p., Sigma). The rate-dependent changes at each stimulation frequency were calculated as a percentage of the response at 0.2 Hz. Data from the H-reflex recordings were calculated and analyzed using the Spike2 (CED, Cambridge, England) software.

Immunohistochemistry

Six weeks after SCI, the rats were deeply anesthetized with sodium pentobarbital and transcardially fixed with a 4% paraformaldehyde (PFA) solution. The lumbar spinal cord (L4–L6) was collected and 20-μm-thick cryosections were prepared as described in the ***Chapter 1***. The tissue sections were incubated with diluted primary antibodies (goat-anti choline acetyltransferase, 1:100, EMD Millipore, #AB144P; rabbit-anti serotonin 2A receptor, 1:200, Calbiochem, #PC176; mouse-anti synaptophysin, 1:100, Abcam, #ab8049; rabbit-anti serotonin transporter, 1:1000, Calbiochem, #PC177L) overnight. The sections were incubated with fluorescent secondary antibodies (Alexa Fluor 488 and 568 for each species-matched types, 1:200, Life Technologies) and DAPI (1:1,000, Sigma) for 2 h on the next day. The images were acquired on a BZ-9000 HS all-in-one fluorescence microscope (KEYENCE BZ-9000).

The area of immunoreactivity was measured using the Image J software (National Institutes of Health, USA). The 5-HT_{2A} receptor (5-HT_{2A}R) levels were measured according to the methods described in the ***Chapter 1***.

To investigate the effect of various interventions on the synapse, the number of synaptophysin puncta[106] were counted from 15 spinal motor neurons in the ventral horn of the lumbar spinal cord per animal. Also, the immunoreactivity of serotonin transporter (SERT) in the ventral horn of the lumbar spinal cord was measured for examining the changes in the pre-synaptic 5-HT system[107,108], using the same method as for measuring 5-HT_{2A} receptor immunoreactivity. I analyzed SERT immunoreactivity using 3 tissue sections per animal.

Statistical analysis

The data were compared using a one-way or two-way analysis of variance (ANOVA) with post-hoc Bonferroni test or Tukey honest significance difference (HSD) test for correction of multiple comparisons. I used Kruskal-Wallis H test to analyze BBB scores. All the statistical analyses were performed using the SPSS software (Version 18, IBM SPSS, Inc.). The error bars represent the standard error of the mean (S.E.M). Results with $p < 0.05$ were considered statistically significant.

Results

Treadmill training and the 5-HT receptor antagonist reduced spastic behavior during the swimming test

Since the variation of severity of spasticity after SCI was observed as described in the ***Chapter 1***, first, I screened 'spasticity-strong' SCI rats to examine the effect of interventions more reliable and selective for targeting spasticity. Therefore, totally, 58% of the SCI animals (n = 37) were assigned to the spasticity-strong group and used for further experiments.

I also performed weekly swimming tests to evaluate the occurrence frequency of spastic behavior during 10 swimming runs after SCI. The occurrence frequency of spastic behaviors slightly decreased in the TMT group, and significantly decreased from the baseline in the cyproheptadine-alone and TMT with cyproheptadine groups after 2 weeks of intervention (P = 0.0355 and P = 0.0481 relatively, one-way ANOVA with post-hoc Tukey HSD test; **Fig. 2-2A**). However, I found that fluoxetine increased the occurrence frequency of spastic behavior during the swimming test, whether or not it was administered in combination with TMT (**Fig. 2-2A** and **2-2B**). At the end of the 2-week-long interventions, the TMT, TMT with cyproheptadine, and only cyproheptadine groups showed significantly lower occurrence frequency of spastic behaviors, compared to the control group (P = 0.011, two-way ANOVA with post-hoc Bonferroni test; **Fig. 2-2B**). These results are consistent with reports on the effects of 5-HT receptor antagonists or SSRIs on human patients with spasticity[66,103,104] and suggest that TMT and cyproheptadine are both effective in alleviating spasticity, while fluoxetine exacerbates these symptoms.

Treadmill training and the 5-HT receptor antagonist, but not the SSRI, increased the rate-dependent depression of the H-reflex

After the final swimming test, I tested the rate-dependent depression (RDD) of the Hoffman reflex (H-reflex). As shown in **Fig. 2-3A**, the M-wave remained unchanged after the stimulation frequency was applied.

Consistent with the results of the swimming test, the RDD values of the TMT, TMT with cyproheptadine, and cyproheptadine alone groups were significantly more increased in response to the stimulation frequency of 5 Hz than that of the control group, suggesting reduced spasticity in these three groups (n = 5 to 6 for each group, $P < 0.001$, one-way ANOVA with post-hoc Bonferroni test; **Fig. 2-3B**). On the contrary, the RDD values of the TMT with fluoxetine and fluoxetine only groups were lower than those of the other groups. At a stimulation frequency of 0.5 Hz, the TMT with cyproheptadine group presented significant differences compared with the other groups. As the changes in the RDD of the H-reflex are generally correlated with spasticity[51,105], these electrophysiological results corroborate the results of the swimming test.

Neither treadmill training nor serotonergic interventions altered locomotor functions

To determine whether TMT and serotonergic interventions affect behavioral functions, I assessed the open field hind limb motor score. Due to the severe contusive SCI, most rats could not walk with weight bearing at 4 weeks after the injury. While the animals received 2 weeks of TMT or combinatorial interventions with cyproheptadine or fluoxetine, I did not observe any significant differences between the experimental groups ($\chi 2(5) = 3.037$, $P = 0.694$, Kruskal-Wallis H test, n = 5 to 6 for each group; **Fig. 2-4**).

Change in immunoreactivity of the 5-HT receptor after 2 weeks of intervention

To examine the effects of interventions on histological changes in the spinal cord after SCI, I analyzed the expression of the 5-HT receptor in lumbar spinal cord motor neurons, which are considered to play a crucial role in the onset of spasticity and its severity. Consistent with the result of ***Chapter 1*** and a previous study[63], the immunoreactivity (IR) of the 5-HT_{2A} receptor in lumbar motor neurons 6 weeks after SCI was significantly higher than that in uninjured animals (**Fig. 2-5A** and **2-5B**). Following 2 weeks of interventions, the IR area of the 5-HT_{2A} receptor in lumbar motor neurons of the TMT and TMT with fluoxetine groups was significantly lower than in lumbar motor neurons of the control group. Furthermore, the IR area of the 5-HT_{2A} receptor in TMT groups with fluoxetine or cyproheptadine was significantly lower than that in the fluoxetine only or cyproheptadine only groups (n =5 for each group, $P < 0.001$, one-way ANOVA with post-hoc Bonferroni test; **Fig. 2-5B**). Despite the similarity of cyproheptadine and TMT in reducing spasticity, administration of cyproheptadine for 2 weeks did not change the IR area of the 5-HT_{2A} receptor. Among all the intervention groups, the TMT with fluoxetine group showed the lowest IR area of the 5-HT_{2A} receptor.

Alteration of 5-HT immunoreactivity in the lumbar spinal cord after the interventions

To identify changes in 5-HT signals in the spinal cord following various interventions, I stained the tissue against 5-HT. Six weeks after severe thoracic injury (250 kd), anti-5-HT signal in the ventral horn of the lumbar spinal cord was almost not reserved compared to the uninjured tissue sections (**Fig. 2-6A**). Aggregations of anti-5-HT signals adjunct to motor neurons were observed in the fluoxetine only group with or without TMT (yellow arrows in

Fig. 2-6A), although there were no prominent changes in 5-HT signals in the cyproheptadine groups. Furthermore, I found that 5-HT within the lumbar motor neurons was commonly observed in the lumbar spinal cord of rats in the TMT and TMT with fluoxetine groups (white arrows in **Fig. 2-6A**). To examine the interaction between 5-HT and its receptor, I stained samples with anti-5-HT and anti-5-HT_{2A} receptor antibodies. I observed co-immunostaining of 5-HT and 5-HT_{2A} receptor within spinal motor neurons. Thus, it is likely that TMT may induce internalization of 5-HT via its receptor (**Fig. 2-6B**).

Synaptic density and SERT immunoreactivity were unchanged in the lumbar spinal cord following intervention

To determine whether the interventions alter synaptic connectivity and serotonergic uptake system or not, I examined synaptophysin[106] and serotonin transporter (SERT)[107,108].

After SCI, the number of synaptophysin puncta of spinal motor neurons (ChAT positive neurons in the ventral horn of lumbar spinal cord) were significantly decreased ($F_{6,25} = 12.877$, $P < 0.001$, one-way ANOVA with post-hoc Bonferroni test, n = 3 to 4 for each group; **Fig. 2-7A** and **2-7B**). After 2 weeks of interventions, there were no significant differences of the number of synaptic puncta between groups ($P > 0.05$, Post-hoc Bonferroni comparisons; **Fig. 2-7B**). I found very little preservation of SERT immunoreactivity in the ventral horn area of the spinal cord in SCI tissue sections when compared with uninjured tissue sections ($F_{6,25} = 22.705$, $P < 0.001$, one-way ANOVA with post-hoc Bonferroni test, n = 3 to 4 for each group; **Fig. 2-7A** and **2-7C**). While there were no significant changes in SERT immunoreactivity following the interventions; there was a decrease in SERT immunoreactivity in the fluoxetine only group with or without TMT when compared with the other groups ($P > 0.05$, Post-hoc Bonferroni comparisons; **Fig. 2-7C**).

Discussion

In this chapter, I examined the effects of combination of physical training and pharmacological modification of the 5-HT system, using cyproheptadine as a 5-HT_2 receptor antagonist, and fluoxetine, an SSRI. I utilized a contusive SCI rat model, and used a swimming test for the screening method to select spasticity-strong rats. Also, as described in the ***Chapter 1***, the occurrence frequency of spastic behavior during the swimming test reflects the severity of spasticity. My results suggest that TMT and cyproheptadine reduce spastic behavior as well as spinal hyperreflexia after 2 weeks of intervention, while the SSRI did not reduce or augment spasticity. I observed no synergistic effect of cyproheptadine and TMT administered together.

To evaluate spasticity, I counted spasms and clonus behaviors during the swimming test and investigated the rate dependent depression (RDD) of the H-reflex in the plantar muscle. In the ***Chapter 1***, spastic rats presented hyperactivity of both the ankle-extensor muscle (medial gastrocnemius muscle; MG) and the plantar-flexor muscle (anterior tibialis muscle; TA) during spastic behaviors. Those excessive and involuntary muscle activations suggested up-regulated spinal hyperexcitability because I identified a correlation between the decrease in the RDD of the H-reflex using the plantar muscle and the hyperactivity of muscles during swimming tests. The plantar muscle is commonly chosen for its selectiveness and robustness of the H-reflex when stimulating the tibial nerve using rodent models of SCI[60,87-89]. In addition, changes in the plantar reflex are similar to those of the other hind limb muscles, i.e., the gastrocnemius and anterior tibialis muscle, in the rat model of SCI[89]. Thus, it would be reasonable to assess spasticity and the hyper active state of spinal motor neurons respectively using the swimming test and RDD of the H-reflex from the plantar muscle.

In this chapter, the decrease of immunoreactivity of 5-HT_{2A} receptor in TMT group indicates that physical training reduces 5-HT receptor expression or changes its distribution so that the hyperactive state of spinal motor neurons can be alleviated. The mechanisms of beneficial effects of physical training such as treadmill training on spasticity were suggested as modulating chloride homeostasis, reinforcing synaptic networks and facilitating inhibitory regulations[67,109,110]. In this study, I could observed neither augmentation of synaptic density on the spinal motor neurons nor significant changes of the serotonergic transporter by any interventions.

Instead, I observed co-localization of 5-HT and the 5-HT_{2A} receptor within spinal motor neurons of the TMT groups, which suggests internalization of the ligand via its receptor. Since the internalization occurs together with down-regulation of receptors at the cell surface, it is likely that internalization is a part of the molecular cascade involved in reducing the hyperactive state of 5-HT system. Internalization of 5-HT receptors has been extensively studied *in vitro* after the ligand stimulation[34,111]. However, it is not clear whether the local concentration of 5-HT surrounding spinal motor neurons contributed to treadmill training-dependent (physical training-dependent) internalization. Considering that ligand-dependent internalization of 5-HT receptor shows fast recycling, co-localized immunosignals which were observed in the steady state tissues of TMT group may not be solely induced by the ligand stimulation. Furthermore, the failure of SSRI, which increases the local 5-HT levels, in promoting internalization indicates that internalization of the receptor is caused by other factors, and not just by enhanced the ligand concentration. Several candidates may connect physical training and 5-HT receptor expression; sensory input from lower limbs, rhythmic firing of motor neurons, or even mechanical stimuli from walking or running performance. Further investigation is needed to identify therapeutic mechanisms for better outcomes.

I predicted that inhibition of the 5-HT receptor would ameliorate the hyperactive state of motor neurons. My results indicate that this treatment successfully reduced the occurrence of spastic behaviors and restored RDD. However, I did not observe synergic effects when the 5-HT_2R antagonist was administered together with TMT. In addition, IHC analyses indicate that cyproheptadine did not change, or slightly increased, 5-HT_{2A} receptor expression in spinal motor neurons after SCI. This could lead to a discrepancy in the perceived relationship between 5-HT_{2A} receptor expression and severity of spasticity. However, the constitutive activation of 5-HT_{2A} receptor has not been reported previously, in comparison to reports that analyze 5-HT_{2C} receptor expression after SCI[58]. Therefore, I argue that although 5-HT_{2A} receptor expression was unchanged, the reduction in spastic symptoms by cyproheptadine administration occurred due to the pharmacological block of the interaction between the 5-HT ligand and its receptor.

On the other hand, chronic SSRI treatments for 3 weeks to several months effectively desensitize the 5-HT receptor in the central nervous system[100,101]. In addition, exposure to SSRIs downregulates the expression of the serotonin transporter, which is a main target of SSRIs[107,112]. In this study, I found a tendency towards decreased expression of the serotonin transporter following administration of fluoxetine. However, I did not observe a downregulation of 5-HT receptors after the administration of fluoxetine for 2 weeks. It is possible that the 2-week period was not long enough to desensitize the hyperactivity of serotonergic receptor. In fact, previous studies have reported that SSRIs exacerbate symptoms related to serotonergic hyperactivity in patients with SCI at the beginning of the prescription or with single-dose administration[103,104]. I expect that further administration of fluoxetine beyond 2 weeks would show therapeutic effects on spasticity in our animal experiments.

Despite the improvement in spasticity in the TMT and cyproheptadine-treated groups, neither group showed improvement in hind limb function, as assessed based on the BBB score. Several studies have reported that physical training and 5-HT activation improves locomotor

function after a SCI. Serotonin receptor agonists facilitate locomotion via activation of rhythmic firing in spinal circuits[95,113,114]. Similarly, physical training activates local spinal circuits via afferent inputs[68,115,116]. The discrepancy between my observation and previous reports may be attributed to our intervention beginning 4 weeks after the severe injury, and thus muscle weakness was already established. Early interventions or mild injury models will be useful to verify enhancement of locomotor functions after physical activity or 5-HT modulations.

In summary, my results present that physical training could resolve the hyperactive state of the 5-HT system and alleviates spasticity. The 5-HT receptor antagonist also reduces spasticity, and its effect is mediated through mechanisms other than treadmill training. This chapter suggests that modification of the 5-HT system, especially related to 5-HT_{2A} receptor expression after the SCI, is crucial to the optimization of therapeutic intervention to alleviate spasticity after SCI. Further assessment of the 5-HT system function will provide molecular-based information for the development of combination therapy involving both, physical training and pharmacological intervention.

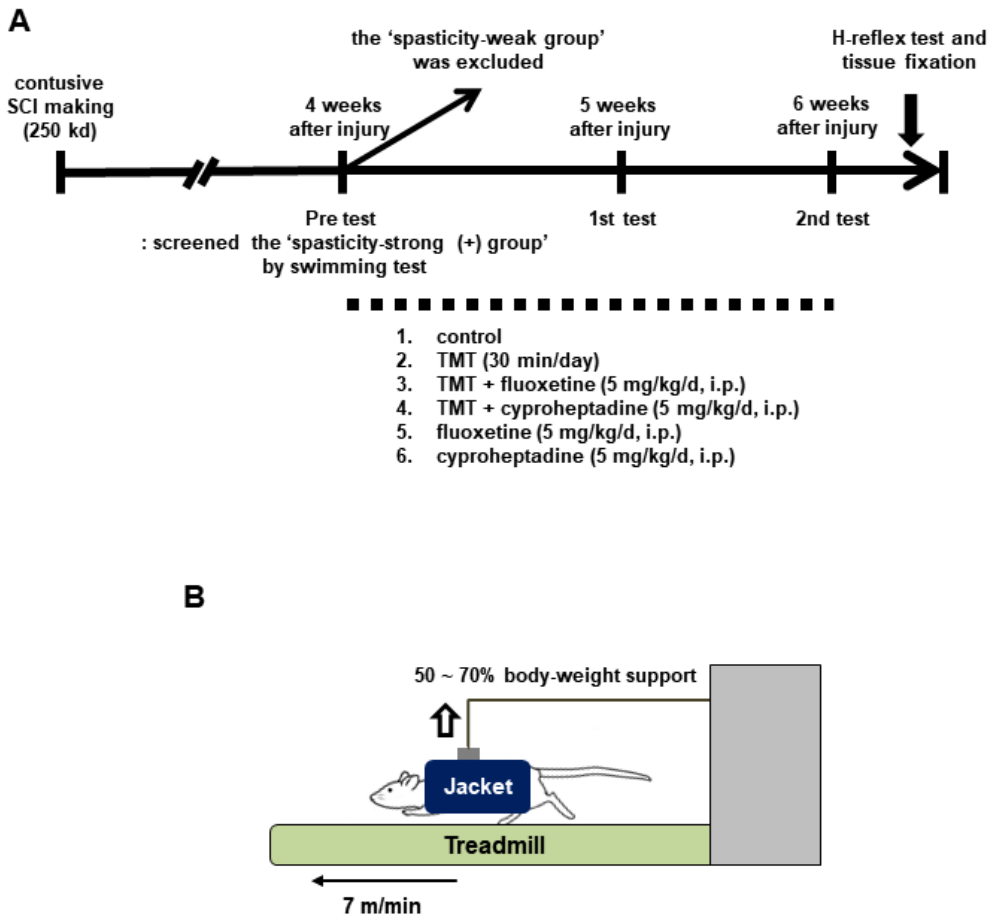

Figure 2-1. Experimental scheme and configuration of methods

(**A**) Experimental time line of this study. Rats received 250 kd of contusive spinal cord injury. After selecting the spasticity-strong group 4 weeks post injury, fluoxetine and cyproheptadine were administrated once daily with or without treadmill training. The H-reflex test and tissue fixation was performed 1 day after the 2nd swimming test. (**B**) Configuration of body-weight supported treadmill training performed in this chapter. The treadmill training (TMT) was conducted to allow animals to perform a plantar placement of their hindlimbs with 50 to 70% of body−weight supported (7 m/min speed). When the rats exhibited dorsal stepping or dragging of their hindlimbs, I re-positioned the animals, temporarily supported their belly, or adjusted their hindlimbs manually.

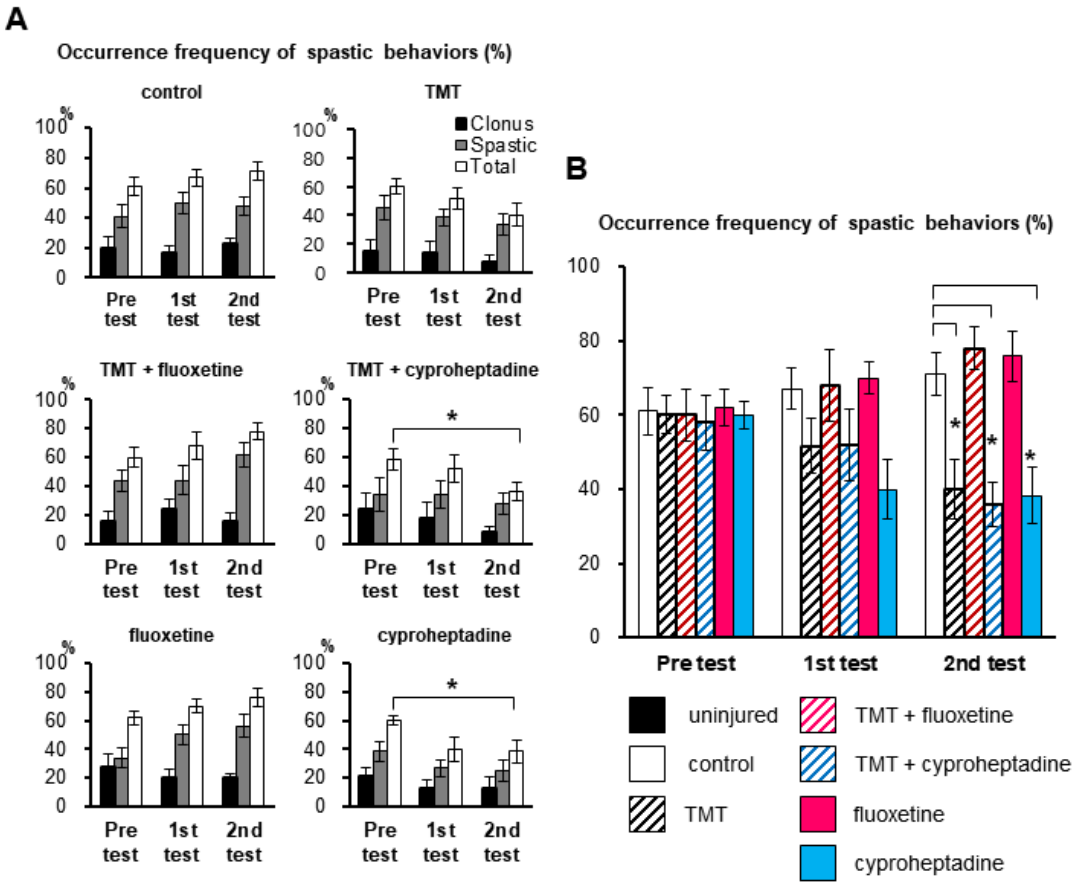

Figure 2-2. Effects of treadmill training and 5-HT receptor antagonist to alleviate spastic behavior during the swimming test

(**A**) Bar graphs showing the mean occurrence frequency of spastic behavior including clonus and spastic phases during weekly swimming tests after spinal cord injury (SCI). The pre, first, and second tests correspond to 4 weeks, 5 weeks, and 6 weeks after the injury, respectively. (**B**) The bars represent the mean occurrence frequency of spastic behavior during the swimming tests observed in each experimental group (white bar: control group, black-dashed bar: TMT group, magenta-dashed bar: TMT with fluoxetine group, blue-dashed bar: TMT with cyproheptadine group, magenta bar: fluoxetine group, blue bar: cyproheptadine group). *, $P < 0.05$, **, $P < 0.01$, #, $P < 0.05$. # present for comparisons with the 'Pre-test'.

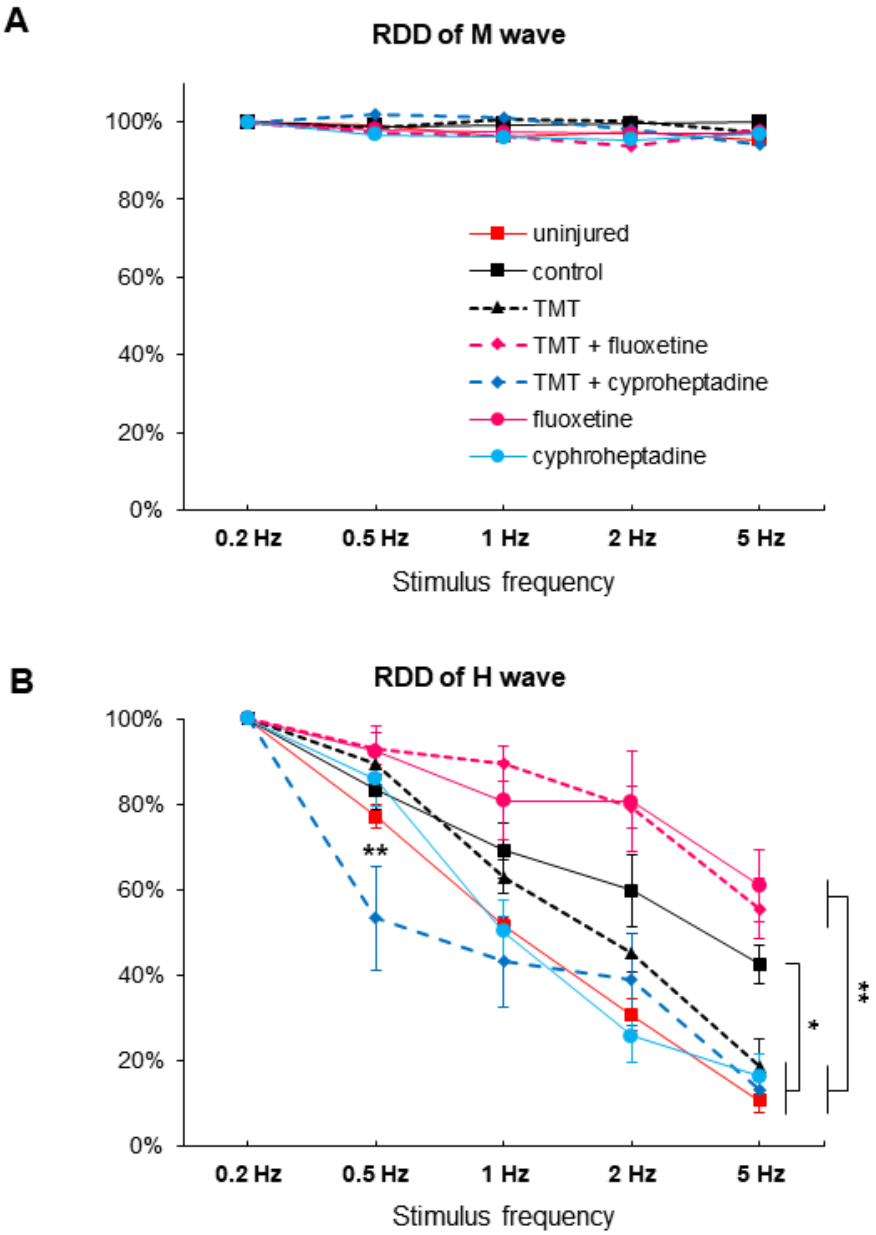

Figure 2-3. Rate-dependent depression (RDD) of the H-reflex increased after treadmill training and a 5-HT receptor antagonist administration

(**A**) The rate-dependent depression (RDD) of the M wave in each group is shown. (**B**) Graphs present the RDD of the H-wave (red line: uninjured group, black line: control group, black-dashed line: TMT group, magenta-dashed line: TMT with fluoxetine group, blue-dashed line: TMT with cyproheptadine group, magenta line: fluoxetine group, blue line: cyproheptadine group). *, $P < 0.05$, **, $P < 0.01$.

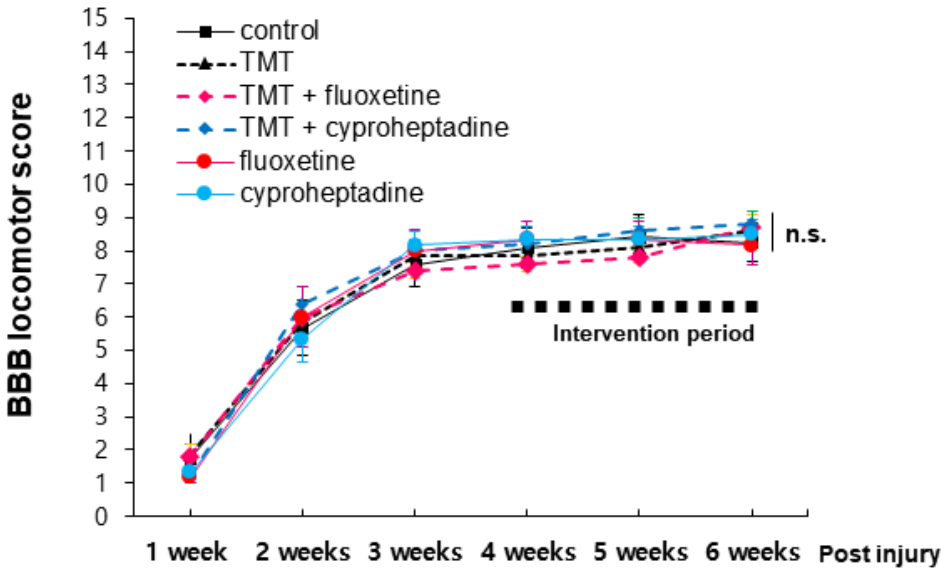

Figure 2-4. The interventions did not significantly altered hind-limb locomotor functions

The BBB locomotor score is shown every week for each group after the injury (black line: control group, black-dashed line: TMT group, magenta-dashed line: TMT with fluoxetine group, blue-dashed line: TMT with cyproheptadine group, magenta line: fluoxetine group, blue line: cyproheptadine group). n.s., non-significant.

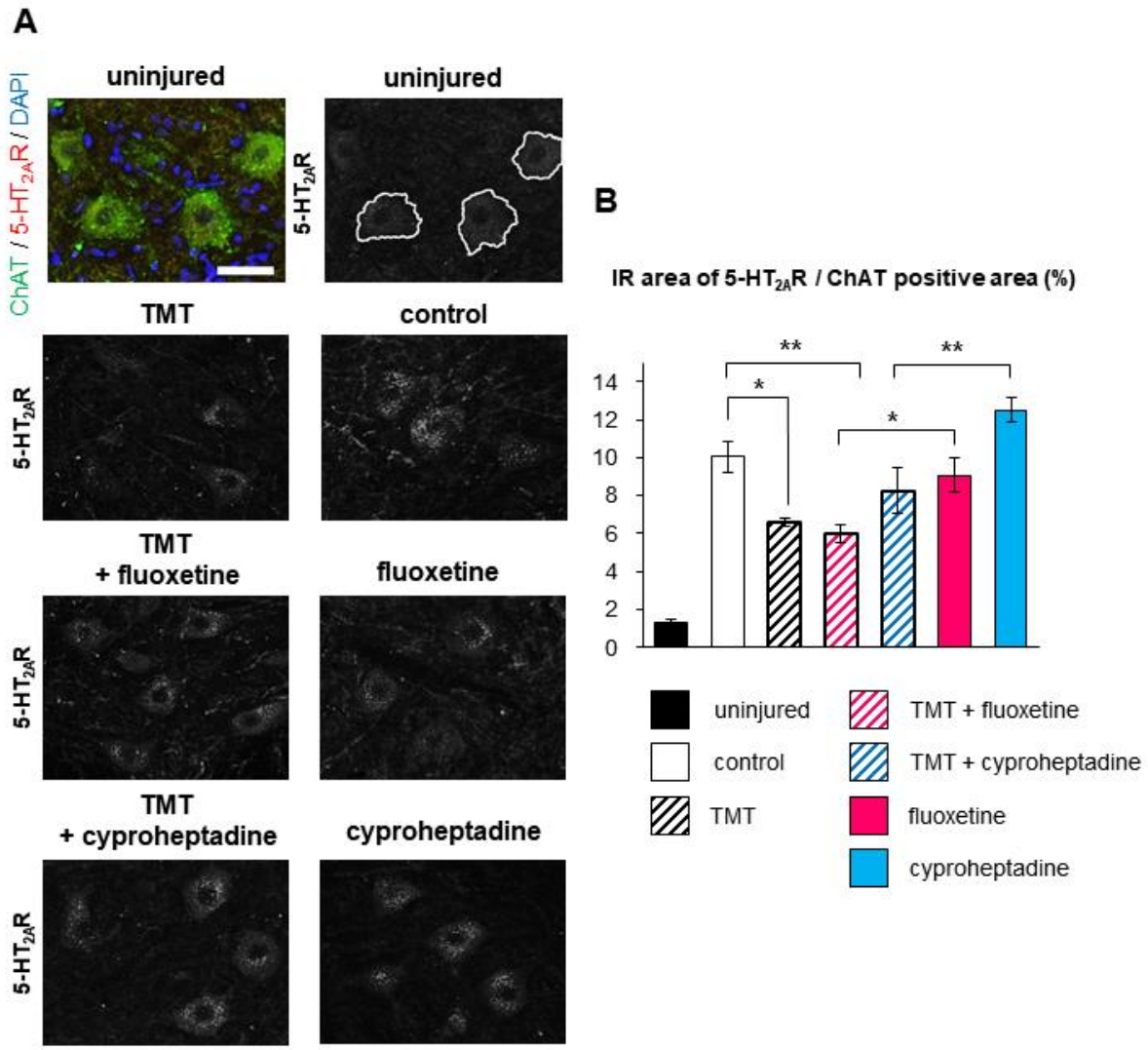
A
uninjured
uninjured
ChAT / 5-HT2AR / DAPI
5-HT2AR
TMT
control
5-HT2AR
TMT
+ fluoxetine
fluoxetine
5-HT2AR
TMT
+ cyproheptadine
cyproheptadine
5-HT2AR
B
IR area of 5-HT2AR / ChAT positive area (%)
14
12
10
8
6
4
2
0
**
*
**
*
uninjured
control
TMT
TMT + fluoxetine
TMT + cyproheptadine
fluoxetine
cyproheptadine

Figure 2-5. Effects of the interventions on immunoreactivity of the 5-HT_{2A} receptor in lumbar spinal cord motor neurons after SCI

(**A**) Representative images of immunoreactivity (IR) of the 5-HT_{2A} receptor (5-HT_{2A}R) on the lumbar motor neurons of each group are shown. As shown at the top, spinal motor neurons were stained by the anti-ChAT (green) antibody and the IR area of the 5-HT_{2A}R was confined to the ChAT-stained area (white lines in the binarized image indicate ChAT margins). The nuclei have been stained by DAPI (blue). Scale bar: 50 μm. (**B**) Quantitative analysis of the IR area of the 5-HT_{2A}R in the ChAT-positive area (lumbar motor neurons) of each group, as shown as a bar graph (black bar: uninjured group, white bar: control group, black-dashed bar: TMT group, magenta-dashed bar: TMT with fluoxetine group, blue-dashed bar: TMT with cyproheptadine group, magenta bar: fluoxetine group, blue bar: cyproheptadine group). *, $P < 0.05$, **, $P < 0.01$.

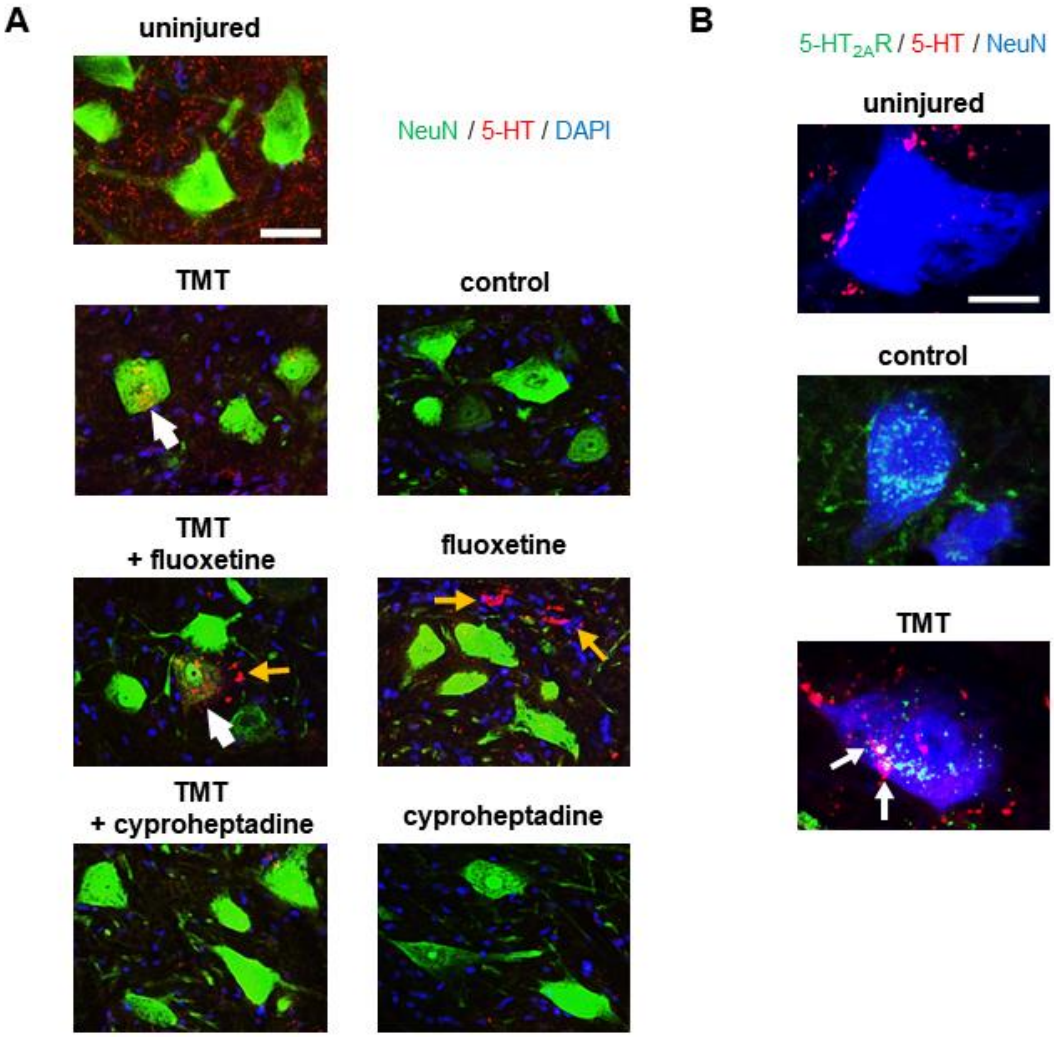

Figure 2-6. Tissue staining against 5-HT and its receptor reveals different distribution dependent on the interventions

(**A**) Representative anti-NeuN (green), 5-HT (red), and DAPI (blue) immunostaining images of motor neurons on the ventral horn of the lumbar spinal cord tissue sections of each group. White arrows represent immunosignals of 5-HT within the lumbar motor neurons, yellow arrows indicate aggregated 5-HT signals around the lumbar motor neurons. Scale bar: 50 μm. (**B**) Representative images of anti-5-HT (red), 5-HT_{2A} receptor (5-HT_{2A}R; green), and NeuN (blue) immunostaining of the lumbar spinal motor neurons are presented. The arrows indicate co-localization of the 5-HT_{2A} receptor and 5-HT immunosignals. Scale bar: 20 μm.

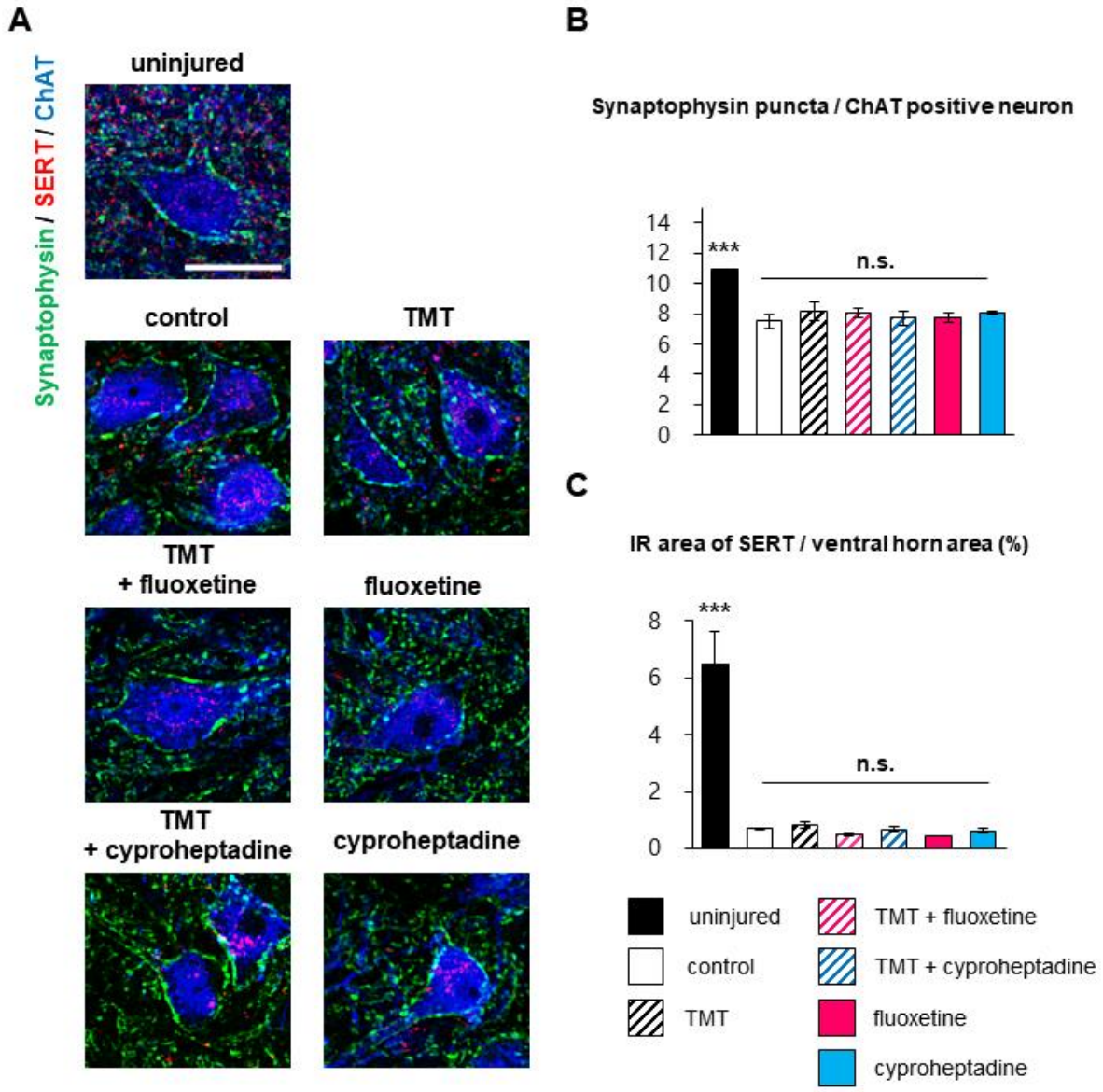
A
Synaptophysin / SERT / ChAT
uninjured
control
TMT
TMT
+ fluoxetine
fluoxetine
TMT
+ cyproheptadine
cyproheptadine
B
Synaptophysin puncta / ChAT positive neuron
14
12
10
8
6
4
2
0
***
n.s.
C
IR area of SERT / ventral horn area (%)
8
6
4
2
0
***
n.s.
uninjured
control
TMT
TMT + fluoxetine
TMT + cyproheptadine
fluoxetine
cyproheptadine

Figure 2-7. The expressions of synaptophysin and serotonin transporter in the lumbar spinal cord were not significantly changed by interventions

(**A**) Representative immunostaining images of motor neurons in the ventral horn of the lumbar spinal cord showing the expression of anti-synaptophysin (green), serotonin transporter (SERT; red), and ChAT (blue) in each group. Scale bar: 50 μm. (**B**) Bar graph showing the mean number of synaptophysin puncta per a spinal motor neuron (black bar: uninjured group, white bar: control group, black-dashed bar: TMT group, magenta-dashed bar: TMT with fluoxetine group, blue-dashed bar: TMT with cyproheptadine group, magenta bar: fluoxetine group, blue bar: cyproheptadine group). (**C**) Bar graph showing quantitative analysis of the SERT immunoreactivity (IR) area in the ventral horn in each group (black bar: uninjured group, white bar: control group, black-dashed bar: TMT group, magenta-dashed bar: TMT with fluoxetine group, blue-dashed bar: TMT with cyproheptadine group, magenta bar: fluoxetine group, blue bar: cyproheptadine group). ***, $P < 0.001$, n.s., non-significant.

Chapter 3.

Effects of physical training on the regulation of serotonin 2A receptor sensitivity of neuronal cells in the central nervous system

Introduction

There is accumulating evidence that physical training (exercise) has beneficial effects on mental disorders including depression, anxiety and schizophrenia[6,14,15]. Among numerous biochemical signals functioning in the nervous system, serotonin (5-HT) has been reported to play an essential role in regulating emotions and behaviors, and has been implicated in psychiatric diseases[16-18]. However, it remains elusive how exercise modulates 5-HT signaling in the central nervous system (CNS).

5-HT receptor, a member of G-protein coupled receptor (GPCR) family, is known to internalize either ligand-dependently or ligand-independently[34,36,117]. As described in the ***Chapter 2***, I observed that treadmill training reduced the expression of 5-HT_{2A} receptor on the spinal motor neurons after spinal cord injury. For the reason of down-regulation of the 5-HT receptor, I hypothesized that physical training induces the ligand-independent internalization of 5-HT_{2A} receptor, rather than ligand-dependent. As described in the ***Section 5*** of ***General introduction***, in particular, I focused fundamental components of physical training, which generates the mechanical stress.

Minimal deforming forces or stress distribution changes are possibly produced in the CNS under physiological conditions such as running. The function of osteocytes is known to be modulated by shear stress that is generated by interstitial fluid flow derived from minimal deformation of bone[118]. Postulating an analogy between osteocytes in bones and neuronal cells in the nervous system, I speculated that minimal stress distribution changes might generate interstitial fluid flow in the CNS, resulting in shear stress-mediated regulation of neuronal functions.

In this chapter, to demonstrate my hypothesis, I conceived a simple and direct method named as 'passive head motion' (PHM) to deliver mechanical stress to the neurons in the brain. PHM is designated to generate vertical accelerations at the head similar to those during treadmill training and, therefore, this system can produce a reminiscent model to investigate the effect of mechanical stress by physical training on spinal neurons shown in the ***Chapter 2***.

Furthermore, I utilized the head-twitch response (HTR) which is a hallucinogenic behavioral action induced by administrating of the 5-HT receptor agonists. Rapid, side to side rotational head movements are presented as unique characteristic behavior of HTR in rodents. HTR has been reported to represent the intensity of 5-HT_{2A} receptor signaling at prefrontal cortex (PFC) of rodents[119-121]. In addition, neuronal responses in the PFC can be evaluated by examining the activation of c-Fos, which has been reported to be downstream of 5-HT signaling[55,122]. Because of its specific onset mechanism and dose-dependent manners, HTR is suitable for using 5-HT_{2A} receptor sensitivity experiments[120,121]. Although HTR is a one to one corresponding *in vivo* model concerning with 5-HT receptors in the brain, to evaluate of 5-HT_{2A} receptor regulation in HTR using PHM system will be an alternative model to understand effects of physical training on mechanical regulation of 5-HT_{2A} receptor function of neuronal cells in the spinal cord. Using these system, I demonstrated that PHM in rodents recapitulates the suppressive effects of running on 5-HT signaling at the PFC in the brain via the internalization of 5-HT_{2A} receptor.

Furthermore, I recapitulated the effect of PHM on the regulation of 5-HT receptor sensitivity using *in vitro* model. Using neuronal cell line, I applied calculated fluid shear stress (FSS) expected to be derived by the head movement during treadmill running. Subsequently, I examined the effect of mechanical stress on the 5-HT receptor internalization and related 5-HT signaling. When 5-HT binds to its receptor, it leads elevation of intracellular calcium concentration and activates signals through extracellular signal-regulated kinase (ERK)

pathways[28]. Generally, 5-HT receptors are temporally internalized and recycled after the receptors interact with 5-HT ligand, which induces the intrinsic regulation of 5-HT receptor sensitivity itself[28,123]. In addition to ligand-dependent internalization of 5-HT receptor, the activation of protein kinase C (PKC), which is known to be induced by FSS[75,124], has been reported to mediate signaling involved in ligand-independent internalization of GPCRs expressed in various types of cells *in vitro* and *in vivo* including 5-HT receptor[125-127].

Materials and methods

Animal Experiments

Animals were housed under a 12 h/12 h light dark cycle with controlled temperature (23~25°C), and treated with humane care under approval from the Animal Care and Use Committee of National Rehabilitation Center for Persons with Disabilities and Tokyo Metropolitan Institute of Gerontology. C57BL/6 mice and Sprague-Dawley (SD) rats were purchased from Charles River (Yokohama, Japan) or SLC (Hamamatsu, Japan) and acclimated to the laboratory environments for at least 1 week. Animals were randomly divided into experimental groups, and used for experiments. I used SD rats to analyze mechanical elements because the larger body size of rats enabled me to utilize various experimental tools required for analysis of physical matters and factors. All the animal behavior tests were conducted between 4 pm and 8 pm.

Acceleration analysis of treadmill running and passive head motion (PHM)

As an animal model of physical exercise, mice were subjected to compulsive running using a belt drive treadmill (MK-680S, Muromachi, Tokyo, Japan) at modest velocities (~10 m/min for mice and ~20 m/min for rats), a typical experimental intervention to test effects of physical exercise after SCI in rodents[128,129]. To measure the accelerations at the head during treadmill running, I fixed an accelerometer (NinjaScan-Light; Switchscience, Tokyo, Japan) on the rats' heads with a surgical tape. Acceleration-specific signals were extracted and average accelerations for 3-D (*x*-, *y*- and *z*-axes; **Fig. 3-2A**) were individually calculated from 10 serial waves using the software applications provided from the manufacture and Spike2 (CED, Cambridge, England). Animals (mice or rats) were subjected to PHM in a prone position using

a platform that was developed to move their heads up and down (schematically represented in **Fig. 3-4D** and **Fig. 3-7A**). During PHM, animals were kept anesthetized with 2% isoflurane and body temperature of tested animals was maintained using a light heater. For recapitulation of the head movement during treadmill training, the PHM system was set up to produce the same acceleration peaks examined during treadmill running.

Analysis of head-twitch response (HTR)

First, HTR was preliminary induced to wild-type C57BL/6 mice to delineate a baseline response by administration of 5-hydroxytryptophan (5-HTP; the precursor of 5-HT which is utilized as a 5-HT_{2A} receptor agonist; 100 mg/kg, i.p., Sigma; **Fig. 3-3**).

Mice were subjected to a week of treadmill running (10 m/min, 30 min per day) or PHM (2Hz, 30 min per day). After that, mice were injected of 5-HTP (100 mg/kg, i.p., Sigma) or its vehicle (normal saline, i.p.) after 3 h of the last bout of treadmill running or PHM. After administration of 5-HTP or saline, animals were individually placed in a Plexiglas box and videotaped for 30 min using a handycam camera (HDR-CX700, Sony, Japan). All animals were observed for 30 min and recorded movies were reviewed to count head twitching.

Immunohistochemical analysis of 5-HT signaling and 5-HT_{2A} receptor in the PFC

Immunohistochemical analysis was performed to visualize the response to 5-HTP injection and the internalization of 5-HT_{2A} receptor in the prefrontal cortex (PFC) of mice following head-twitch response analysis. After the completion of the behavioral tests, animals were immediately anesthetized by administrating combinations of midazolam, butorphanol and medetomidine, and perfused with 4% paraformaldehyde (PFA) transcardially. Then, brains

were excised, post-fixed in 4% PFA for additional 24 h at 4 ºC, and stored in 30% sucrose/PBS until they sank. Fixed brains were frozen in OCT (Sakura, Japan) and cut into 20 μm-thick sagittal sections using a cryostat (Leica Microsystems). Sliced sections were permeabilized with 0.1% Tween-20 in TBS, blocked with 4% donkey serum (Millipore), stained by incubating with primary antibodies at appropriate concentrations as follows: mouse-anti NeuN (1:500, EMD Millipore #MAB377,), goat-anti 5-HT_{2A} receptor (1:100, Santa cruz biotechnology, #sc-15073) and rabbit-anti c-Fos (1: 100, Santa cruz biotechnology, #sc-52). Their species-matched secondary antibodies conjugated with Alexa Fluor 488, 568 or 645 (Life Technologies) were applied, and viewed with a fluorescence microscope (BZ-9000 HS, Keyence).

To quantify 5-HT_{2A} receptor internalization in PFC neurons, I defined 'internalized' and 'membrane-associated' 5-HT_{2A} receptor-positive signals based on the distance from soma margins and the connectivity with perimarginal regions. I first outlined the somas of individual PFC neurons by tracing the margins of NeuN-positive area (yellow lines in **Fig. 3-5C**). As the anti-5-HT_{2A} receptor immunosignals within 2 μm of soma margins appeared to be distributed along the marginal outlines, I defined them as 'membrane-associated'. Resultantly, the anti-5-HT_{2A} receptor immunosignals distributed at >2 μm from soma margins (blue lines in **Fig. 3-5C**) were defined as 'internalized'. Regardless of the distance from soma margins, anti-5-HT_{2A} receptor immunosignals connected with perimarginal regions were defines as 'membrane-associated'. Only the somas larger than 10 μm in short diameter were subjected to the quantification of 5-HT_{2A} receptor internalization. Images were quantified using Photoshop CC (Adobe systems, USA) and ImageJ (NIH, USA) software.

Quantitative PCR analysis (reverse transcription and real-time PCR) of 5-HT_{2A} receptor expression in the PFC

Total RNA (500 ng) extracted from mouse PFC excised immediately after cervical dislocation were subjected to reverse transcription, using ISOGEN II (NIPPONGENE, Japan) and PrimeScript® RT reagent Kit (TaKaRa, Japan). The resulting cDNA was subjected to real-time PCR analysis to evaluate the expression of 5-HT_{2A} receptor mRNA in the PFC using glyceraldehyde-3-phosphate dehydrogenase (GAPDH) as an internal control in Applied Biosystems 7500 Real Time PCR System with Power SYBR Green PCR Master Mix (Life Technologies).

The primers (sense and antisense, respectively) were as follows: mouse HT2AR, 5′-TGCCGTCTGGATTTACCTGG-3′ and 5-TGGTTCTGGAGTTGAAGCGG-3, and mouse GAPDH, 5′-GCAAAGTGGAGATTGTTGCCAT-3′ and 5′- CCTTGACTGTGCCGTTGAATTT -3′.

Immunoblot analysis of 5-HT_{2A} receptor expression in the PFC

Mouse PFC tissue was excised immediately after cervical dislocation, mechanically homogenized, solubilized with sodium dodecyl sulfate (SDS) sample buffer (50 mM Tris HCl pH 7.0, 18% glycerol, 2% SDS), and subjected to SDS-PAGE followed by anti-5-HT_{2A} receptor (goat, Santa cruz biotechnology, #sc-15073) and anti-GADPH (rabbit, Cell signaling technology, #5174) immunoblotting. Specific signals were visualized and quantified using Odyssey infrared imaging system and ImageJ software (NIH, USA).

In vivo analysis of the distribution dynamics of cerebral interstitial fluid using MRI

MRI Scanning: 8-week-old male SD rats were scanned in an ICON 1.0-Tesla bench top MRI system (Bruker BioSpin, Esslingen, Germany) using a T1-weighted-fast low angle shot-navigation-highers-three-dimensional (T1-FLASH-nav-highers-3-D) sequence. Parameters for the T1-FLASH-nav-highers-3-D sequence were as follows; echo time (TE): 12.0 ms, repetition time (TR): 50.0 ms, flip angle (FA): 30°, slice thickness (SL): 0.84 mm, field of view (FOV): 35 × 35 × 27 mm, voxel: 0.137 × 0.137 × 0.84 mm^3. Each scanning took 10 min.

Intracerebral microinjection of Gd-DTPA solution: Rats were first subjected to brain pre-scanning with MRI under isoflurane anesthesia, and then to intracerebral microinjection of Gd-DTPA (Magnevist®, Beyer) as previously reported with some modifications. In brief, after rats were anesthetized with 2 mg/kg of midazolam (Sandoz), 2.5 mg/kg of butorphanol (Meiji Seika, Japan) and 0.15 mg/kg of medetomidine (Kyoritsu Seiyaku, Japan), a 31-G needle connected with microsyringe (Hamilton Bonaduz AG, Bonaduz, Switzerland) was placed on prefrontal cortex (PFC) of rats according to the stereotaxic measurements as follows; anterior: 2.5 - 3 mm, lateral: 1.5 - 2.0 mm, ventral: 2 - 3 mm from the bregma. One microliter of Gd-DTPA solution (diluted to 25 mM with normal saline) was infused with the rate fixed at 0.2 μl/min using a microsyringe pump instrument (KD scientific, MA). After the injection, we held the microsyringe for 5 min to avoid reflux, pulled out the needle carefully, and sutured the skin.

MRI data acquisition and post-processing: Following intracerebral Gd-DTPA injection, rats were subjected to brain MRI scanning 10, 60 and 90 min after microinjection. PHM was either applied or left unapplied (kept sedentary) for 30 min just before the scanning at 60 min post-injection (**Fig. 3-8A**). MR images were analyzed using a software package rSPM[130], which is a modified version of SPM12 (http://www.fil.ion.ucl.ac.uk/spm/software/spm12/) developed

for human neuroimaging data analyses. The original data were converted from the DICOM format to the NIfTI format. Each individual rat brain image was realigned to the first volume and spatially normalized to a template brain image provided by rSPM. The normalized data had a 86 x 121 x 66 matrix with a 0.2 x 0.2 x 0.2 mm^3 isotropic voxel. The Gd-DPTA cluster was defined as voxels with top 0.05% signal intensity in each volume.

Measurement of intracerebral pressure (ICP) at rats' PFC

ICP was measured using a blood pressure telemeter (Millar, Houston, TX) with its sensor placed in rats' PFC (**Fig. 3-9A**). During ICP measurement, respiration was monitored using a respiration sensor attached to the tested rats. Low-pass (50 Hz) filtered ICP waves were analyzed using LabChart 8 (ADInstruments) software. I observed ~0.5-Hz respiration-synchronized ICP changes with ~2.5 mmHg magnitude (peak to peak) as well as 2-Hz PHM-specific waves with ~1 mmHg magnitude (peak to peak).

Simulative calculation of the magnitude of fluid shear stress on the PFC neurons during PHM

Interstitial fluid flow in the brain tissue follows the Henry Darcy's law, which defines the flux density of penetrating fluid per unite time. The velocity of interstitial fluid flow (u) is assumed to approach the superficial velocity (u_∞) and zero (u=0) at the cell surface (*i.e.* a no-slip condition). Using these two boundary conditions together with the Brinkman equation, fluid shear stress (τ) at the cell surface can be obtained as described in **Table 3-1**.

Neuronal cell culture and plasmid transfection

Neuro2A cells (mouse neuroblastoma; provided from Dr. Ichijo, The University of Tokyo, Japan) were cultured in DMEM (Wako, Japan) with 10% fetal bovine serum (GE Healthcare Life Science) at 37 °C in a 5% CO_2 incubator. At approximately 70% confluence in a 10-cm culture dish (Falcon), Neuro2A cells were transfected with 10 μg of a human 5-HT_{2A} receptor expression vector plasmid using lipofectamine® 3000 (Invitrogen) for 48 hr according to the manufacturer's directions. After transfection, cells were transferred and grown in a poly-D-lysine coated 35-mm culture dish (Corning). Before further experiments, cells were cultured in serum-free DMEM for 48 h (**Fig. 3-1A**).

Application of fluid shear stress (FSS) to neuronal cells in culture

According to a previous report[131], a parallel plate flow-chamber and roller pump (Masterflex; Cole-Parmer, IL) were used to apply FSS (**Fig. 3-1B**). The flow-chamber, which was composed of a cell culture dish, a polycarbonate I/O unit, and a silicone gasket, generated a 23-mm-long 10-mm-wide 0.5-mm-high flow channel. The flow circuit was filled with serum-free medium. The fluid flow was delivered as 0.5 Hz frequency to deliver average 2 Pa of FSS on transfected Neuro2A cells for 30 min (**Fig. 3-1C**). To maintain pH and temperature of culture medium, I used a 5% CO_2-containing reservoir and a temperature-controlled bath.

Live imaging of cultured neuronal cells exposed by FSS

To monitor the functional and physiological effect of FSS on Neuro2A cells including morphological changes and calcium ion influx, I conducted live cell imaging. Neuro2A cells grown in a 10-cm dish were transfected with 10 μg of 5-HT_{2A} receptor expression plasmid vector using lipofectamine® 3000 (Invitrogen). Cells were also transfected 5 μg of mCherry

expression plasmid to visualize cell morphology. After transfection, cells were transferred and grown in a poly-D-lysine coated 35-mm dish, which was placed in a 37ºC/5%-CO_2 plate type incubator (Tokai Hit, Japan) attached to a microscope (BZ-9000 HS, Keyence). Then, a flow chamber was set to the dish plate and FSS was applied. To compare with ligand-dependent internalization 5-HT_{2A} receptor, 10 μM of 5-HT was administrated on Neuro2A without flow chamber mounting.

Morphological changes of Neuro2A cells were examined after application of FSS or 5-HT administration. Activation of caspase-3 was also evaluated to elucidate that whether FSS burdened too much stress to induce apoptotic cell death on Neuro2A cells.

Analysis of modulation of the 5-HT receptor sensitivity by FSS on neuronal cells

To evaluate cellular changes of 5-HT receptor sensitivity by FSS, intracellular Ca^{2+} concentration and ERK phosphorylation which are activated by 5-HT binding to its receptor were evaluated. After FSS application (average 2 Pa, 30 min), cells were loaded with Fluo 4-AM dye (Dojindo, Japan) for 60 min in a 37ºC/5%-CO_2 incubator. Cells were then placed on an incubator-attached fluorescence microscope, and treated with 5-HT (10 μM). After 10 min of 5-HT administration, green fluorescence emitted from Fluo 4-AM bound to Ca^{2+} was viewed with the microscope. ERK phosphorylation in Neuro2A cells by 5-HT administration was evaluated by immunocytochemistry, before and after FSS.

Immunocytochemistry on Neuro2A cells

Neuro2A cells were washed once with ice-cold PBS, fixed with 4% PFA in PBS permeabilized with 0.1% Triton X-100 in PBS, incubated with a blocking solution (10% fetal bovine serum, Thermo Fisher Scientific), and stained using target-specific primary antibodies as follows: mouse-anti 5-HT_{2A} receptor (1:100, #sc-166775), mouse and rabbit-anti TUJ-1 (1: 500, abcam, #ab78078 and #ab18207), rabbit-anti PKCγ (1: 200, Santa cruz biotechnology, #sc-211), rabbit-anti phospho-MARCKS (Ser152/156; 1: 200, Sigma, #P0370), rabbit-anti phospho-ERK1/2 (Thr202/Tyr204; 1:500, Cell signaling technology, #4370), and rabbit-anti cleaved caspase-3 (Asp175; 1: 500, Cell signaling technology, #9661). Their species-matched secondary antibodies were applied and DAPI was used for nuclear staining. Cells were then viewed with a fluorescence microscope (BZ-9000 HS, Keyence).

To quantify 5-HT_{2A} receptor internalization in Neuro2A cells, I defined 5-HT_{2A} receptor-internalized cells based on the ratio of anti-5-HT_{2A} receptor immunosignals distributed at >2 μm from the soma margins defined by outlining TUJ-1-positive areas (yellow lines in **Fig. 3-10A**). I counted cells with >25% of total anti-5-HT_{2A} receptor immunosignal intensity distributed >2 μm away from the margins (i.e. inside the blue lines in **Fig. 3-10A**) as '5-HT_{2A} receptor-internalized'. Only somas larger than 10 μm in short diameter were subjected to the quantification of 5-HT_{2A} receptor internalization. Images were analyzed using BZ-H1C (BZ-9000 HS related application, Keyence), Photoshop CC (Adobe systems, USA) and ImageJ (NIH, USA) software.

PKC inhibition tests *in vitro* and *in vivo*

As for *in vitro* PKC inhibition, Neuro2A cells were pre-treated by Ro 31-8220 (a PKC inhibitor; 4 μM, 1 h) before 5-HT (10 μM) administration or FSS application (average 2 Pa, 0.5 Hz, 30 min).

To evaluate whether PKC inhibition hampers the effect of PHM on HTR or not, I injected Ro 31-8220 (5 mg/kg, i.p., Sigma) to mice before each bout of daily PHM for a week. Then, HTR was analyzed after 5-HT injection (**Fig. 3-14C**). As a control, normal saline was injected instead of Ro 31-8220. To confirm the single effect of Ro 31-8220, HTR analysis was also performed with mice that were not subjected to PHM. Immunohistochemical analysis of c-Fos expression and 5-HT_{2A} receptor internalization in neurons of the PFC was performed as described above.

Statistical analysis

All the quantitative data are presented as means ± SEM. Statistical analyses were conducted by two-tailed Student's *t*-test or one-way ANOVA with post hoc Bonferroni test for comparison, using SPSS software (IBM SPSS, Inc.). Differences were considered as significant at *P* values below 0.05.

Results

PHM system reproduces the gravity-derived mechanical stimulation generated by treadmill running

I first measured the acceleration generated at the head during treadmill running., I observed that the peak magnitude of the vertical acceleration generated at the rats' heads (*z*-axis in **Fig. 3-2A**) during treadmill running (20 m/min) was ~1.0 *g* (**Fig. 3-2B** and **3-2C**). I therefore set up our custom-designed 'passive head motion' (PHM) system to produce 1.0 *g* of vertical acceleration peaks at the heads of rodents (mice and rats) to be tested (**Fig. 3-2B** and **3-2C**). I examined the head-twitch response (HTR) of mice because of the ease and reliability of quantitative analysis due to frequent and immediate head twitching of mice after 5-HTP administration[132,133]

Treadmill running and PHM similarly modulate behavioral response to 5-HT

Then, I quantitatively analyzed HTR induced by 5-HTP in wild-type C57/BL6 mice (n = 10 for 5-HTP treated group, n = 5 for saline treated group, $P < 0.001$, Student's unpaired two-tailed *t*-test; **Fig. 3-3A** and **3-3B**). Mice showed HTR immediately after 5-HTP administration and the episodes reached the peak after 15 min. Further, I found that a week of treadmill running significantly decreased HTR (n = 10 for each group, 10 m/min, 30 min per day, $P = 0.0269$, Student's unpaired two-tailed *t*-test; **Fig. 3-4A**), suggesting a suppressive effect of exercise on 5-HT signaling (**Fig. 3-4B** and **3-4C**). Application of PHM to mice under anesthesia led to a decrease in HTR (n = 10 for each group, 2 Hz; 30 min per day; 7 days, $P = 0.0349$, Student's unpaired two-tailed *t*-test; **Fig. 3-4D, 3-4E** and **3-4F**), similar to that after treadmill running.

Mice that underwent PHM exhibited neither apparent alert problems nor detrimental consequences on behavioral activity. Collectively, these results suggest that PHM and treadmill running have a comparable effect on 5-HT signaling in the PFC of rodents.

Both treadmill running and PHM induce decreased neuronal response to 5-HT and the internalization of 5-HT$_{2A}$ receptor

To examine how treadmill running and PHM modulated 5-HT-related signaling in neurons in PFC of mice, I conducted immunostaining of brain tissue sections using NeuN as a biomarker for neurons[134]. I observed an increase in c-Fos expression, which has been reported to be downstream of 5-HT signaling[55,122], in PFC neurons of mice after 5-HTP injection while no apparent c-Fos expression was observed in vehicle (saline)-injected control mice. Consistent with the suppressive effect of 5-HT signaling by daily treadmill running or PHM (30 min, 7 days) on HTR (**Fig. 3-4**), both interventions down-regulated 5-HTP-induced c-Fos expression in the PFC neurons (n = 3 to 4 for each group, Left chart:, $P < 0.001$, one-way ANOVA with post hoc Bonferroni test, Right chart:, $P = 0.001$, Student's unpaired two-tailed *t*-test; **Fig. 3-5A** and **3-5B**).

To verify the reason of reduced neuronal response to 5-HT, I observed distribution of 5-HT$_{2A}$ receptor on neurons in the PFC of brain (**Fig. 3-5C**). It revealed that 5-HT$_{2A}$ receptor internalization in mouse PFC neurons was significantly enhanced by both treadmill running and PHM (n = 3 for each group, Internalized: Left chart, $P < 0.001$, one-way ANOVA; Right chart, $P = 0.002$, Student's unpaired two-tailed *t*-test, Membrane-associated: Left chart, $P = 0.011$, one-way ANOVA with post hoc Bonferroni test; Right chart, $P = 0.0338$, Student's unpaired two-tailed *t*-test; **Fig. 3-5D** and **3-5E)**. When I conducted immunoblot and quantitative polymerase chain reaction (PCR) analyses, I found that neither treadmill running

nor PHM significantly changed the expression levels of 5-HT_{2A} receptor in mouse PFC (n = 6 for each group, $P = 0.095$ and $P = 0.364$ for n.s., one-way ANOVA with post hoc Bonferroni test; **Fig. 3-6A** and **3-6B**). Considering that 5-HT_{2A} receptor expression is highly neuron-specific in rodent cerebral cortex[135], 5-HT_{2A} receptor expression in the PFC neurons appears not to be significantly altered by treadmill running or PHM. These findings suggest that 5-HT_{2A} receptor internalization, rather than repression of its expression, is involved in the desensitization of 5-HT signaling in PFC neurons by treadmill running or PHM.

PHM facilitates cerebral interstitial fluid flow and changes intracerebral pressure at the PFC

As described in the ***Section 5*** of ***General introduction*** and the ***introduction*** in this chapter, I speculated that fluid shear stress (FSS) generated by the flow of interstitial fluid in the nervous system is the mechanical stress from physical training such as treadmill running.

To examine whether PHM affected the interstitial fluid movement (flow) in the brain, I injected an extracellular fluid contrast agent, gadolinium-diethylenetriaminepentaacetic acid (Gd-DTPA) into the PFC of anesthetized rats (**Fig. 3-7A**), and tracked its distribution with magnetic resonance imaging (MRI) (**Fig. 3-8A** and **3-8B**). When I compared rats with and without PHM, I found that PHM promoted Gd-DTPA spreading in the rostral-caudal (*y*-axis, **Fig. 3-7B**) and left-right (*x*-axis, **Fig. 3-7B**) directions (n = 5 for each group, Two-way ANOVA with Bonferroni's post hoc test, *x*-axis: $P = 0.0081$ and $P = 0.4136$; *y*-axis: $P < 0.001$ and $P = 0.0231$; *z*-axis: $P = 0.1068$ and $P = 0.4289$; **Fig. 3-7C** and **3-7D**). Notably, PHM did not significantly affect the dorsal-ventral spreading (*z*-axis, **Fig. 3-7B**) of Gd-DTPA (**Fig. 3-7D**). This suggests that PHM enhances interstitial fluid flow in the PFC along defined axes, rather than isotropically.

To further analyze the physical effects that PHM produced on the brain, I measured the local pressure in rats' PFC using a telemetry pressure sensor (**Fig. 3-9A**). I found that PHM generated pressure waves (changes) with ~1 mmHg peak amplitude (10 segments analyzed for each, $P < 0.001$, Student's unpaired two-tailed *t*-test; **Fig. 3-9B, 3-9C** and **3-9D**). This supports the notion that PHM brings about changes of pressure distribution, thereby driving local interstitial fluid flow in the PFC. My simulative calculation suggests that the PHM subjected the PFC neurons to interstitial fluid flow-derived shear stress with the average magnitude of 0.6 ~ 3.6 Pa (**Table 3-1**), which was demonstrated *in vitro* to modify the physiological function such as intracellular Ca^{2+} influx of astrocytes[136], the most abundant type of cells distributed in the brain.

Fluid shear stress internalizes 5-HT_{2A} receptor expressed in neuronal cells, and modulates neuronal response to 5-HT *in vitro*

Next, I conducted *in vitro* experiments to examine whether 5-HT_{2A} receptor expressed in neuronal cells internalized in response to FSS. Based on my simulation mentioned above, I applied pulsatile FSS with the average magnitude of 2 Pa to cultured Neuro2A cells, using a system previously reported[131] (**Fig. 3-1B** and **3-1C**). As was observed after 5-HT administration, FSS application (0.5 Hz, 30 min) caused internalization of 5-HT_{2A} receptors expressed in Neuro2A cells (**Fig. 3-10B** and **3-10C**). However, FSS-induced 5-HT_{2A} receptor internalization appeared different from that after 5-HT administration. As shown in **Fig. 3-10D**, 5-HT_{2A} receptor internalization increased incrementally up to 3 h after termination of FSS (3.5 h after the initiation of FSS, n = 3 for each group, $P < 0.001$, one-way ANOVA with post hoc *t*-test comparison), whereas it became insignificant 3 h after 5-HT administration. Notably, 5-HT_{2A} receptor internalization was significantly enhanced even 24 h after FSS (**Fig. 3-10D**).

Such short duration of 5-HT-induced 5-HT_{2A} receptor internalization in neuronal cells is consistent with the lack of significant changes regarding 5-HT_{2A} receptor internalization in the PFC neurons between mice with and without 5-HTP injected >30 min before the transcardial PFA infusion for *in vivo* analysis. Further, morphological changes of Neuro2A cells into round shape were observed after FSS, while Neuro2A cells kept their morphology with the processes after 5-HT administration (**Fig. 3-11A**) I did not detect significant caspase-3 activation, which is typically observed in apoptotic cells[98], for at least 24 h subsequent to FSS (n = 3 for each group, P = 0.119, Student's unpaired two-tailed *t*-test, >30 cells counted; **Fig. 3-11B** and **3-11C**). These findings suggest that the mechanisms of 5-HT_{2A} receptor shuttling/recycling are at least partially distinct between post-FSS application and post-5-HT administration.

On the other hand, 5-HT administration increased intracellular Ca^{2+} concentration in Neuro2A cells, however, this effect was attenuated by pre-FSS treatment (n = 4 for each group, P = 0.0138, one-way ANOVA with Bonferroni's post hoc test, 50 cells analyzed; **Fig. 3-12A** and **3-12B**). Consistent with the result of intracellular Ca^{2+} concentration, I observed via immunostaining analysis that FSS alleviated 5-HT-induced extracellular signal-regulated kinase (ERK) activation (n = 4 for each group, P = 0.0058, one-way ANOVA with Bonferroni's post hoc test, 50 cells analyzed; **Fig. 3-12C** and **3-12D**). Collectively, these results indicate that FSS desensitizes neuronal cells to 5-HT by inducing prolonged 5-HT_{2A} receptor internalization that involves a mechanism discrete from apoptotic processes.

PKC is involved in both FSS-induced 5-HT_{2A} receptor internalization *in vitro* and PHM-attenuated HTR *in vivo*

Next, I looked into whether FSS-induced desensitization of neuronal cells to 5-HT was relevant to the attenuation of HTR by PHM. It has been reported that HTR is up-regulated in mice that are genetically defective in PKCγ[137], the major PKC subtype expressed in neuronal cells[138]. As described above, PKC is activated by FSS. Therefore, I examined whether PKCγ was involved in 5-HT_{2A} receptor internalization after the application of FSS *in vitro*. When I analyzed Neuro2A cells by immunostaining, I found that FSS (2 Pa, 30 min) enhanced phosphorylation of MARCKS, a major PKC substrate[139]. However, FSS-induced MARCKS phosphorylation was hardly observed in Neuro2A cells pre-treated with a PKC inhibitor, Ro 31-8220 (**Fig. 3-13A**). In addition, after FSS application I observed decreased nuclear distribution of PKCγ, which has been demonstrated to relate to its activation in cultured neurons[140] (**Fig. 3-13B**). Furthermore, PKC inhibition significantly attenuated 5-HT_{2A} receptor internalization in Neuro2A cells after 5-HT administration or FSS application (n = 3 for each group, Left chart: $P < 0.001$; Right chart: $P = 0.0107$, Student's unpaired two-tailed *t*-test, 100 cells counted; **Fig. 3-14A** and **3-14B**). These results suggest that PKC activation is responsible for FSS-induced desensitization of neuronal cells to 5-HT.

Then, I tested if PKC activation was involved in 5-HT_{2A} receptor internalization *in vivo*, as indicated in the suppressive effect of PHM on HTR. When we injected Ro 31-8220 prior to each bout of daily PHM for a week (**Fig. 3-14C**), there was an increase in HTR after 5-HTP administration, nullifying the effects of PHM on HTR (n = 5 for Ro 31-8220 group, n = 8 for PHM groups with or without Ro 31-8220, details are described in the ***legend*** of **Fig. 3-14D** and **3-14E**). Histologically, the effects of PHM on c-Fos expression (n = 4 for each group, $P > 0.5$ for n.s., one-way ANOVA with Bonferroni's post hoc test; **Fig. 3-15A** and **3-15B**) and 5-HT_{2A}

receptor internalization in the PFC neurons were significantly reduced by Ro 31-8220 pre-administration (n = 3 for each group, Internalized: $P > 0.5$ for n.s., one-way ANOVA; Membrane-associated: $P > 0.5$ for n.s., one-way ANOVA with Bonferroni's post hoc test; **Fig. 3-15C** and **3-15D**). All in all, I conclude that PKCγ activation is at least partly responsible for FSS-induced desensitization of neuronal cells to 5-HT *in vitro* as well as the suppressive effect of PHM on HTR after 5-HTP administration *in vivo*. These findings support the notion that FSS-induced desensitization of neuronal cells *in vitro* is relevant to the suppression of HTR by PHM *in vivo*.

Discussion

In this chapter, I demonstrated that mechanical perturbation on brain *in vivo*, as well as on cultured neuronal cells *in vitro*, gives rise to desensitization to 5-HT through mechanically-induced, ligand-independent internalization of a 5-HT receptor. Furthermore, I show that an inhibition of protein kinase C (PKC) hampers mechanical desensitization of neurons *in vivo* and neuronal cells *in vitro* to 5-HT.

Internalization of 5-HT_{2A} receptor was commonly observed in PFC neurons of mice after treadmill running or PHM, therefore, I postulated a common regulatory mechanism underlying this internalization. Exercise is known to increase 5-HT production and release in rodent brain[23,141]. However, the effects of exercise are site-dependent, and 5-HT concentration in the rodent cerebral cortex stays unchanged[142] or even decreases after exercise[143]. Therefore, 5-HT_{2A} receptor internalization observed after a week of daily treadmill running is likely to be instigated ligand-independently, rather than result from increased local 5-HT concentration in the PFC. In addition, extracellular 5-HT concentration in rat brain has been reported to be significantly decreased by isoflurane anesthesia[144], which was used during our PHM experiments. Because ligand-dependent internalization thus appeared unlikely to be responsible, I hypothesized that 5-HT_{2A} receptor might be internalized in PFC neurons as a cellular response to mechanical forces generated by treadmill running or PHM.

I observed mechanical stress facilitates ligand-independent internalization of 5-HT_{2A} receptor both *in vivo* and *in vitro*. In particular, fluid shear stress (FSS) showed prolonged internalization of the receptor. On the other hand, in consistent with previous reports[34,117], 5-HT_{2A} receptor undergoes ligand-dependent internalization which presents rapid endocytosis, desensitization of the receptor and recycling to the plasma membrane. Some studies reported

FSS induces endocytosis of GPCR, but specific mechanisms are poorly understood[78]. But, it is suggested that changes of actin fiber formation by FSS may be related to the effect of endocytosis[145]. I also observed the changes of cellular morphology after FSS application whereas 5-HT exposure did not change cellular formations. Thus, it is possible that cytoskeletal transformation may lead prolonged desensitization of 5-HT receptor. Moreover, considering that FSS-induced internalized GPCR activates ERK signaling and is co-localized with late endosome and LAMP-1[78,146,147], I assumed that prolonged internalized 5-HT_{2A} receptor may undergo to degradation processes; like angiotensin type 1 receptor[148]. However, in this study, I could not prove decreased 5-HT_{2A} receptor level using immunoblots with PFC tissue sample.

It is evident that activation of PKC induces internalization of GPCRs[125-127]. Activation PKC phosphorylates 5-HT_{2A} receptor which causes beta-arrestin to bind the receptor[123]. Then, receptor and G protein coupling is compromised and the arrestin-mediated internalization is facilitated. On the other hand, application of fluid shear stress activates PKC[75,124]. It is described that increased intracellular calcium concentration which is mediated by phospholipase C causes activation of PKC[149,150]. However, the specific mechanisms by which FSS-induced phospholipase C activation are unknown although several signal transducers have been proposed[151]. Along with PKC, many studies proposed that FSS-stimulated signal transductions are integrin-mediated events[152-154]. This suggests that the cytoskeletal adaptations to mechanical stress fundamentally involve in cellular regulations. Overall, in consistent with previously described studies, I observed that FSS facilitates the internalization of 5-HT receptor.

The most important observation in this chapter is that mechanical head movement recapitulates the effect of treadmill running on the neurological behavior response. To date, mechanical stress on the brain has been almost solely documented in the context of traumatic brain injury. However, my result may shed light on the positive aspect of mechanical effects on the CNS. I demonstrated that PHM in rodents, which generates vertical accelerations at their

heads similar to those during treadmill running, changes interstitial fluid flow and produces fluid shear stress in the CNS. Subsequently, I showed that responses of neuronal cells to FSS derived from head motion-induced interstitial fluid flow in the brain are responsible for the suppression of 5-HT signaling.

In summary, my results indicate that mechanical perturbation on the brain modulates 5-HT_{2A} receptor signaling in the PFC, and could partially answer the question of how physical training (exercise) have influences on CNS functions. This suggestion can explain the result of ***Chapter 2*** in my thesis. While I could not directly demonstrate mechanical stress-induced suppression of 5-HT receptor hypersensitivity in the spinal cord, I believe that physical training would induce the suppression of 5-HT receptor sensitivity which leads to ameliorate spasticity after spinal cord injury by similar mechanism.

In addition, this chapter suggests that the effects of walking and running on emotional regulation[155] may involve serotonergic modulations in the cerebral cortex induced by mechanical impact on the head. The beneficial effects of exercises as the prevention and treatment for a variety of diseases and health disorders may rely at least partly on modest impact on the brain, which generates optimal fluid shear stress on the CNS.

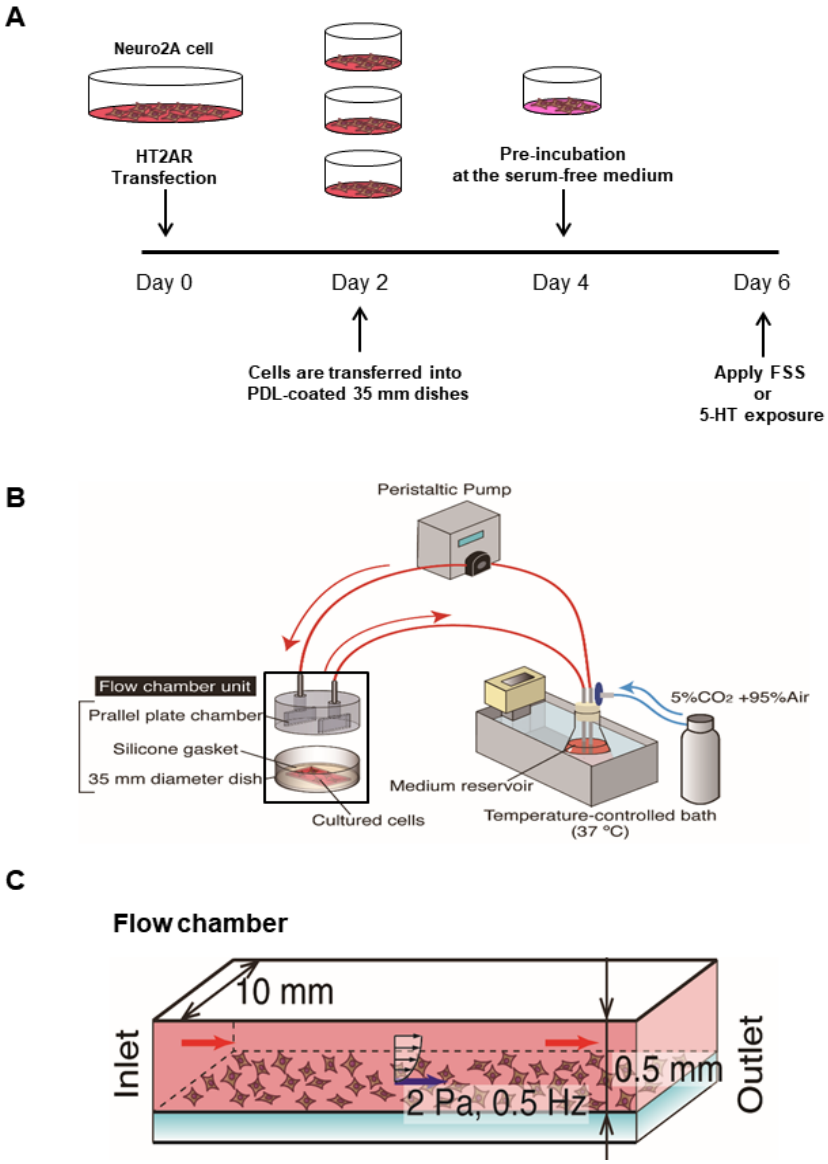

Figure 3-1. Configuration of cultured neuronal cell preparation and experimental set-up to exert fluid shear stress (FSS) on the cells

(**A**) Experimental scheme about preparation of transfected Neuro2A cells for FSS application and 5-HT exposure. (**B**) Experimental configuration about flow exposure system for applying FSS on the neuronal cells. This system is consisting of one flow chamber, a roller pump, two reservoirs and temperature-controlled bath. (**C**) Detailed illustration of a flow chamber used in this study (the black box represented in **B**). The fluid flow was delivered as 0.5 Hz frequency via 10-mm-wide and 0.5-mm-high flow chamber to deliver average 2 Pa of FSS.

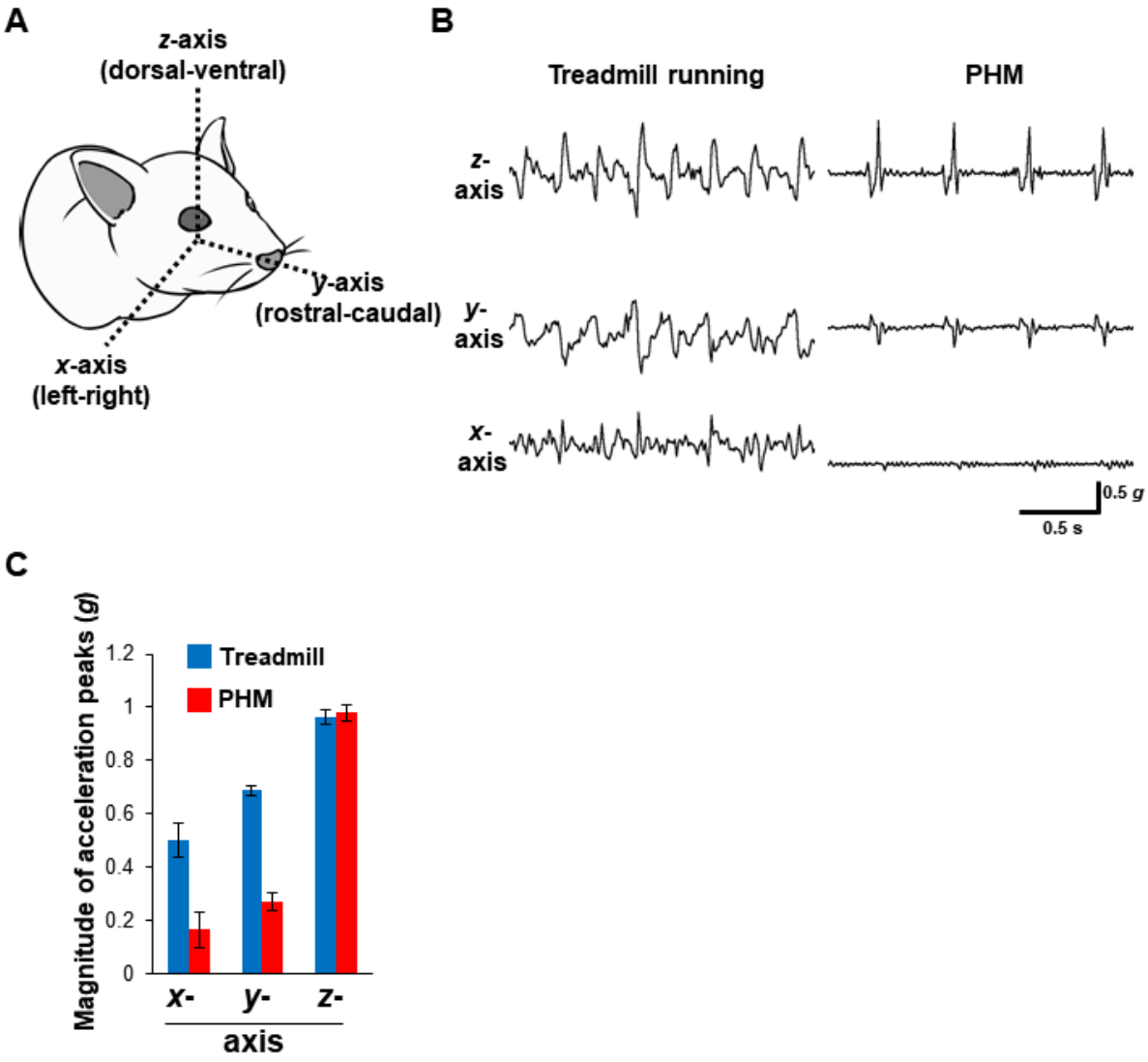

Figure 3-2. Measurement of accelerations generated at rats' heads during treadmill running and PHM

(**A**) Definition of *x*-(left-right), *y*-(rostral-caudal), and *z*-(dorsal-ventral) axes used in this study. (**B**) Accelerations generated at the rats' heads during treadmill running (velocity: 20 m/min) and PHM (frequency: 2 Hz). The head drop by the PHM system was adjusted to 5 mm to produce 1.0 *g* vertical acceleration peaks. Right-angled scale bar, 0.5 *g* / 0.5 s. (**C**) Peak magnitudes of accelerations for *x*-, *y*-, and *z*-axes during treadmill running and PHM (n = 3 for each group).

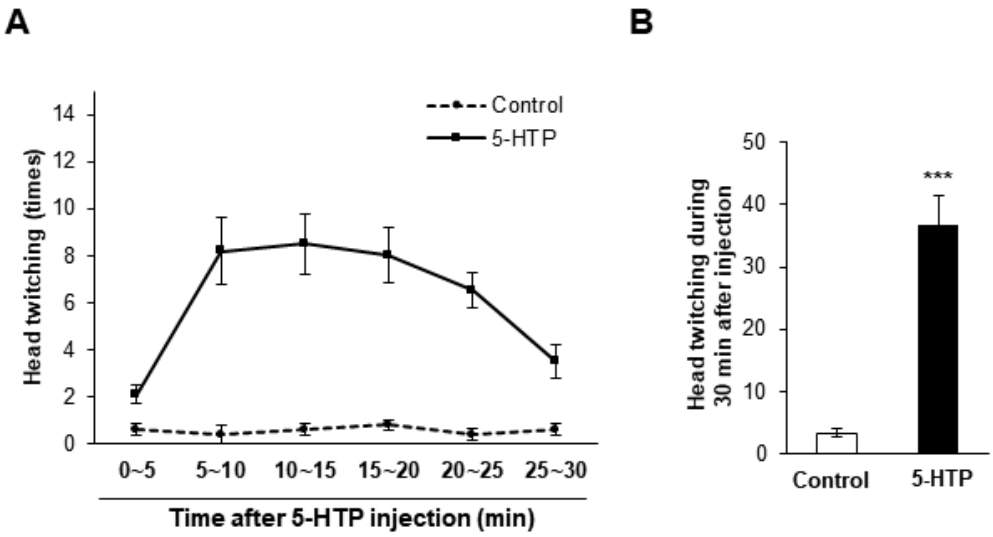

Figure 3-3. Counting head twitching after 5-HTP administration in wild-type C57/BL6 mice

(**A**) and (**B**) Quantification of 5-HTP-induced HTR. Line chart of head twitching count in 5-min blocks for 30 min (**A**) and histogram of total head twitching count (**B**) after injection of 5-HTP or saline (Control). ***, $P < 0.001$.

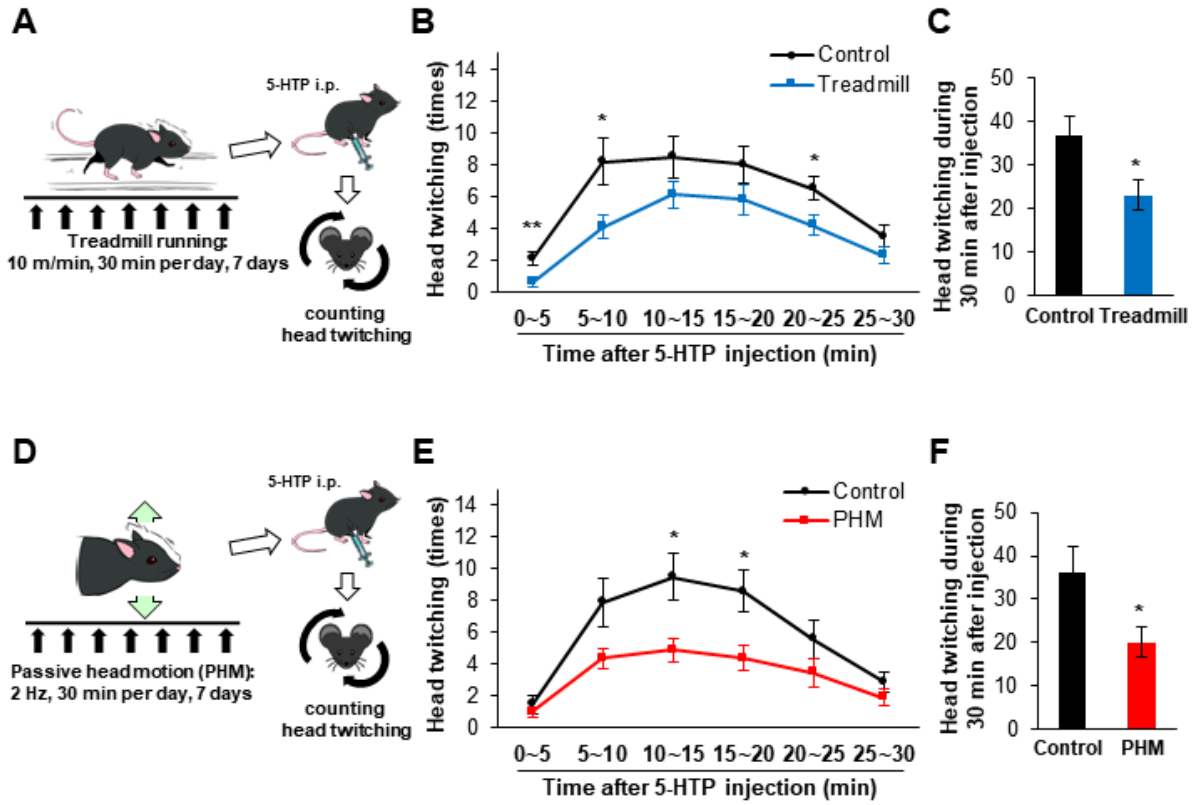

Figure 3-4. Treadmill running and PHM decrease head-twitch response

(**A**) Schematic representation of experimental protocol for analysis of the effects of treadmill running on HTR. (**B**) and (**C**) Treadmill running alleviated 5-HTP-induced HTR. Count of head twitching in 5-min blocks (**B**) and for 30 min (**C**) post-5-HTP injection. (**D**) Schematic representation of experimental protocol for analysis of the effects of PHM on HTR. PHM (cyclical 5-mm head drop) was applied to generate vertical accelerations of 1.0 *g* peaks at the heads of mice (2 Hz, 30 min per day, 7 days). (**E**) and (**F**) PHM alleviated 5-HTP-induced HTR. Head twitching was counted as in (**B**) and (**C**), respectively.

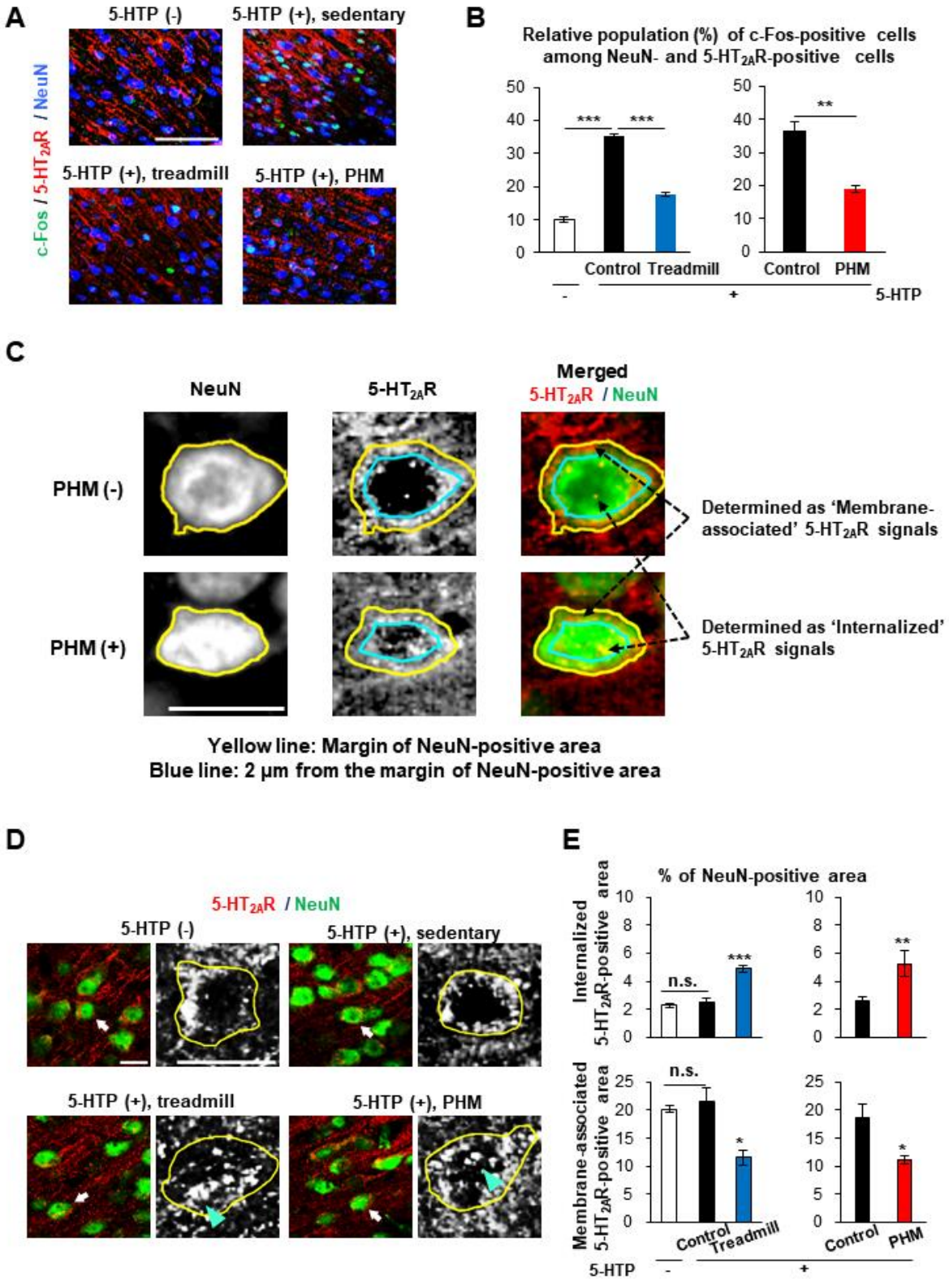
A
5-HTP (-)
5-HTP (+), sedentary
5-HTP (+), treadmill
5-HTP (+), PHM
c-Fos / 5-HT2AR / NeuN
B
Relative population (%) of c-Fos-positive cells among NeuN- and 5-HT2AR-positive cells
Control Treadmill
Control PHM
5-HTP
C
NeuN
5-HT2AR
Merged
5-HT2AR / NeuN
PHM (-)
PHM (+)
Determined as 'Membrane-associated' 5-HT2AR signals
Determined as 'Internalized' 5-HT2AR signals
Yellow line: Margin of NeuN-positive area
Blue line: 2 μm from the margin of NeuN-positive area
D
5-HT2AR / NeuN
5-HTP (-)
5-HTP (+), sedentary
5-HTP (+), treadmill
5-HTP (+), PHM
E
% of NeuN-positive area
Internalized 5-HT2AR-positive area
Membrane-associated 5-HT2AR-positive area
n.s.
Control Treadmill
Control PHM
5-HTP

Figure 3-5. Treadmill running and PHM modulate neuronal response to 5-HT

(**A**) Micrographic images of anti-c-Fos (green), anti-5-HT_{2A} receptor (5-HT_{2A}R; red) and anti-NeuN (blue) immunostaining of the PFC of mice injected with saline or 5-HTP (upper column) and 5-HTP injected mice after a week of daily treadmill running or PHM (lower column). Scale bar, 100 μm. (**B**) Both treadmill running and PHM decreased c-Fos expression in 5-HT_{2A} receptor-positive neurons of mouse PFC. Relative population (%) of c-Fos-positive cells out of 300 NeuN- and 5-HT_{2A} receptor-positive cells is shown. (**C**) Schematic representation of the definition as to 'membrane-associated' and 'internalized' anti-5-HT_{2A} receptor immunosignals used for the quantification in (**D**) and (**E**). Yellow lines indicate the margins of somas outlined by anti-NeuN immunosignals. Blue lines represent 2 μm inside the soma margins. Scale bars, 20 μm. (**D**) Micrographic images of anti-5-HT_{2A} receptor (red) and anti-NeuN (green) immunostaining of the PFC of mice injected with vehicle or 5-HTP (upper column) and 5-HTP injected mice after a week of daily treadmill running or PHM (lower column). High magnification images of anti-5-HT_{2A} receptor immunostaining of arrow-pointed cells are presented with a gray scale. Yellow lines indicate the margins of somas outlined by NeuN-positive signals, and cyan arrowheads point to internalized anti-5-HT_{2A} receptor immunosignals. Scale bars, 20 μm. (**E**) Quantification of internalized and membrane-associated 5-HT_{2A} receptor-positive area relative to NeuN-positive area in mouse PFC. Approximately, 40 NeuN-positive neuronal somas were analyzed for each animal.

*, $P < 0.05$; **, $P < 0.01$; ***, $P < 0.001$; n.s., not significant.

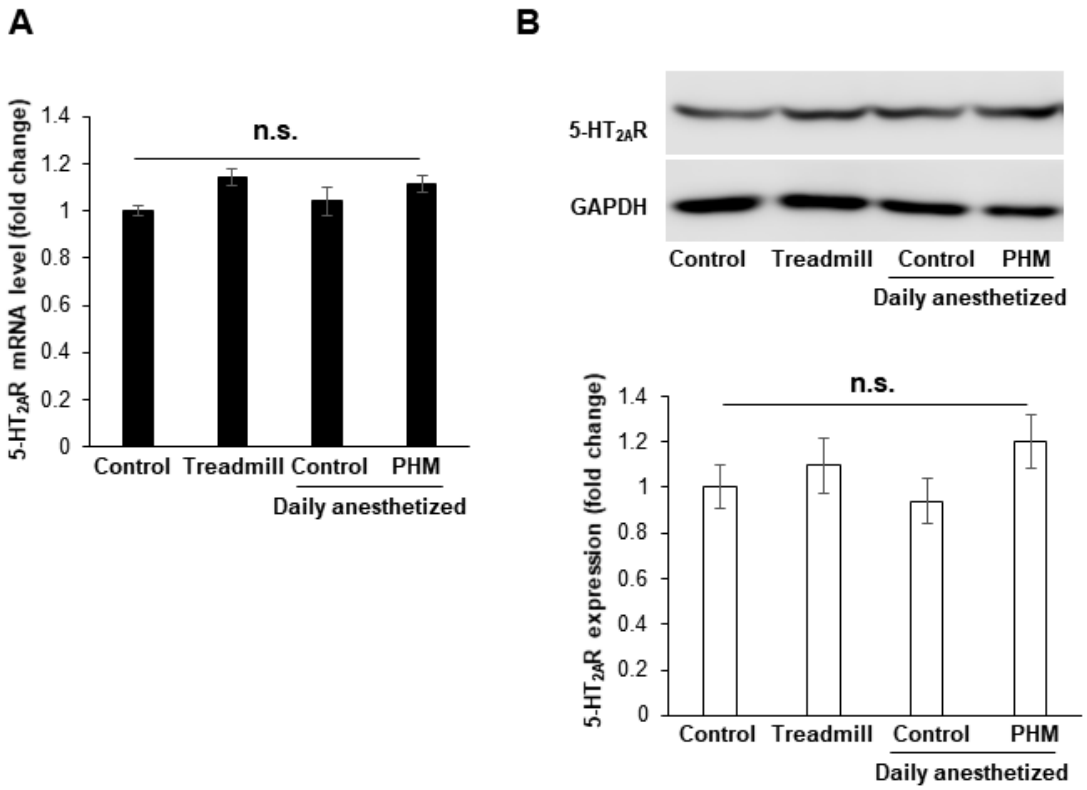

Figure 3-6. Neither treadmill running nor PHM significantly alters expression levels of 5-HT$_{2A}$ receptor in mouse PFC

mRNA (**A**) and protein (**B**) expressions of 5-HT$_{2A}$ receptor in mouse PFC were quantified with the mean value of control samples (column 1 or lane 1 in each panel) set as 1. n.s., not significant.

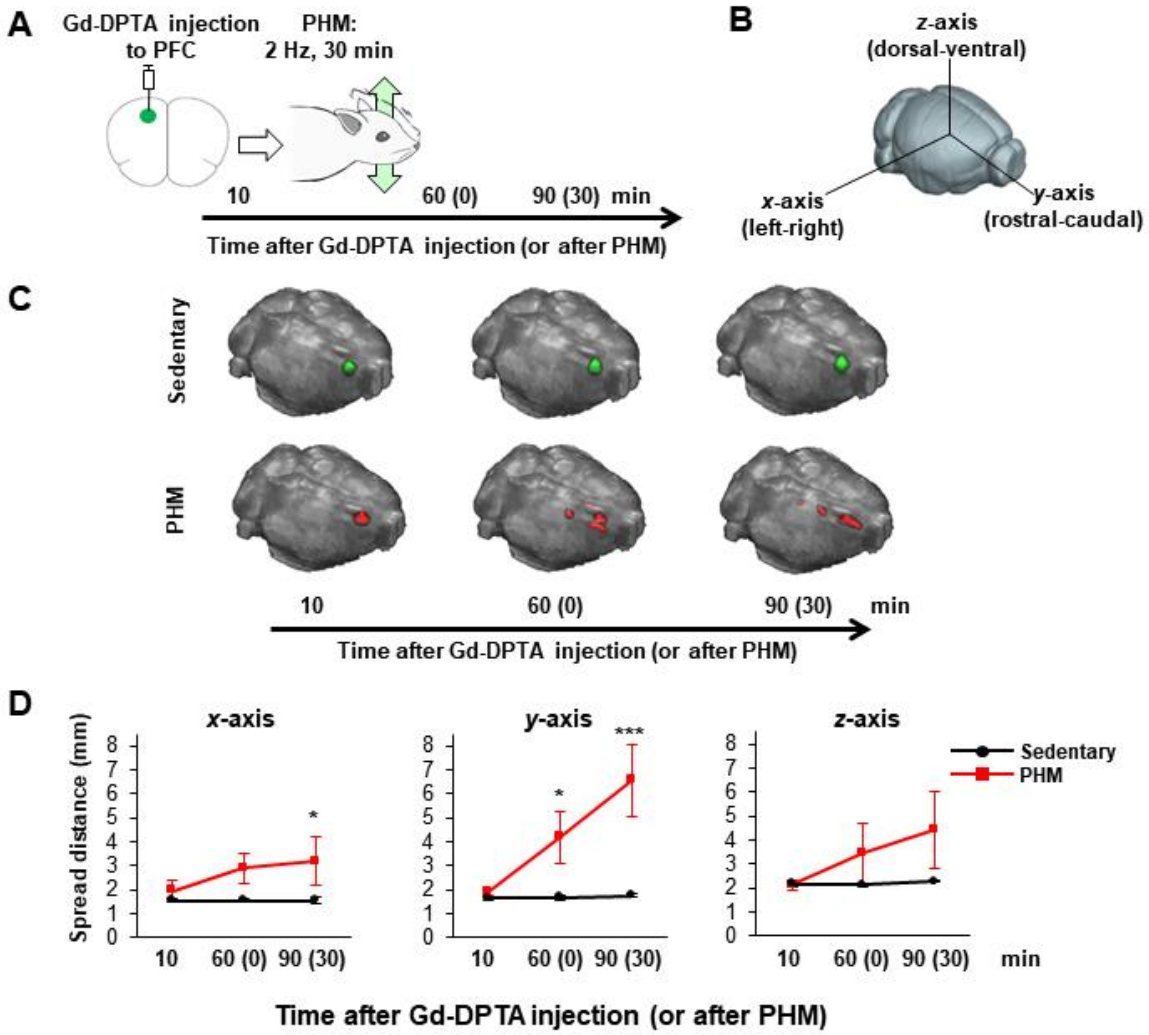

Figure 3-7. MRI analysis reveals the distribution of cerebral interstitial fluid flow at the PFC is altered by PHM

(**A**) Schematic representation of experimental protocol for MRI analysis of Gd-DTPA injected in rats' PFC. (**B**) Definition of *x*-(left-right), *y*-(rostral-caudal), and *z*-(dorsal-ventral) axes used in this study. (**C**) Representative Gd-DTPA spreading presented on a surface rendered brain. Gd-DTPA clusters are indicated by green (sedentary) and red (PHM). (**D**) Quantification of Gd-DTPA spreading along each axis. Red line: PHM (n = 5), Black line: sedentary (n = 5). *, $P < 0.05$, ***, $P < 0.001$.

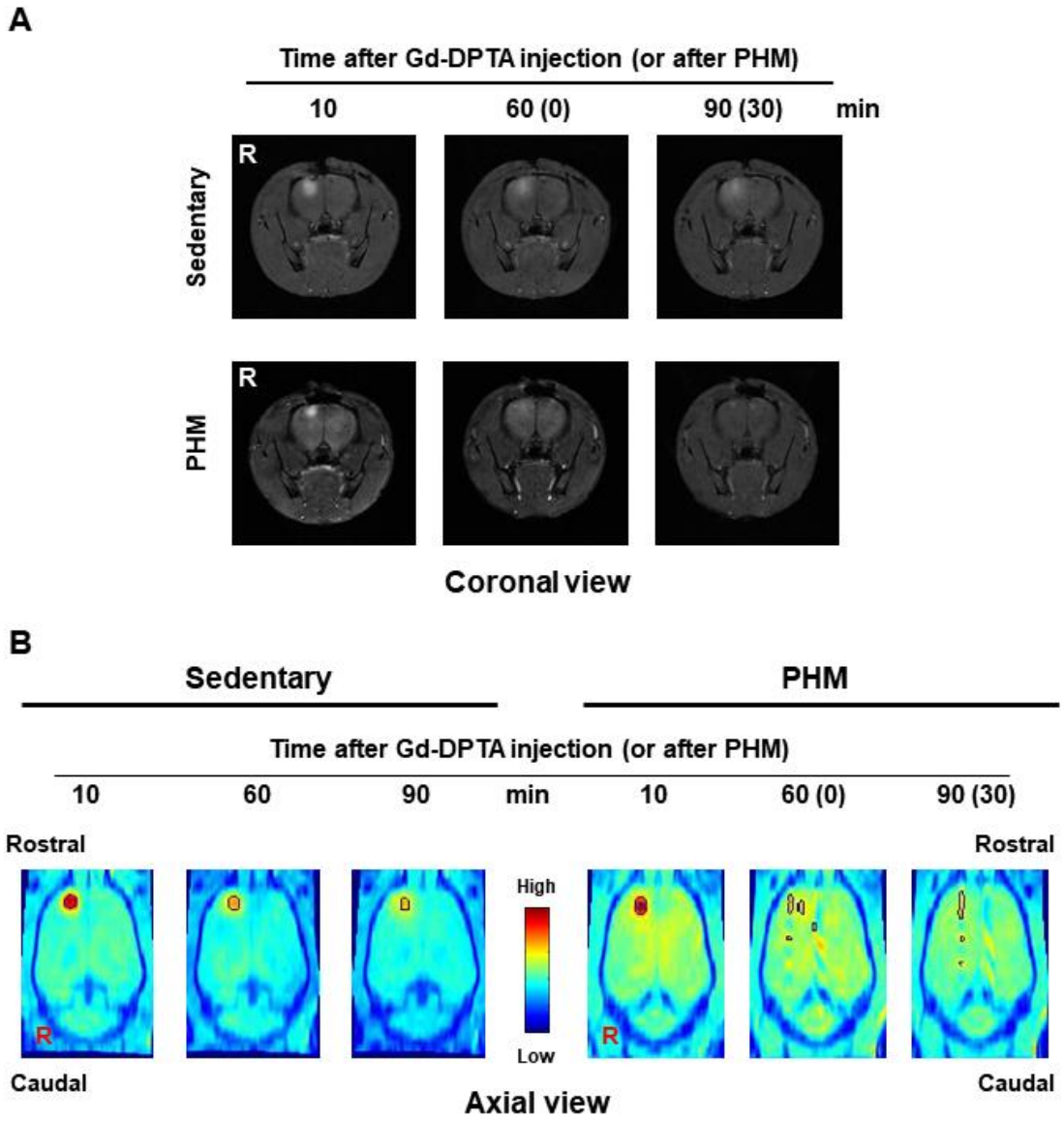

Figure 3-8. MRI analysis of spreading of Gd-DPTA injected in rats' PFC

(**A**) Representative coronal view slices of MRI scanned 10, 60 and 90 min after Gd-DTPA injection (before, and 0 and 30 min after PHM). 'R' indicates the right side. (**B**) Pseudo-color presentation of MR signal intensity. Gd-DPTA clusters were defined as voxels of top 0.05% intensity marked with black lines. The original MRI data for the slices shown in (**A**) and for the intensity shown in (**B**) are identical (from the same rats) in both sedentary and PHM-applied rats.

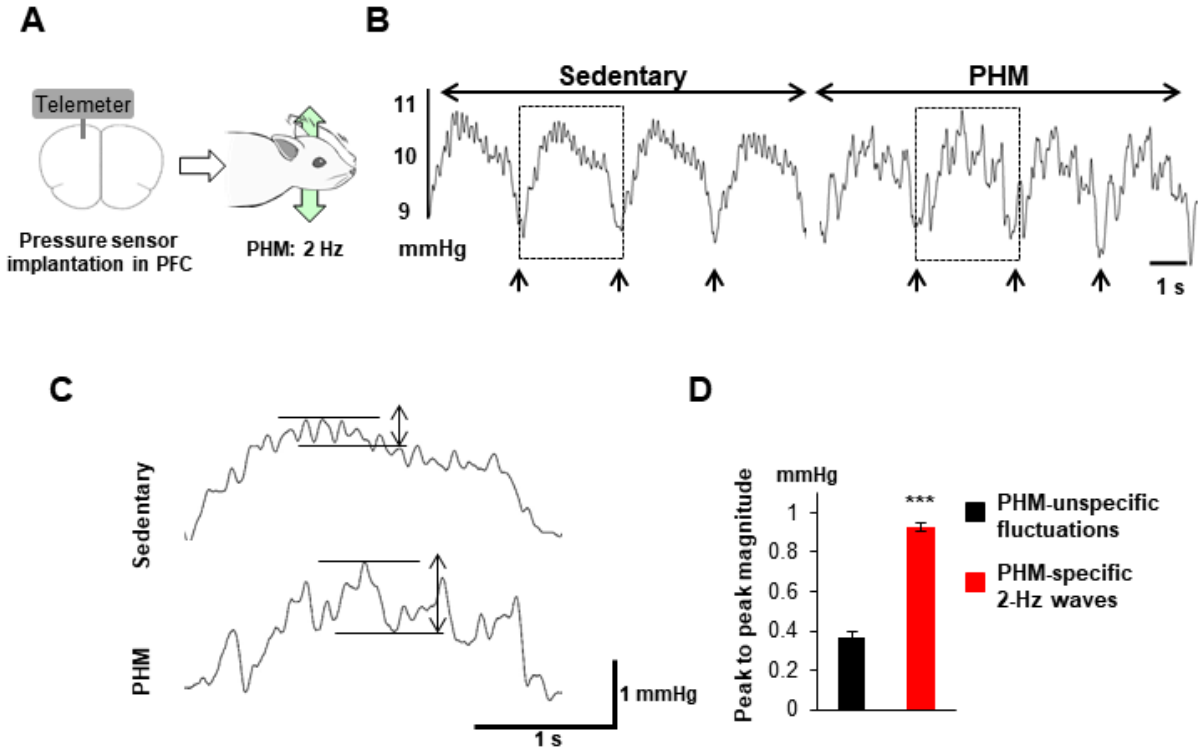

Figure 3-9. PHM changes intracerebral pressure at the PFC

(**A**) Schematic representation of ICP measurement at rats' PFC. (**B**) Representative ICP waves recorded in rats' PFC during sedentary condition and PHM. Arrows indicate the time points of transition from inhalation to exhalation detected by simultaneous respiration monitoring. Scale bar, 1 s. (**C**) Respiration-unsynchronized ICP changes. Respiration-synchronized ICP waves indicated by rectangles in (**B**) are presented with high magnification. Right-angled scale bar, 1 s / 1 mmHg. Note that 2-Hz ICP waves indicated by an arrow were specifically generated during PHM. (**D**) Magnitude of PHM-specific and -unspecific ICP changes unsynchronized with respiration. Peak to peak magnitudes indicated by arrows in (**C**) were quantified. ***, $P < 0.001$.

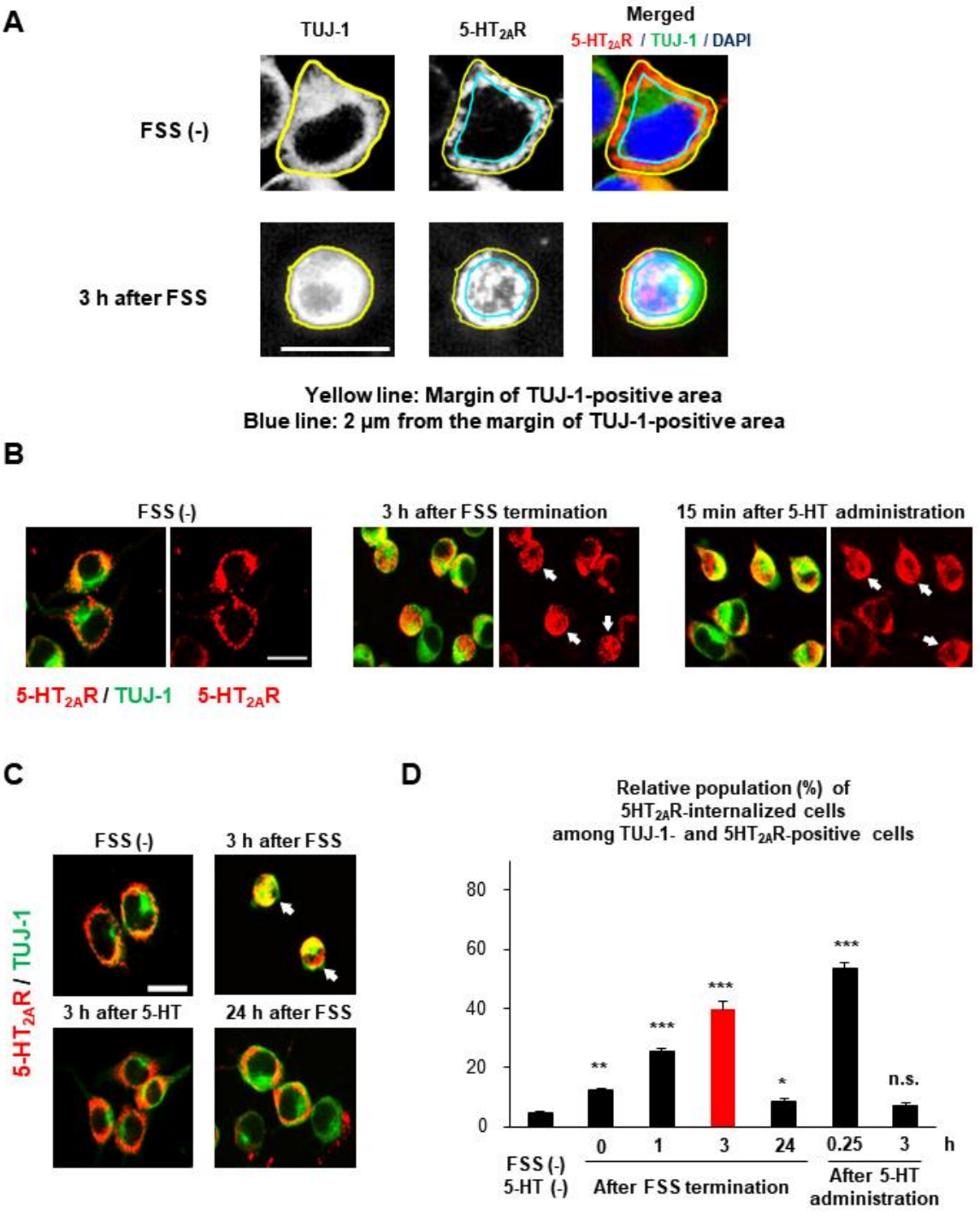
A
TUJ-1
5-HT2AR
Merged
5-HT2AR / TUJ-1 / DAPI
FSS (-)
3 h after FSS
Yellow line: Margin of TUJ-1-positive area
Blue line: 2 μm from the margin of TUJ-1-positive area
B
FSS (-)
3 h after FSS termination
15 min after 5-HT administration
5-HT2AR / TUJ-1
5-HT2AR
C
FSS (-)
3 h after FSS
3 h after 5-HT
24 h after FSS
5-HT2AR / TUJ-1
D
Relative population (%) of
5HT2AR-internalized cells
among TUJ-1- and 5HT2AR-positive cells
80
60
40
20
0
**
***
***
*
***
n.s.
0
1
3
24
0.25
3
h
FSS (-)
5-HT (-)
After FSS termination
After 5-HT
administration

Figure 3-10. Fluid shear stress internalizes 5-HT$_{2A}$ receptor expressed in neuronal cells

(**A**) Schematic images related to counting 5-HT$_{2A}$ receptor-internalized cells used for the quantification in (**D**). Yellow lines indicate the margins of neuronal somas outlined by anti-TUJ-1 immunosignals. Blue lines represent 2 μm inside from the soma margins. Scale bars, 20 μm. (**B**) 5-HT$_{2A}$ receptor was internalized after fluid shear stress (FSS). Neuro2A cells grown in a poly-D-lysine-coated dish were subjected to pulsatile FSS (average 2 Pa, 0.5 Hz, 30 min) or treated with 5-HT (10 μM), fixed, and stained for 5-HT$_{2A}$ receptor (5-HT$_{2A}$R; red). To differentiate the cytoplasm of neuronal cells from their cell membranes, co-immunostaining of TUJ-1 was conducted (green). Left, control. Middle, 3 h after the termination of FSS. Right, 15 min after 5-HT administration. Arrows point to cells with internalized 5-HT$_{2A}$ receptor. Scale bar, 20 μm. (**C**) 5-HT$_{2A}$ receptor internalization lasted longer after FSS, as compared with after 5-HT administration. Micrographic images of Neuro2A cells, with and without FSS application, stained for 5-HT$_{2A}$ receptor (5-HT$_{2A}$R; red) and TUJ-1 (green). Arrows point to cells with internalized 5-HT$_{2A}$ receptor. Scale bar, 20 μm. (**D**) Quantification of 5-HT$_{2A}$ receptor internalization. Cells with internalized 5-HT$_{2A}$ receptor were counted out of 100 TUJ-1- and 5-HT$_{2A}$ receptor-positive cells in micrographs of immunostaining. *, $P < 0.05$; **, $P < 0.01$; ***, $P < 0.001$.

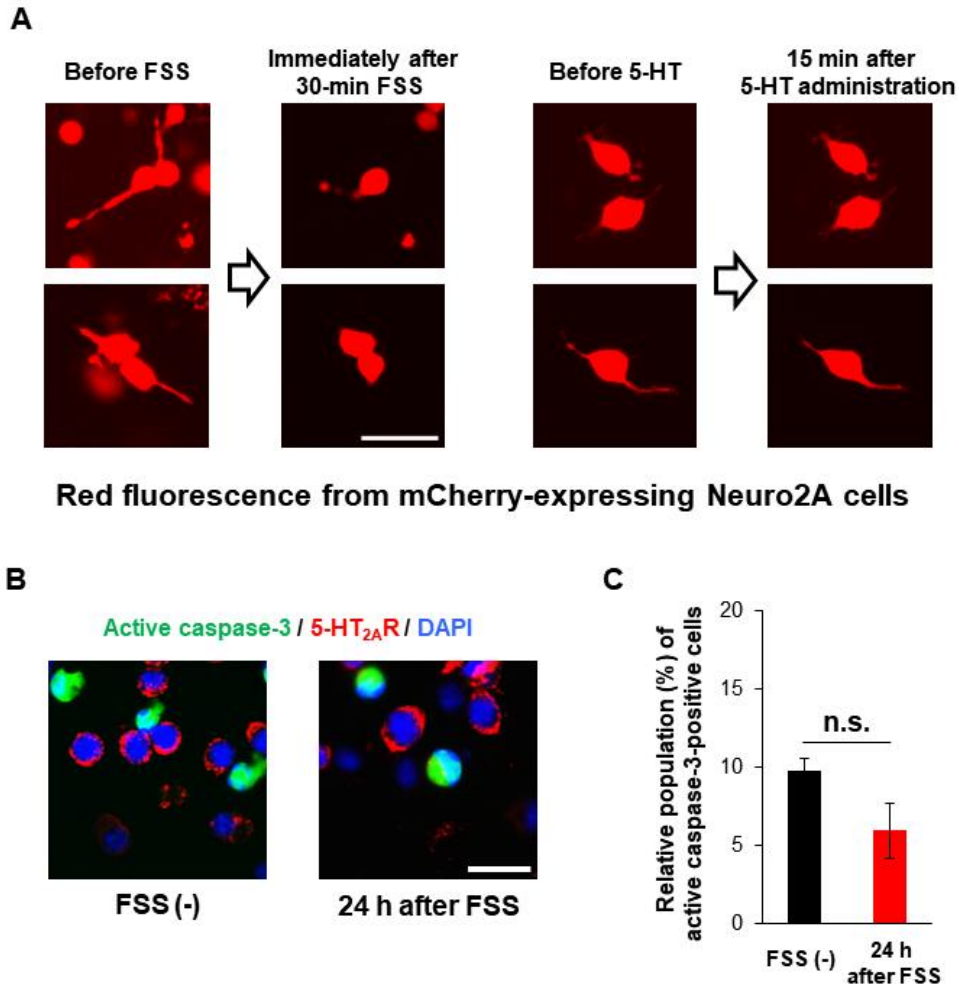

Figure 3-11. FSS induce morphological change of neuronal cells without apparent apoptosis

(**A**) Neuronal cells became rounded after FSS. mCherry was exogenously expressed in Neuro2A cells to facilitate monitoring cell shape changes. Live cell images of mCherry-expressing cells before and after FSS application (average 2 Pa, 0.5 Hz, 30 min) or 5-HT administration (10 μM, 15 min) are shown. Scale bar, 50 μm. (**B**) Micrographic images of anti-active caspase-3 (green) and anti-5-HT_{2A} receptor (5-HT_{2A}R; red) immunostaining of Neuro2A cells 24 h after 30-min FSS application (right) and cells left unexposed to FSS (left) are shown together with nuclear staining (DAPI, blue). Scale bar, 25 μm. (**C**) Relative population of active caspase-3-positive cells among total cells. n.s., not significant.

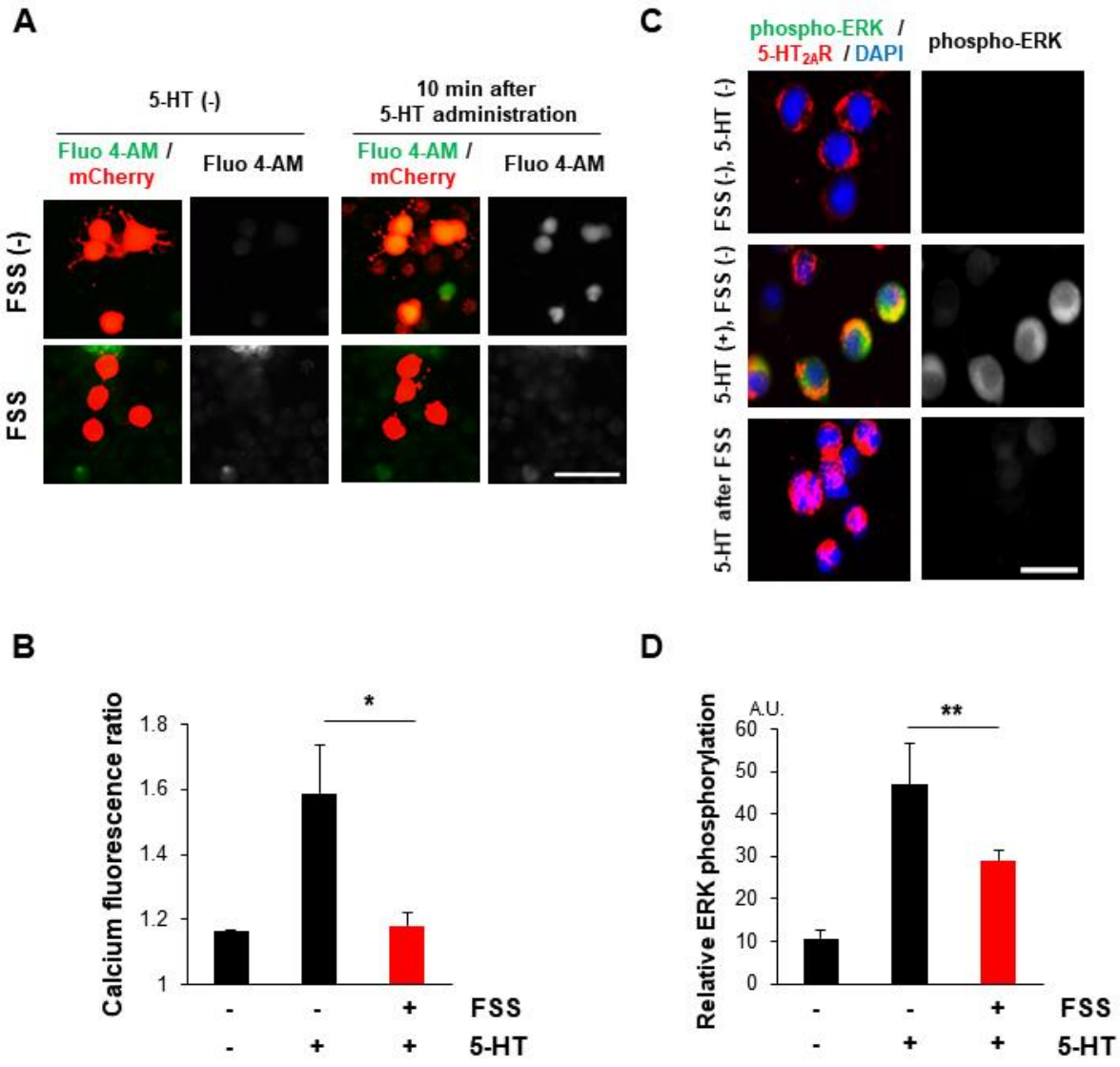
A
5-HT (-)
10 min after
5-HT administration
Fluo 4-AM /
mCherry
Fluo 4-AM
Fluo 4-AM /
mCherry
Fluo 4-AM
FSS (-)
FSS
C
phospho-ERK /
5-HT2AR / DAPI
phospho-ERK
FSS (-), 5-HT (-)
5-HT (+), FSS (-)
5-HT after FSS
B
Calcium fluorescence ratio
1.8
1.6
1.4
1.2
1
*
- - +
FSS
- + +
5-HT
D
Relative ERK phosphorylation
A.U.
60
50
40
30
20
10
0
**
- - +
FSS
- + +
5-HT

Figure 3-12. FSS modulates neuronal response to 5-HT *in vitro*

(**A**) FSS attenuated 5-HT-induced increase in intracellular Ca^{2+} concentration. Neuro2A cells were either exposed or left unexposed to FSS (average 2 Pa, 0.5 Hz, 30 min). After 3 h from the termination of FSS, cells were treated with 5-HT (10 μM) for 10 min, and subjected to measurement of intracellular Ca^{2+} concentration using Fluo 4-AM as described in Methods. Scale bar, 50 μm. (**B**) Intracellular Ca^{2+} concentration represented as relative fluorescence intensity with the mean fluorescence value from cells before 5-HT administration set at 1. *, $P < 0.05$; ***, $P < 0.001$. (**C**) FSS alleviated 5-HT-induced ERK phosphorylation in neuronal cells. Neuro2A cells were either exposed or left unexposed to pulsatile FSS (average 2 Pa, 0.5 Hz, 30 min). After 3 h from FSS termination, cells were treated with 5-HT (10 μM) for 15 min, fixed and stained for 5-HT_{2A} receptor (5-HT_{2A}R; red), phospho-ERK (green) and DAPI. Scale bar, 25 μm. (**D**) Quantification of anti-phospho-ERK immuno-intensity: Signal intensity of anti-phospho-ERK immunostaining was quantified using 'auto-threshold' of ImageJ (NIH, USA), and immuno-intensity was determined as arbitrary units (A.U.) by referring the cumulated intensity values to the total positive signal area.

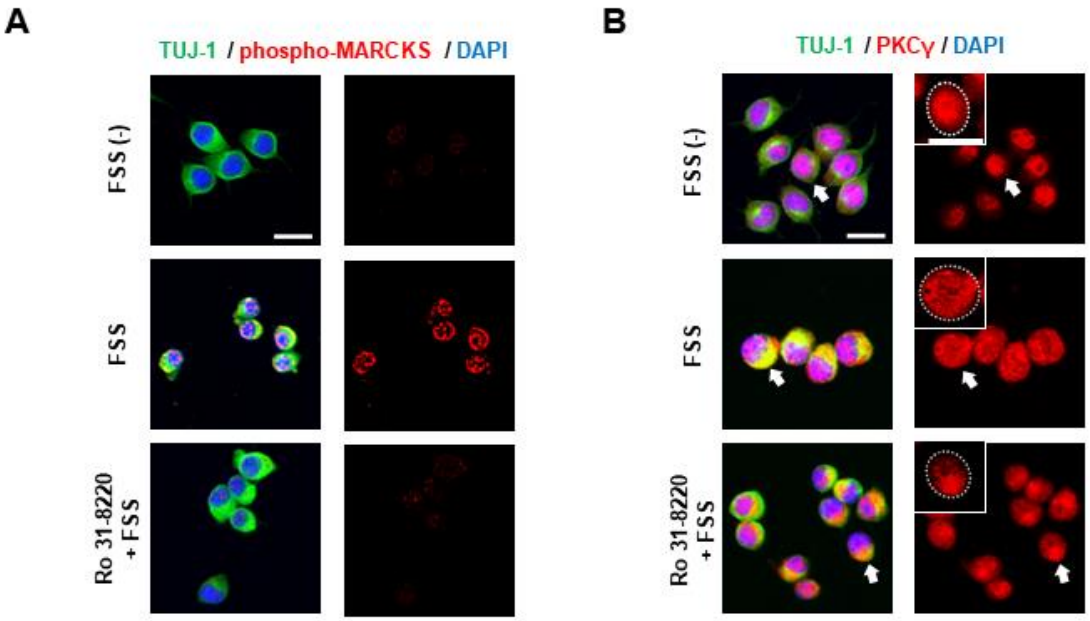

Figure 3-13. FSS is involved in the activation of protein kinase C

(**A**) and (**B**) MARCKS was phosphorylated in neuronal cells after FSS, depending on protein kinase C (PKC) activity. Neuro2A cells, either exposed or left unexposed to FSS (average 2 Pa, 0.5 Hz, 30 min) with and without PKC inhibitor pretreatment (Ro 31-8220; 4 μM, 1 h), were subjected to anti-TUJ-1 (green) and anti-phospho-MARCKS (red in **A**) or anti-PKCγ (red in **B**) immunostaining. Nuclei were stained with DAPI. High magnification images of anti-PKCγ immunostaining of arrow-pointed cells are presented with cell margins (white dash lines) as insets (**B**). Scale bars, 20 μm.

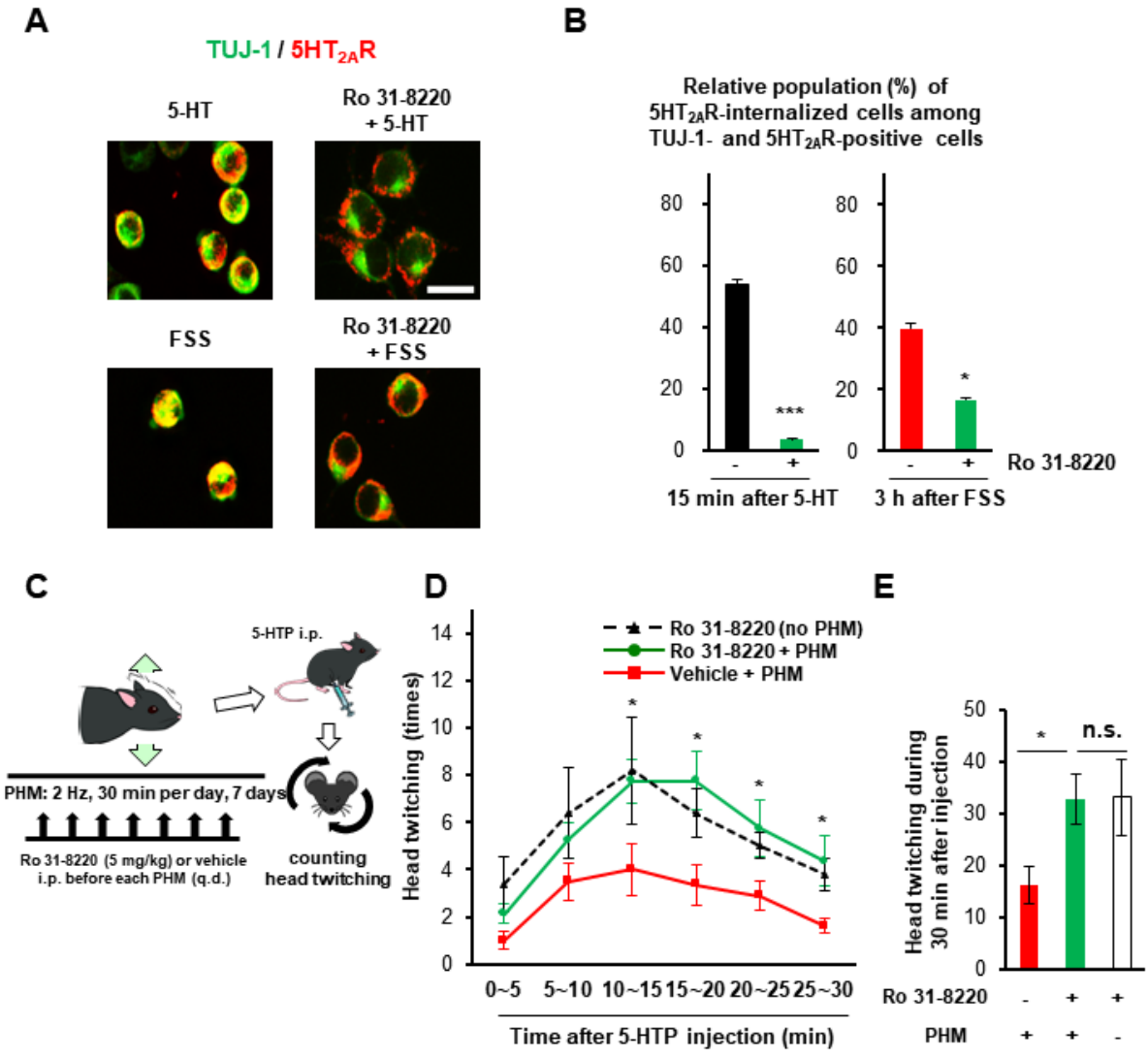
A
TUJ-1 / 5HT2AR
5-HT
Ro 31-8220 + 5-HT
FSS
Ro 31-8220 + FSS
B
Relative population (%) of 5HT2AR-internalized cells among TUJ-1- and 5HT2AR-positive cells
80
60
40
20
0
***
*
- +
Ro 31-8220
15 min after 5-HT
3 h after FSS
C
5-HTP i.p.
PHM: 2 Hz, 30 min per day, 7 days
Ro 31-8220 (5 mg/kg) or vehicle i.p. before each PHM (q.d.)
counting head twitching
D
Ro 31-8220 (no PHM)
Ro 31-8220 + PHM
Vehicle + PHM
Head twitching (times)
14
12
10
8
6
4
2
0
0~5 5~10 10~15 15~20 20~25 25~30
Time after 5-HTP injection (min)
E
Head twitching during 30 min after injection
50
40
30
20
10
0
*
n.s.
Ro 31-8220 - + +
PHM + + -

Figure 3-14. Inhibition of protein kinase C blocks FSS-mediated internalization of 5-HT2A receptor *in vitro* and PHM-attenuated HTR *in vivo*

(**A**) PKC inhibition hampered both 5-HT- and FSS-induced 5-HT_{2A} receptor internalization. Neuro2A cells with combinations of Ro 31-8220 pretreatment and 5-HT (10 μM) administration or FSS application (average 2 Pa, 0.5 Hz, 30 min) were fixed and stained for 5-HT_{2A} receptor (5-HT_{2A}R; red) and TUJ-1 (green). Scale bars, 20 μm. (**B**) Quantification of 5-HT_{2A} receptor internalization. (**C**) Schematic representation of the experimental protocol for PHM with PKC inhibition. Ro 31-8220 or vehicle was injected just before each bout of PHM. (**D**) and (**E**) PKC inhibition nullified the effect of PHM on 5-HTP-induced HTR. *, $P < 0.05$; **, $P < 0.01$, n.s., not significant. Asterisks (*) in (**D**) indicate statistical significance between PHM with (green line) and without (red line) Ro 31-8220 ($P = 0.158$, Student's unpaired two-tailed *t*-test), whereas there were no significant differences at any time point between Ro 31-8220 with (green line) and without (black line) PHM ($P = 0.981$, Student's unpaired two-tailed *t*-test).

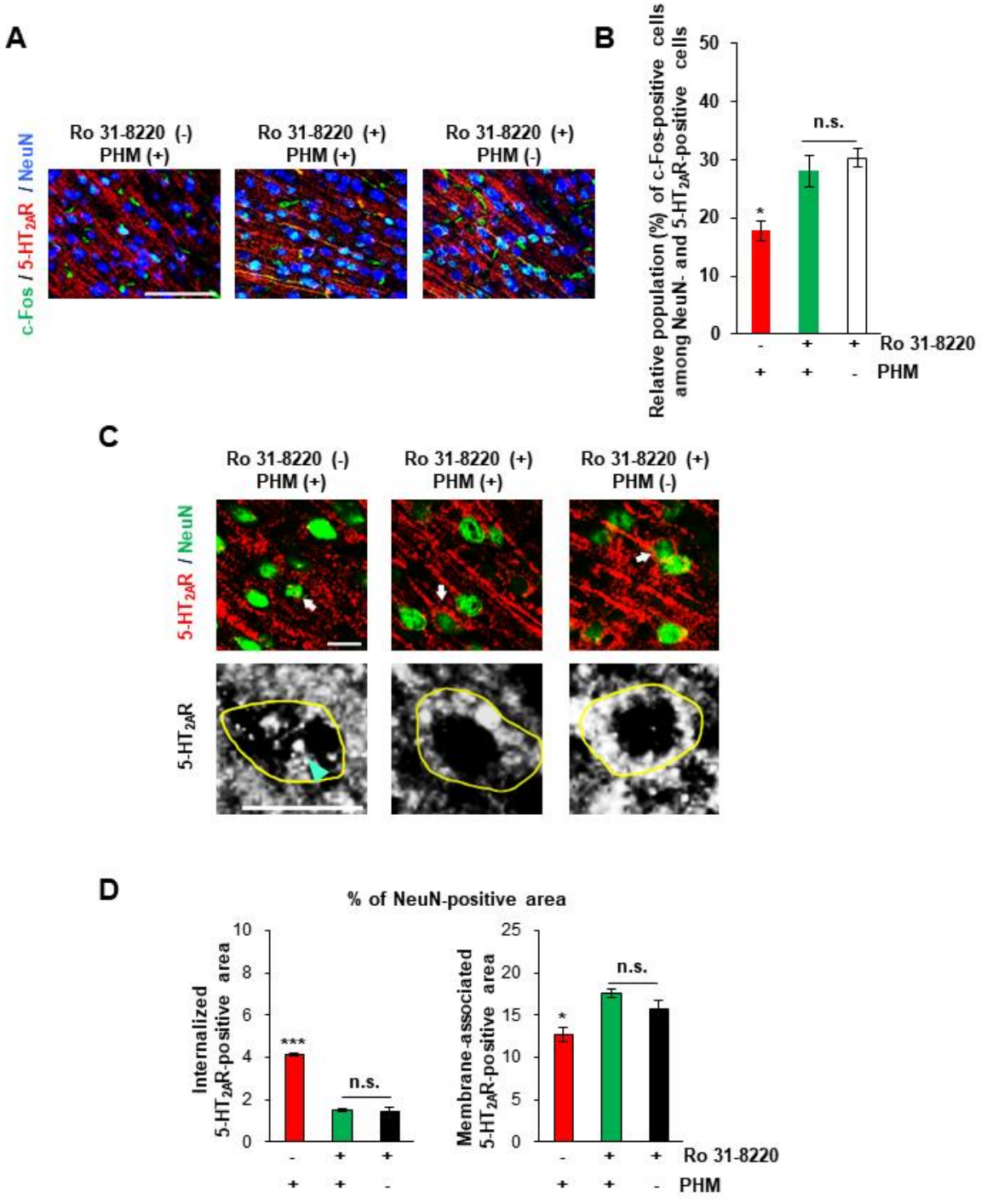
A
Ro 31-8220 (-)
PHM (+)
Ro 31-8220 (+)
PHM (+)
Ro 31-8220 (+)
PHM (-)
c-Fos / 5-HT2AR / NeuN
B
Relative population (%) of c-Fos-positive cells among NeuN- and 5-HT2AR-positive cells
50
40
30
20
10
0
*
n.s.
Ro 31-8220
PHM
C
Ro 31-8220 (-)
PHM (+)
Ro 31-8220 (+)
PHM (+)
Ro 31-8220 (+)
PHM (-)
5-HT2AR / NeuN
5-HT2AR
D
% of NeuN-positive area
Internalized 5-HT2AR-positive area
10
8
6
4
2
0
***
n.s.
Membrane-associated 5-HT2AR-positive area
25
20
15
10
5
0
*
n.s.
Ro 31-8220
PHM

Figure 3-15. Protein kinase C inhibition eliminates the effect of PHM on c-Fos expression and 5-HT$_{2A}$ receptor internalization in mouse PFC neurons

(**A**) Representative micrographic images of anti-c-Fos (green), anti-5-HT$_{2A}$ receptor (5-HT$_{2A}$R; red) and anti-NeuN (blue) immunostaining of the PFC of mice administrated with Ro 31-8220 or its vehicle (saline) prior to each bout of daily PHM. Scale bar, 100 μm. (**B**) PKC inhibition nullified the effect of PHM on c-Fos expression in 5-HT$_{2A}$ receptor-positive neurons of mouse PFC. Relative population (%) of c-Fos-positive cells out of 300 NeuN- and 5-HT$_{2A}$ receptor-positive cells is shown. (**C**) Representative micrographic images of anti-5-HT$_{2A}$ receptor (red) and anti-NeuN (green) immunostaining of mouse PFC from each group. High magnification images of anti-5-HT$_{2A}$ receptor immunostaining of arrow-pointed cells are presented with a gray scale. Yellow lines represent the margins of neuronal somas outlined by anti-NeuN immunosignals, and cyan arrowhead points to internalized anti-5-HT$_{2A}$ receptor immunosignals. Scale bars, 20 μm. (**D**) Internalized and membrane-associated 5-HT$_{2A}$ receptor-positive areas were quantified. 35 - 40 NeuN-positive cells were analyzed for each animal. *, $P < 0.05$; ***, $P < 0.001$; n.s., not significant.

A

Property	Value
Pressure (ΔP; mmHg)	0.93
Viscosity (μ; mPa·s)	1 ~ 20 *
Spread distance along x-axis (Δx; μm)	0.1587
Spread distance along y-axis (Δy; μm)	0.1933
Spread distance along z-axis (Δz; μm)	0.1778
Velocity of interstitial fluid flow along x-axis ($u_{\infty,x}$; μm/s)	0.4370
Velocity of interstitial fluid flow along y-axis ($u_{\infty,y}$; μm/s)	1.0356
Velocity of interstitial fluid flow along z-axis ($u_{\infty,z}$; μm/s)	0.4978

B

Fluid shear stress (τ_x) along along x-axis at the cell surface:

$$\tau_x = \frac{\mu u_{\infty,x}}{\sqrt{K_{p,x}}}$$

$$K_{p,x} = \frac{\mu u_{\infty,x} \Delta x}{\Delta P}$$

, where $K_{p,x}$ is the Darcy permeability of brain tissue along x-axis.

The shear stresses along y- and z-axis can be calculated in a similar manner.

When the values listed in **a** are introduced in these equations, the magnitude of fluid shear stress is estimated as 0.6 ~ 3.6 Pa.

Table 3-1. Simulative calculation of the magnitude of PHM-generated fluid shear stress on the PFC neurons

(**A**) Values referenced for simulative calculation of the magnitude of fluid shear stress that PHM generated in the PFC. All referenced values except viscosity (marked by an asterisk) were drawn from analyses with Gd-DTPA-enhanced MRI and ICP measurement (**Fig. 3-7** and **Fig. 3-9**). The property of interstitial fluid viscosity was referenced from previous studies[156-158]. (**B**) Calculation of the magnitude of PHM-generated fluid shear stress. Fluid shear stress (τ) at the cell surface can be calculated as reported previously[159].

Conclusion

Spasticity occurs chronically with involuntary muscular contractions resulting from hyperexcitability of spinal circuit after SCI. As one of the crucial factors for development of spasticity, up-regulated expression of 5-HT receptors on the spinal motor neurons due to the 5-HT denervation is considered. Although physical training or exercise shows significant benefits for spasticity after spinal cord injury (SCI), the underlying mechanism of how physical training (exercise) regulates the 5-HT receptors on the spinal cord has not been elicited. Further, not only confined to the spinal cord, it is believed that physical training is also beneficial for several 5-HT-receptor related mood disorders such as depression and anxiety.

Thus, the objective of my thesis was to investigate the effects of physical training and its mechanism related 5-HT signaling in the CNS for better understanding and for developing novel strategies or therapeutic programs. To do so, I first set up a proper evaluation model for assessing spasticity. Using the swimming test, I investigated the effect of physical training (treadmill training) on the 5-HT_{2A} receptor after traumatic SCI. Then, by exploiting the 5-HT_{2A} receptor related neuronal behavior and the region in the brain, I explored the mechanism about how physical activities regulate the 5-HT_{2A} receptor sensitivity.

In the ***Chapter 1***, I evaluated the feasibility of the swimming test with a rat model of contusive SCI to determine and assess spasticity along with examination of the expression of 5-HT_{2A} receptor. Based on the results of the swimming test, SCI rats could accurately and easily be categorized into “spasticity-positive” and “spasticity-negative” groups, and these results were not only reproducible across tests and time but also corresponded to the results of behavioral, electrophysiological, and histological feature assessments. Therefore, a swimming test using data based on the occurrence of spastic episodes (spasm and clonus) can accurately reflect the severity of spasticity in a contusive SCI rat model. I further uncovered a mechanism for the variation in spasticity among animals with SCI related to the expression of 5-HT_{2A} receptor at the lumbar spinal motor neurons, which was more up-regulated in the spasticity-

positive group. This indicates that the 5-HT_{2A} receptor hypersensitivity may be correlated to the development and severity of spasticity following SCI. This chapter represents the first demonstration of spasticity evaluation in a contusive SCI animal model, demonstrating the utility of the swimming test for classification. Furthermore, I demonstrated a correlation between 5-HT hypersensitivity and spasticity severity for the same level of SCI. Thus, the ***Chapter 1*** demonstrates that a swimming test is a useful method for evaluating spastic behaviors related to the 5-HT receptor that should help toward the development of new therapeutic interventions for spasticity.

Utilizing the developed evaluating method in the ***Chapter 1***, I investigated the effect of physical training (treadmill training) on spasticity, with or without combinational therapies using administration of serotonergic drugs (cyproheptadine or fluoxetine). In the ***Chapter 2***, I observed beneficial effects of treadmill training and the 5-HT_2 receptor antagonist (cyproheptadine) on spasticity assessed by a multimodal assessment approach, including behavior assessment, electrophysiology, and histology. Besides, I found no synergistic effect of the combined administration of treadmill training and the 5-HT antagonist. Moreover, my results indicate that treadmill training and the 5-HT receptor antagonist have different effects on the hyperactive state of the 5-HT_{2A} receptor expressed on motor neurons. On the other hand, administration of the selective serotonin re-uptake inhibitor (fluoxetine) exacerbated spastic behaviors. In particular, using immunohistochemical analysis, I observed decrease 5-HT_{2A} receptor expression by treadmill training and suggested that this result may be due to the internalization of the 5-HT receptor. The findings in the ***Chapter 2*** successfully demonstrated the effect of combination therapy involving treadmill training and serotonergic drugs, and provide an insight into the mechanism underlying its effect. Thus, the ***Chapter 2*** suggests that a new concept that is a fusion of locomotive and pharmacological rehabilitation, and provide a

reliable experimental approach to explore new therapeutic interventions for spasticity in contusive SCI.

Last, in the ***Chapter 3***, I further examined the effect of physical training on the regulation of 5-HT receptor based on the observation in the ***Chapter 2***. To elicit how the physical training affects the regulation of 5-HT receptor, I used the brain of rodents and its 5-HT_{2A} receptor related functions because of the possibility for utilizing as a reminiscent model to investigate the spinal neurons and for better understanding. I focused on physical movements of an animal, especially the head part, during treadmill training and hypothesized that the mechanical stress generated from physical activities regulates 5-HT receptor sensitivity in the CNS. Subsequently, I designed a 'passive head motion' system which generates vertical accelerations at rodent's heads similar to those during treadmill running to deliver simple mechanical stress. I demonstrated that passive head motion in rodents recapitulates the effects of physical activity on the decreased neuronal response to overdose 5-HT injection. As the reason for desensitization to 5-HT, mainly, I observed the internalization of 5-HT_{2A} receptor of neurons at the prefrontal cortex in the brain. Also, I determined the change of distribution dynamics of cerebral interstitial fluid using MRI analysis as well as the change of intracerebral pressures when the passive head motion applied to animals. From these results, I derived that fluid shear stress is generated in the brain of rodent, from the head motion, which also may occurred by treadmill running. Next, I presented *in vitro* evidences that neuronal cells exposed to fluid shear stress which is a similar level of passive head motion-induced shear stress showed the internalization of 5-HT_{2A} receptor. Fluid shear stress exposed neuronal cells presented suppressed 5-HT signaling in consistent with *in vivo* analysis. Furthermore, I presented that an inhibition of protein kinase C (PKC) blocks mechanical desensitization of neurons *in vivo* and neuronal cells *in vitro* to 5-HT. Overall, the ***Chapter 3*** suggests that the mechanical regulation

of neuronal cell function in the brain is partly responsible for the effects of physical activity, such as treadmill running, on the CNS.

In conclusion, this study revealed that physical training (exercise) which generates the mechanical stress in the CNS could regulate the sensitivity of 5-HT_{2A} receptor and alleviate spasticity after SCI. My results showed that the physical activities could desensitize 5-HT signaling toward hypersensitivity of 5-HT_{2A} receptor after spinal cord injury or response of the 5-HT receptor to overdose 5-HT receptor agonist in the brain. Considering these points, my study may help to develop novel rehabilitation programs or therapies for not only spasticity, but the other 5-HT receptor related disorders, focusing to maintain the homeostasis of 5-HT signaling. In addition, although my study confined its focus to the 5-HT receptor, beneficial effects of physical training on the CNS are evidently not limited to regulation of the 5-HT receptor in the neuronal cells.

Physical training has been generally accepted as an effective and safest practice to maintain our health as well as a rehabilitation tool to promote impaired body functions. Various physical activities, such as running, swimming and bicycling, have been proven beneficial as prevention and therapy for a variety of health problems, including metabolic diseases, cardiovascular disorders and mental illnesses. Although the effects of physical activities are well documented, the mechanisms behind them are still uncovered. Thus, I assume that the other known physical activity-induced beneficial effects which especially related to GPCRs may be due to generated mechanical stress on the receptors. Also, given that mechanical regulation of the brain and spinal cord functions has not been extensively studied or even supposed so far, further studies are expected.

Acknowledgement

As a foreigner student and as a fresh veterinarian, five years study in Japan is an unforgettable experience in my life. I learned not just scientific knowledge and techniques, but also another broad view of life and culture.

First of all, I would like to express my deepest gratitude to my supervisor, **Professor Ryohei Nishimura** for choosing me as a Ph.D. student and for his guidance in the course of study. Due to his generosity and comfortable atmosphere, I was able to concentrate my work. I also thanks his great support and cares on each projects.

I am sincerely thanks to **Dr. Naoki Fujita** for his guidance and great supports on this thesis. Also, he always provided me valuable comments and advises. Without his guidance, I could not do my experiments about the spinal cord and brain at the National Rehabilitation Center for Persons with Disabilities (NRCD).

I greatly appreciate **Dr. Toru Ogata** (NRCD) for leading me to the experiment and the field of neuroscience. He taught me how to do experiments and to write papers from step one. I thanks for his enthusiastic discussion, efforts for my works and for being a corresponding author of three of my papers. Also, his generosity offered me valuable opportunity to do my experimental activities at NRCD.

I would like to express my gratitude to **Dr. Yasuhiro Sawada** (NRCD) for his great ideas, philosophy to science and enthusiastic scientific discussion with me. Thanks to his detailed ways of working and enthusiasm toward science which inspire me to move on.

I am grateful to **Dr. Motoshi Nagao** (NRCD) for his kind advises and supports. In addition, I thanks for his generous care about progression of my projects and valuable comments.

I express my gratitude to **Dr. Jun Toyohara** (Tokyo Metropolitan Institute of Gerontology) for his generosity to help MRI experiments and to **Dr. Michiru Makuuchi** (NRCD) for his kind analysis and explanation about MRI data. Also, I would like to appreciate **Dr. Daisuke Yoshino** (Tohoku University) for his genuine discussion and his help for shear stress experiments. I was able to do fluid shear stress experiment due to his instruction and calculation.

I specially thanks to members of National Rehabilitation Center: **Dr. Takahiro Maekawa** for spending his valuable time to develop passive head motion machines and for his kindness as well as patient teaching about several experimental techniques; **Dr. Toru Doi** for his interesting discussion and for sharing issues of experiments during 4 years; and **Dr. Shuhei Murase** for valuable discussion and his kind support. Furthermore, I am grateful to **Dr. Masakuni Tokunaga**, **Dr. Atsushi Takashima, Kumiko Saitou**, **Naoko Kume** and **Kayoko Nakanishi** for their kind supports and generosity. I also would like to thanks to **Dr. Taku Kitamura** for his genuine guidance about electrophysiological analysis and **Dr. Kazuhito Morioka** for his valuable comments on my project.

Furthermore, I would like to thank **Associate professor Takayuki Nakagawa, Professor Manabu Mochizuki** and all teaching & research assistant staffs for their precious cares and help. My heartfelt and sincere gratitude goes to the members of The University of Tokyo: **Maresuke Morita, Yuiko Tanaka, Kentaro Endo, Tae Takeda,** and **Junyan Chen**. Thanks for sharing so much great time and a lots of advisements. It is my pleasure to meet you all in Tokyo. I also appreciate all the members of laboratory of veterinary surgery, The University of Tokyo.

I greatly appreciate **Professor Hwi yool Kim** (Konkuk University, South Korea) for introducing me to The University of Tokyo and for providing me wise advices and cares.

I express my deep gratitude to **Professor Sang min Jung,** now in heaven**.**

I would like to express my deepest gratitude and dedicate this thesis to **my parents** and **my family**. Thanks for your unconditional supports and cares.

Last, above all, I would like to thank to **Ministry of Education, Culture, Sports, Science, and Technology of Japan (MEXT)** and **The University of Tokyo** for giving me an opportunity as being a Japanese government scholarship student to get my Ph.D. degree, here.

PER ASPERA AD ASTRA

References

1 Warburton, D. E., Nicol, C. W. & Bredin, S. S. Health benefits of physical activity: the evidence. *CMAJ* **174**, 801-809, doi:10.1503/cmaj.051351 (2006).

2 World Health Organization. *Physical activity*, <http://www.who.int/topics/physical_activity/en/> (2017).

3 Neufer, P. D. *et al.* Understanding the Cellular and Molecular Mechanisms of Physical Activity-Induced Health Benefits. *Cell Metab* **22**, 4-11, doi:10.1016/j.cmet.2015.05.011 (2015).

4 Cotman, C. W., Berchtold, N. C. & Christie, L. A. Exercise builds brain health: key roles of growth factor cascades and inflammation. *Trends Neurosci* **30**, 464-472, doi:10.1016/j.tins.2007.06.011 (2007).

5 Faulkner, G. E. & Taylor, A. H. *Exercise, health and mental health: Emerging relationships*. (Taylor & Francis, 2005).

6 Salmon, P. Effects of physical exercise on anxiety, depression, and sensitivity to stress: a unifying theory. *Clin Psychol Rev* **21**, 33-61 (2001).

7 Adamopoulos, S. *et al.* Physical training reduces peripheral markers of inflammation in patients with chronic heart failure. *Eur Heart J* **22**, 791-797, doi:10.1053/euhj.2000.2285 (2001).

8 Gokce, N. *et al.* Effect of exercise on upper and lower extremity endothelial function in patients with coronary artery disease. *Am J Cardiol* **90**, 124-127 (2002).

9 Ristow, M. *et al.* Antioxidants prevent health-promoting effects of physical exercise in humans. *Proc Natl Acad Sci U S A* **106**, 8665-8670, doi:10.1073/pnas.0903485106 (2009).

10 Berg, A., Halle, M., Franz, I. & Keul, J. Physical activity and lipoprotein metabolism: epidemiological evidence and clinical trials. *Eur J Med Res* **2**, 259-264 (1997).

11 Carro, E., Nunez, A., Busiguina, S. & Torres-Aleman, I. Circulating insulin-like growth factor I mediates effects of exercise on the brain. *J Neurosci* **20**, 2926-2933 (2000).

12 Cotman, C. W. & Berchtold, N. C. Exercise: a behavioral intervention to enhance brain health and plasticity. *Trends Neurosci* **25**, 295-301 (2002).

13 van Praag, H., Christie, B. R., Sejnowski, T. J. & Gage, F. H. Running enhances neurogenesis, learning, and long-term potentiation in mice. *Proc Natl Acad Sci U S A* **96**, 13427-13431 (1999).

14 Strohle, A. Physical activity, exercise, depression and anxiety disorders. *J Neural Transm (Vienna)* **116**, 777-784, doi:10.1007/s00702-008-0092-x (2009).

15 Firth, J., Cotter, J., Elliott, R., French, P. & Yung, A. R. A systematic review and meta-analysis of exercise interventions in schizophrenia patients. *Psychol Med* **45**, 1343-1361, doi:10.1017/S0033291714003110 (2015).

16 Berger, M., Gray, J. A. & Roth, B. L. The expanded biology of serotonin. *Annu Rev Med* **60**, 355-366, doi:10.1146/annurev.med.60.042307.110802 (2009).

17 Roth, B. L., Hanizavareh, S. M. & Blum, A. E. Serotonin receptors represent highly favorable molecular targets for cognitive enhancement in schizophrenia and other disorders. *Psychopharmacology (Berl)* **174**, 17-24, doi:10.1007/s00213-003-1683-8 (2004).

18 Canli, T. & Lesch, K. P. Long story short: the serotonin transporter in emotion regulation and social cognition. *Nat Neurosci* **10**, 1103-1109, doi:10.1038/nn1964 (2007).

19 Babyak, M. *et al*. Exercise treatment for major depression: maintenance of therapeutic benefit at 10 months. *Psychosom Med* **62**, 633-638 (2000).

20 Greist, J. H. *et al.* Running as treatment for depression. *Compr Psychiatry* **20**, 41-54 (1979).

21 Chaouloff, F., Elghozi, J. L., Guezennec, Y. & Laude, D. Effects of conditioned running on plasma, liver and brain tryptophan and on brain 5-hydroxytryptamine metabolism of the rat. *Br J Pharmacol* **86**, 33-41 (1985).

22 Greenwood, B. N. *et al.* Freewheel running prevents learned helplessness/behavioral depression: role of dorsal raphe serotonergic neurons. *J Neurosci* **23**, 2889-2898 (2003).

23 Meeusen, R. & De Meirleir, K. Exercise and brain neurotransmission. *Sports Med* **20**, 160-188 (1995).

24 Adams, M. M. & Hicks, A. L. Comparison of the effects of body-weight-supported treadmill training and tilt-table standing on spasticity in individuals with chronic spinal cord injury. *J Spinal Cord Med* **34**, 488-494, doi:10.1179/2045772311Y.0000000028 (2011).

25 Elbasiouny, S. M., Moroz, D., Bakr, M. M. & Mushahwar, V. K. Management of spasticity after spinal cord injury: current techniques and future directions. *Neurorehabil Neural Repair* **24**, 23-33, doi:10.1177/1545968309343213 (2010).

26 Edgerton, V. R. *et al.* Retraining the injured spinal cord. *J Physiol* **533**, 15-22 (2001).

27 Harkema, S. J. Neural plasticity after human spinal cord injury: application of locomotor training to the rehabilitation of walking. *Neuroscientist* **7**, 455-468, doi:10.1177/107385840100700514 (2001).

28 Nichols, D. E. & Nichols, C. D. Serotonin receptors. *Chem Rev* **108**, 1614-1641, doi:10.1021/cr078224o (2008).

29 Millan, M. J., Marin, P., Bockaert, J. & Mannoury la Cour, C. Signaling at G-protein-coupled serotonin receptors: recent advances and future research directions. *Trends Pharmacol Sci* **29**, 454-464, doi:10.1016/j.tips.2008.06.007 (2008).

30 Graeff, F. G., Guimaraes, F. S., De Andrade, T. G. & Deakin, J. F. Role of 5-HT in stress, anxiety, and depression. *Pharmacol Biochem Behav* **54**, 129-141 (1996).

31 van Praag, H. M. & de Haan, S. Central serotonin metabolism and frequency of depression. *Psychiatry Res* **1**, 219-224 (1979).

32 Yates, M. *et al.* 5HT2 receptor changes in major depression. *Biol Psychiatry* **27**, 489-496 (1990).

33 Vermeire, S. *et al.* Neuro-imaging the serotonin 2A receptor as a valid biomarker for canine behavioural disorders. *Res Vet Sci* **91**, 465-472, doi:10.1016/j.rvsc.2010.09.021 (2011).

34 Raote, I., Bhattacharyya, S. & Panicker, M. M. Functional selectivity in serotonin receptor 2A (5-HT2A) endocytosis, recycling, and phosphorylation. *Mol Pharmacol* **83**, 42-50, doi:10.1124/mol.112.078626 (2013).

35 Gainetdinov, R. R., Premont, R. T., Bohn, L. M., Lefkowitz, R. J. & Caron, M. G. Desensitization of G protein-coupled receptors and neuronal functions. *Annu Rev Neurosci* **27**, 107-144, doi:10.1146/annurev.neuro.27.070203.144206 (2004).

36 Hanyaloglu, A. C. & von Zastrow, M. Regulation of GPCRs by endocytic membrane trafficking and its potential implications. *Annu Rev Pharmacol Toxicol* **48**, 537-568, doi:10.1146/annurev.pharmtox.48.113006.094830 (2008).

37 Lance, J. W. The control of muscle tone, reflexes, and movement: Robert Wartenberg Lecture. *Neurology* **30**, 1303-1313 (1980).

38 Pandyan, A. D. *et al.* Spasticity: clinical perceptions, neurological realities and meaningful measurement. *Disabil Rehabil* **27**, 2-6 (2005).

39 Roy, R. R. & Edgerton, V. R. Neurobiological perspective of spasticity as occurs after a spinal cord injury. *Exp Neurol* **235**, 116-122, doi:10.1016/j.expneurol.2012.01.017 (2012).

40 Skold, C., Levi, R. & Seiger, A. Spasticity after traumatic spinal cord injury: nature, severity, and location. *Arch Phys Med Rehabil* **80**, 1548-1557, doi:S0003-9993(99)90329-5 [pii] (1999).

41 Adams, M. M. & Hicks, A. L. Spasticity after spinal cord injury. *Spinal Cord* **43**, 577-586, doi:10.1038/sj.sc.3101757 (2005).

42 Kapitza, S. *et al.* Tail spasms in rat spinal cord injury: changes in interneuronal connectivity. *Exp Neurol* **236**, 179-189, doi:10.1016/j.expneurol.2012.04.023 S0014-4886(12)00195-1 [pii] (2012).

43 Hsieh, T. H. *et al.* Time course quantification of spastic hypertonia following spinal hemisection in rats. *Neuroscience* **167**, 185-198, doi:10.1016/j.neuroscience.2010.01.064 (2010).

44 D'Amico, J. M., Condliffe, E. G., Martins, K. J., Bennett, D. J. & Gorassini, M. A. Recovery of neuronal and network excitability after spinal cord injury and implications for spasticity. *Front Integr Neurosci* **8**, 36, doi:10.3389/fnint.2014.00036 (2014).

45 van Cooten, I. P., Snoek, G. J., Nene, A. V., de Groot, S. & Post, M. W. Functional hindrance due to spasticity in individuals with spinal cord injury during inpatient rehabilitation and 1 year thereafter. *Spinal Cord*, doi:10.1038/sc.2015.41 (2015).

46 Barnes, M. P. An overview of the clinical management of spasticity. *Upper motor neurone syndrome and spasticity: clinical management and neurophysiology*, 1-11 (2001).

47 Abbruzzese, G. The medical management of spasticity. *Eur J Neurol* **9 Suppl 1**, 30-34; discussion 53-61 (2002).

48 Kirshblum, S. Treatment alternatives for spinal cord injury related spasticity. *J Spinal Cord Med* **22**, 199-217 (1999).

49 Rekand, T. Clinical assessment and management of spasticity: a review. *Acta Neurol Scand Suppl*, 62-66, doi:10.1111/j.1600-0404.2010.01378.x (2010).

50 Bose, P., Parmer, R. & Thompson, F. J. Velocity-dependent ankle torque in rats after contusion injury of the midthoracic spinal cord: time course. *J Neurotrauma* **19**, 1231-1249, doi:10.1089/08977150260338029 (2002).

51 Corleto, J. A. *et al.* Thoracic 9 Spinal Transection-Induced Model of Muscle Spasticity in the Rat: A Systematic Electrophysiological and Histopathological Characterization. *PLoS One* **10**, e0144642, doi:10.1371/journal.pone.0144642 (2015).

52 Thompson, F. J., Parmer, R. & Reier, P. J. Alteration in rate modulation of reflexes to lumbar motoneurons after midthoracic spinal cord injury in the rat. I. Contusion injury. *J Neurotrauma* **15**, 495-508 (1998).

53 Bennett, D. J., Sanelli, L., Cooke, C. L., Harvey, P. J. & Gorassini, M. A. Spastic long-lasting reflexes in the awake rat after sacral spinal cord injury. *J Neurophysiol* **91**, 2247-2258, doi:10.1152/jn.00946.2003 91/5/2247 [pii] (2004).

54 Kitzman, P. Alteration in axial motoneuronal morphology in the spinal cord injured spastic rat. *Exp Neurol* **192**, 100-108, doi:10.1016/j.expneurol.2004.10.021 (2005).

55 Li, Y., Harvey, P. J., Li, X. & Bennett, D. J. Spastic long-lasting reflexes of the chronic spinal rat studied in vitro. *J Neurophysiol* **91**, 2236-2246, doi:10.1152/jn.01010.2003 91/5/2236 [pii] (2004).

56 Murray, K. C., Stephens, M. J., Ballou, E. W., Heckman, C. J. & Bennett, D. J. Motoneuron excitability and muscle spasms are regulated by 5-HT2B and 5-HT2C receptor activity. *J Neurophysiol* **105**, 731-748, doi:10.1152/jn.00774.2010 jn.00774.2010 [pii] (2011).

57 Boulenguez, P. *et al.* Down-regulation of the potassium-chloride cotransporter KCC2 contributes to spasticity after spinal cord injury. *Nat Med* **16**, 302-307, doi:10.1038/nm.2107 nm.2107 [pii] (2010).

58 Murray, K. C. *et al.* Recovery of motoneuron and locomotor function after spinal cord injury depends on constitutive activity in 5-HT2C receptors. *Nat Med* **16**, 694-700, doi:10.1038/nm.2160 (2010).

59 Brown, P. Pathophysiology of spasticity. *J Neurol Neurosurg Psychiatry* **57**, 773-777 (1994).

60 Lee, J. K., Johnson, C. S. & Wrathall, J. R. Up-regulation of 5-HT2 receptors is involved in the increased H-reflex amplitude after contusive spinal cord injury. *Exp Neurol* **203**, 502-511, doi:10.1016/j.expneurol.2006.09.003 (2007).

61 Li, Y., Gorassini, M. A. & Bennett, D. J. Role of persistent sodium and calcium currents in motoneuron firing and spasticity in chronic spinal rats. *J Neurophysiol* **91**, 767-783, doi:10.1152/jn.00788.2003 (2004).

62 Harvey, P. J., Li, X., Li, Y. & Bennett, D. J. 5-HT2 receptor activation facilitates a persistent sodium current and repetitive firing in spinal motoneurons of rats with and without chronic spinal cord injury. *J Neurophysiol* **96**, 1158-1170, doi:10.1152/jn.01088.2005 (2006).

63 Kong, X. Y., Wienecke, J., Chen, M., Hultborn, H. & Zhang, M. The time course of serotonin 2A receptor expression after spinal transection of rats: an immunohistochemical study. *Neuroscience* **177**, 114-126, doi:10.1016/j.neuroscience.2010.12.062 (2011).

64 Ren, L. Q. *et al.* The time course of serotonin 2C receptor expression after spinal transection of rats: an immunohistochemical study. *Neuroscience* **236**, 31-46, doi:10.1016/j.neuroscience.2012.12.063 (2013).

65 Nance, P. W. A comparison of clonidine, cyproheptadine and baclofen in spastic spinal cord injured patients. *J Am Paraplegia Soc* **17**, 150-156 (1994).

66 Wainberg, M., Barbeau, H. & Gauthier, S. The effects of cyproheptadine on locomotion and on spasticity in patients with spinal cord injuries. *J Neurol Neurosurg Psychiatry* **53**, 754-763 (1990).

67 Cote, M. P., Gandhi, S., Zambrotta, M. & Houle, J. D. Exercise modulates chloride homeostasis after spinal cord injury. *J Neurosci* **34**, 8976-8987, doi:10.1523/JNEUROSCI.0678-14.2014 (2014).

68 Hubli, M. & Dietz, V. The physiological basis of neurorehabilitation--locomotor training after spinal cord injury. *J Neuroeng Rehabil* **10**, 5, doi:10.1186/1743-0003-10-5 (2013).

69 Reese, N. B. *et al.* Restoration of frequency-dependent depression of the H-reflex by passive exercise in spinal rats. *Spinal Cord* **44**, 28-34, doi:10.1038/sj.sc.3101810 (2006).

70 Wirz, M. *et al.* Effectiveness of automated locomotor training in patients with chronic incomplete spinal cord injury: a multicenter trial. *Arch Phys Med Rehabil* **86**, 672-680, doi:10.1016/j.apmr.2004.08.004 (2005).

71 Abbott, N. J. Evidence for bulk flow of brain interstitial fluid: significance for physiology and pathology. *Neurochem Int* **45**, 545-552, doi:10.1016/j.neuint.2003.11.006 (2004).

72 Lei, Y., Han, H., Yuan, F., Javeed, A. & Zhao, Y. The brain interstitial system: Anatomy, modeling, in vivo measurement, and applications. *Prog Neurobiol*, doi:10.1016/j.pneurobio.2015.12.007 (2016).

73 Han, H. *et al.* A novel MRI tracer-based method for measuring water diffusion in the extracellular space of the rat brain. *IEEE J Biomed Health Inform* **18**, 978-983, doi:10.1109/JBHI.2014.2308279 (2014).

74 Zuo, L., Li, K. & Han, H. Comparative analysis by magnetic resonance imaging of extracellular space diffusion and interstitial fluid flow in the rat striatum and thalamus. *Applied Magnetic Resonance* **46**, 623-632 (2015).

75 Berk, B. C., Corson, M. A., Peterson, T. E. & Tseng, H. Protein kinases as mediators of fluid shear stress stimulated signal transduction in endothelial cells: a hypothesis for calcium-dependent and calcium-independent events activated by flow. *J Biomech* **28**, 1439-1450 (1995).

76 Cunningham, K. S. & Gotlieb, A. I. The role of shear stress in the pathogenesis of atherosclerosis. *Lab Invest* **85**, 9-23, doi:10.1038/labinvest.3700215 (2005).

77 Niebauer, J. & Cooke, J. P. Cardiovascular effects of exercise: role of endothelial shear stress. *J Am Coll Cardiol* **28**, 1652-1660, doi:10.1016/S0735-1097(96)00393-2 (1996).

78 Ramkhelawon, B., Rivas, D. & Lehoux, S. Shear stress activates extracellular signal-regulated kinase 1/2 via the angiotensin II type 1 receptor. *FASEB J* **27**, 3008-3016, doi:10.1096/fj.12-222299 (2013).

79 Bennett, D. J. *et al.* Spasticity in rats with sacral spinal cord injury. *J Neurotrauma* **16**, 69-84 (1999).

80 Thompson, F. J., Parmer, R., Reier, P. J., Wang, D. C. & Bose, P. Scientific basis of spasticity: insights from a laboratory model. *J Child Neurol* **16**, 2-9 (2001).

81 Lee, J. K., Emch, G. S., Johnson, C. S. & Wrathall, J. R. Effect of spinal cord injury severity on alterations of the H-reflex. *Exp Neurol* **196**, 430-440, doi:10.1016/j.expneurol.2005.08.018 (2005).

82 Courtine, G. *et al.* Recovery of supraspinal control of stepping via indirect propriospinal relay connections after spinal cord injury. *Nat Med* **14**, 69-74, doi:10.1038/nm1682 (2008).

83 Singh, A., Balasubramanian, S., Murray, M., Lemay, M. & Houle, J. Role of spared pathways in locomotor recovery after body-weight-supported treadmill training in contused rats. *J Neurotrauma* **28**, 2405-2416, doi:10.1089/neu.2010.1660 (2011).

84 Magnuson, D. S. *et al.* Swimming as a model of task-specific locomotor retraining after spinal cord injury in the rat. *Neurorehabil Neural Repair* **23**, 535-545, doi:10.1177/1545968308331147 (2009).

85 Smith, R. R. *et al.* The Louisville Swim Scale: a novel assessment of hindlimb function following spinal cord injury in adult rats. *J Neurotrauma* **23**, 1654-1670, doi:10.1089/neu.2006.23.1654 (2006).

86 Gonzenbach, R. R. *et al.* Nogo-A antibodies and training reduce muscle spasms in spinal cord-injured rats. *Ann Neurol* **68**, 48-57, doi:10.1002/ana.22009 (2010).

87 Gozariu, M., Roth, V., Keime, F., Le Bars, D. & Willer, J. C. An electrophysiological investigation into the monosynaptic H-reflex in the rat. *Brain Res* **782**, 343-347 (1998).

88 Lee, H. J. *et al.* Better functional outcome of compression spinal cord injury in mice is associated with enhanced H-reflex responses. *Exp Neurol* **216**, 365-374, doi:10.1016/j.expneurol.2008.12.009 (2009).

89 Valero-Cabre, A., Fores, J. & Navarro, X. Reorganization of reflex responses mediated by different afferent sensory fibers after spinal cord transection. *J Neurophysiol* **91**, 2838-2848, doi:10.1152/jn.01177.2003 (2004).

90 Trompetto, C. *et al.* Pathophysiology of spasticity: implications for neurorehabilitation. *Biomed Res Int* **2014**, 354906, doi:10.1155/2014/354906 (2014).

91 Schindler-Ivens, S. & Shields, R. K. Low frequency depression of H-reflexes in humans with acute and chronic spinal-cord injury. *Experimental brain research* **133**, 233-241 (2000).

92 Thompson, F. J., Reier, P. J., Lucas, C. C. & Parmer, R. Altered patterns of reflex excitability subsequent to contusion injury of the rat spinal cord. *J Neurophysiol* **68**, 1473-1486 (1992).

93 Skold, C. Spasticity in spinal cord injury: self- and clinically rated intrinsic fluctuations and intervention-induced changes. *Arch Phys Med Rehabil* **81**, 144-149 (2000).

94 Grey, M. J. *et al.* Post-activation depression of soleus stretch reflexes in healthy and spastic humans. *Exp Brain Res* **185**, 189-197, doi:10.1007/s00221-007-1142-6 (2008).

95 Schmidt, B. J. & Jordan, L. M. The role of serotonin in reflex modulation and locomotor rhythm production in the mammalian spinal cord. *Brain Res Bull* **53**, 689-710 (2000).

96 Navarrett, S., Collier, L., Cardozo, C. & Dracheva, S. Alterations of serotonin 2C and 2A receptors in response to T10 spinal cord transection in rats. *Neurosci Lett* **506**, 74-78, doi:10.1016/j.neulet.2011.10.052 (2012).

97 Doly, S. *et al.* The 5-HT2A receptor is widely distributed in the rat spinal cord and mainly localized at the plasma membrane of postsynaptic neurons. *J Comp Neurol* **472**, 496-511, doi:10.1002/cne.20082 (2004).

98 Stahl, S. M. Mechanism of action of serotonin selective reuptake inhibitors. Serotonin receptors and pathways mediate therapeutic effects and side effects. *J Affect Disord* **51**, 215-235 (1998).

99 Vaswani, M., Linda, F. K. & Ramesh, S. Role of selective serotonin reuptake inhibitors in psychiatric disorders: a comprehensive review. *Prog Neuropsychopharmacol Biol Psychiatry* **27**, 85-102 (2003).

100 Meyer, J. H. *et al.* The effect of paroxetine on 5-HT(2A) receptors in depression: an [(18)F]setoperone PET imaging study. *Am J Psychiatry* **158**, 78-85, doi:10.1176/appi.ajp.158.1.78 (2001).

101 Yamauchi, M., Miyara, T., Matsushima, T. & Imanishi, T. Desensitization of 5-HT2A receptor function by chronic administration of selective serotonin reuptake inhibitors. *Brain Res* **1067**, 164-169, doi:10.1016/j.brainres.2005.10.075 (2006).

102 Basso, D. M., Beattie, M. S. & Bresnahan, J. C. A sensitive and reliable locomotor rating scale for open field testing in rats. *J Neurotrauma* **12**, 1-21 (1995).

103 Stolp-Smith, K. A. & Wainberg, M. C. Antidepressant exacerbation of spasticity. *Arch Phys Med Rehabil* **80**, 339-342 (1999).

104 Thompson, C. K. & Hornby, T. G. Divergent modulation of clinical measures of volitional and reflexive motor behaviors following serotonergic medications in human incomplete spinal cord injury. *J Neurotrauma* **30**, 498-502, doi:10.1089/neu.2012.2515 (2013).

105 Skinner, R. D., Houle, J. D., Reese, N. B., Berry, C. L. & Garcia-Rill, E. Effects of exercise and fetal spinal cord implants on the H-reflex in chronically spinalized adult rats. *Brain Res* **729**, 127-131 (1996).

106 Thiel, G. Synapsin I, synapsin II, and synaptophysin: marker proteins of synaptic vesicles. *Brain Pathol* **3**, 87-95 (1993).

107 Schloss, P. & Williams, D. C. The serotonin transporter: a primary target for antidepressant drugs. *J Psychopharmacol* **12**, 115-121, doi:10.1177/026988119801200201 (1998).

108 Greenwood, B. N. *et al.* Wheel running alters serotonin (5-HT) transporter, 5-HT1A, 5-HT1B, and alpha 1b-adrenergic receptor mRNA in the rat raphe nuclei. *Biol Psychiatry* **57**, 559-568, doi:10.1016/j.biopsych.2004.11.025 (2005).

109 Ilha, J. *et al.* The beneficial effects of treadmill step training on activity-dependent synaptic and cellular plasticity markers after complete spinal cord injury. *Neurochem Res* **36**, 1046-1055, doi:10.1007/s11064-011-0446-x (2011).

110 Khristy, W. *et al.* Changes in GABA(A) receptor subunit gamma 2 in extensor and flexor motoneurons and astrocytes after spinal cord transection and motor training. *Brain Res* **1273**, 9-17, doi:10.1016/j.brainres.2009.03.060 (2009).

111 Baldys, A. & Raymond, J. R. Role of c-Cbl carboxyl terminus in serotonin 5-HT2A receptor recycling and resensitization. *J Biol Chem* **286**, 24656-24665, doi:10.1074/jbc.M110.119891 (2011).

112 Weaver, K. J., Paul, I. A., Lin, R. C. & Simpson, K. L. Neonatal exposure to citalopram selectively alters the expression of the serotonin transporter in the hippocampus: dose-dependent effects. *Anat Rec (Hoboken)* **293**, 1920-1932, doi:10.1002/ar.21245 (2010).

113 Slawinska, U., Majczynski, H., Dai, Y. & Jordan, L. M. The upright posture improves plantar stepping and alters responses to serotonergic drugs in spinal rats. *J Physiol* **590**, 1721-1736, doi:10.1113/jphysiol.2011.224931 (2012).

114 Ichiyama, R. M. *et al.* Dose dependence of the 5-HT agonist quipazine in facilitating spinal stepping in the rat with epidural stimulation. *Neurosci Lett* **438**, 281-285, doi:10.1016/j.neulet.2008.04.080 (2008).

115 Hayashibe, M. *et al.* Locomotor improvement of spinal cord-injured rats through treadmill training by forced plantar placement of hind paws. *Spinal Cord* **54**, 521-529, doi:10.1038/sc.2015.186 (2016).

116 Rossignol, S. & Frigon, A. Recovery of locomotion after spinal cord injury: some facts and mechanisms. *Annu Rev Neurosci* **34**, 413-440, doi:10.1146/annurev-neuro-061010-113746 (2011).

117 Bhattacharyya, S., Puri, S., Miledi, R. & Panicker, M. M. Internalization and recycling of 5-HT2A receptors activated by serotonin and protein kinase C-mediated mechanisms. *Proc Natl Acad Sci U S A* **99**, 14470-14475, doi:10.1073/pnas.212517999 (2002).

118 Klein-Nulend, J., Bakker, A. D., Bacabac, R. G., Vatsa, A. & Weinbaum, S. Mechanosensation and transduction in osteocytes. *Bone* **54**, 182-190, doi:10.1016/j.bone.2012.10.013 (2013).

119 Corne, S. J. & Pickering, R. W. A possible correlation between drug-induced hallucinations in man and a behavioural response in mice. *Psychopharmacologia* **11**, 65-78 (1967).

120 Canal, C. E. & Morgan, D. Head-twitch response in rodents induced by the hallucinogen 2,5-dimethoxy-4-iodoamphetamine: a comprehensive history, a re-evaluation of mechanisms, and its utility as a model. *Drug Test Anal* **4**, 556-576, doi:10.1002/dta.1333 (2012).

121 Halberstadt, A. L. & Geyer, M. A. Characterization of the head-twitch response induced by hallucinogens in mice: detection of the behavior based on the dynamics of head movement. *Psychopharmacology (Berl)* **227**, 727-739, doi:10.1007/s00213-013-3006-z (2013).

122 Gonzalez-Maeso, J. *et al.* Hallucinogens recruit specific cortical 5-HT(2A) receptor-mediated signaling pathways to affect behavior. *Neuron* **53**, 439-452, doi:10.1016/j.neuron.2007.01.008 (2007).

123 Roth, B. L., Berry, S. A., Kroeze, W. K., Willins, D. L. & Kristiansen, K. Serotonin 5-HT2A receptors: molecular biology and mechanisms of regulation. *Crit Rev Neurobiol* **12**, 319-338 (1998).

124 Kroll, M. H. *et al.* Protein kinase C is activated in platelets subjected to pathological shear stress. *J Biol Chem* **268**, 3520-3524 (1993).

125 Chapell, R., Bueno, O. F., Alvarez-Hernandez, X., Robinson, L. C. & Leidenheimer, N. J. Activation of protein kinase C induces gamma-aminobutyric acid type A receptor internalization in Xenopus oocytes. *J Biol Chem* **273**, 32595-32601 (1998).

126 Liles, W. C., Hunter, D. D., Meier, K. E. & Nathanson, N. M. Activation of protein kinase C induces rapid internalization and subsequent degradation of muscarinic acetylcholine receptors in neuroblastoma cells. *J Biol Chem* **261**, 5307-5313 (1986).

127 Park, J. S. *et al.* Persistent inflammation induces GluR2 internalization via NMDA receptor-triggered PKC activation in dorsal horn neurons. *J Neurosci* **29**, 3206-3219, doi:10.1523/JNEUROSCI.4514-08.2009 (2009).

128 Kim, S. E. *et al.* Treadmill exercise prevents aging-induced failure of memory through an increase in neurogenesis and suppression of apoptosis in rat hippocampus. *Exp Gerontol* **45**, 357-365, doi:10.1016/j.exger.2010.02.005 (2010).

129 Li, H. *et al.* Regular treadmill running improves spatial learning and memory performance in young mice through increased hippocampal neurogenesis and decreased stress. *Brain Res* **1531**, 1-8, doi:10.1016/j.brainres.2013.07.041 (2013).

130 Gaser, C. *et al.* Deformation-based brain morphometry in rats. *Neuroimage* **63**, 47-53, doi:10.1016/j.neuroimage.2012.06.066 (2012).

131 YOSHINO, D., SAKAMOTO, N., TAKAHASHI, K., INOUE, E. & SATO, M. Development of Novel Flow Chamber to Study Endothelial Cell Morphology: Effects of Shear Flow with Uniform Spatial Gradient on Distribution of Focal Adhesion. *Journal of Biomechanical Science and Engineering* **8**, 233-243 (2013).

132 Bedard, P. & Pycock, C. J. "Wet-dog" shake behaviour in the rat: a possible quantitative model of central 5-hydroxytryptamine activity. *Neuropharmacology* **16**, 663-670 (1977).

133 Goodwin, G. M. & Green, A. R. A behavioural and biochemical study in mice and rats of putative selective agonists and antagonists for 5-HT1 and 5-HT2 receptors. *Br J Pharmacol* **84**, 743-753 (1985).

134 Mullen, R. J., Buck, C. R. & Smith, A. M. NeuN, a neuronal specific nuclear protein in vertebrates. *Development* **116**, 201-211 (1992).

135 Cornea-Hebert, V., Riad, M., Wu, C., Singh, S. K. & Descarries, L. Cellular and subcellular distribution of the serotonin 5-HT2A receptor in the central nervous system of adult rat. *J Comp Neurol* **409**, 187-209 (1999).

136 Maneshi, M. M. *et al.* Mechanical stress activates NMDA receptors in the absence of agonists. *Sci Rep* **7**, 39610, doi:10.1038/srep39610 (2017).

137 Bowers, B. J., Miyamoto-Ditmon, J. & Wehner, J. M. Regulation of 5-HT2A/C receptors and DOI-induced behaviors by protein kinase Cgamma. *Pharmacol Biochem Behav* **85**, 441-447, doi:10.1016/j.pbb.2006.09.022 (2006).

138 Saito, N. & Shirai, Y. Protein kinase C gamma (PKC gamma): function of neuron specific isotype. *J Biochem* **132**, 683-687 (2002).

139 Hartwig, J. H. *et al.* MARCKS is an actin filament crosslinking protein regulated by protein kinase C and calcium-calmodulin. *Nature* **356**, 618-622, doi:10.1038/356618a0 (1992).

140 Menard, C., Bastianetto, S. & Quirion, R. Neuroprotective effects of resveratrol and epigallocatechin gallate polyphenols are mediated by the activation of protein kinase C gamma. *Front Cell Neurosci* **7**, 281, doi:10.3389/fncel.2013.00281 (2013).

141 Chaouloff, F. Physical exercise and brain monoamines: a review. *Acta Physiol Scand* **137**, 1-13, doi:10.1111/j.1748-1716.1989.tb08715.x (1989).

142 Blomstrand, E., Perrett, D., Parry-Billings, M. & Newsholme, E. A. Effect of sustained exercise on plasma amino acid concentrations and on 5-hydroxytryptamine metabolism in six different brain regions in the rat. *Acta Physiol Scand* **136**, 473-481, doi:10.1111/j.1748-1716.1989.tb08689.x (1989).

143 Gomez-Merino, D., Bequet, F., Berthelot, M., Chennaoui, M. & Guezennec, C. Y. Site-dependent effects of an acute intensive exercise on extracellular 5-HT and 5-HIAA levels in rat brain. *Neurosci Lett* **301**, 143-146 (2001).

144 Mukaida, K., Shichino, T., Koyanagi, S., Himukashi, S. & Fukuda, K. Activity of the serotonergic system during isoflurane anesthesia. *Anesth Analg* **104**, 836-839, doi:10.1213/01.ane.0000255200.42574.22 (2007).

145 Han, J. *et al.* Acute and chronic shear stress differently regulate endothelial internalization of nanocarriers targeted to platelet-endothelial cell adhesion molecule-1. *ACS Nano* **6**, 8824-8836, doi:10.1021/nn302687n (2012).

146 Eskelinen, E. L. Roles of LAMP-1 and LAMP-2 in lysosome biogenesis and autophagy. *Mol Aspects Med* **27**, 495-502, doi:10.1016/j.mam.2006.08.005 (2006).

147 Zerial, M. & McBride, H. Rab proteins as membrane organizers. *Nat Rev Mol Cell Biol* **2**, 107-117, doi:10.1038/35052055 (2001).

148 Ramkhelawon, B. *et al.* Shear stress regulates angiotensin type 1 receptor expression in endothelial cells. *Circ Res* **105**, 869-875, doi:10.1161/CIRCRESAHA.109.204040 (2009).

149 Davies, P. F. Mechanical sensing mechanisms: shear stress and endothelial cells. *J Vasc Surg* **13**, 729-731 (1991).

150 Nollert, M. U., Eskin, S. G. & McIntire, L. V. Shear stress increases inositol trisphosphate levels in human endothelial cells. *Biochem Biophys Res Commun* **170**, 281-287 (1990).

151 Watson, P. A. Function follows form: generation of intracellular signals by cell deformation. *FASEB J* **5**, 2013-2019 (1991).

152 Bhullar, I. S. *et al.* Fluid shear stress activation of IkappaB kinase is integrin-dependent. *J Biol Chem* **273**, 30544-30549 (1998).

153 Chen, K. D. *et al.* Mechanotransduction in response to shear stress. Roles of receptor tyrosine kinases, integrins, and Shc. *J Biol Chem* **274**, 18393-18400 (1999).

154 Tzima, E. *et al.* A mechanosensory complex that mediates the endothelial cell response to fluid shear stress. *Nature* **437**, 426-431, doi:10.1038/nature03952 (2005).

155 Edwards, M. K., Rhodes, R. E. & Loprinzi, P. D. A Randomized Control Intervention Investigating the Effects of Acute Exercise on Emotional Regulation. *Am J Health Behav* **41**, 534-543, doi:10.5993/AJHB.41.5.2 (2017).

156 Huang, N. & Bonn, D. Viscosity of a dense suspension in Couette flow. *Journal of Fluid Mechanics* **590**, 497-507 (2007).

157 Sugiyama, S. *et al.* Computational simulation of convection-enhanced drug delivery in the non-human primate brainstem: a simple model predicting the drug distribution. *Neurol Res* **35**, 773-781, doi:10.1179/1743132813Y.0000000215 (2013).

158 Yao, W., Shen, Z. & Ding, G. Simulation of interstitial fluid flow in ligaments: comparison among Stokes, Brinkman and Darcy models. *Int J Biol Sci* **9**, 1050-1056, doi:10.7150/ijbs.7242 (2013).

159 Tarbell, J. M. & Shi, Z.-D. Effect of the glycocalyx layer on transmission of interstitial flow shear stress to embedded cells. *Biomechanics and modeling in mechanobiology*, 1-11 (2013).